Bernhard Blümich

Essential NMR

Bernhard Blümich
Essential NMR

Bernhard Blümich

Essential NMR
for Scientists and Engineers

With 110 Figures

Springer

Professor Dr. Bernhard Blümich
Institute of Technical Chemistry and
Macromolecular Chemistry
RWTH University of Aachen
52056 Aachen
Germany
bluemich@RWTH-aachen.de

Preface

NMR means Nuclear Magnetic Resonance. It is a phenomenon in physics which has been exploited for more than 50 years in a manifold of different forms with numerous applications in chemical analysis, medical diagnostics, biomedical research, materials characterization, chemical engineering, and well logging. Although the phenomenon is comparatively simple, the different realizations of NMR in terms of methods to gather molecular information steadily increase following the advances in electronics and data processing.

A scientist or engineer who wants to gain first insight into the basic principles and applications of NMR is faced with the problem of finding a comprehensive and sufficiently short presentation of the essentials of NMR. This is what this book is meant to be. Preferably it is used to accompany a course or to review the material. The figures and the text are arranged in pairs guiding the reader through the different aspects of NMR. Following the introduction, the principles of the NMR phenomenon are covered in chapter 2. Chapter 3 on spectroscopy addresses the scientist's quest for learning about molecular structure, order, and dynamics. Chapters 4 and 5 deal with imaging and low-field NMR. They are more of interest to the engineer concerned with imaging, transport phenomena, and quality control. It is hoped, that this comprehensive presentation of NMR essentials is a helpful source of information to students and professionals in the applied sciences and in engineering.

Aachen, May 2004   Bernhard Blümich

Suggested Readings

For selective studies, the following combination of chapters is recommended:

Topic of Interest	Chapters	Reader
Basic NMR physics	1, 2	All
NMR spectroscopy	1, 2, 3	Chemists, physicists, biologists
NMR imaging	1, 2, 4	Materials scientists, engineers
NMR for quality control	1, 2, 5	Materials scientists, engineers

Contents

1. Introduction

Definition
Uses of NMR
Equipment
History
Cost
Literature

NMR: Nuclear Magnetic Resonance

NMR is a physical phenomenon
utilized to investigate molecular properties of matter
by irradiating atomic nuclei in a magnetic field
with radio waves

Uses of NMR

- *Chemical analysis*: molecular structures and dynamics
- *Materials science*: characterization of physical properties of matter
- *Medical imaging*: magnetic resonance tomography
  (largest area of application)
- *Chemical engineering*: measurements of diffusion, flow profiles,
  and distributions of velocities
- *Well logging* in geophysics and oil exploration: characterization of
  carbohydrates in rocks
- *Process- and quality control* by low-field NMR and
  by unilateral NMR Sensors

Equipment for NMR

- Spectroscopy: *NMR spectrometer* consisting of a magnet, a radio-frequency transmitter, a receiver, and a computer
- Imaging: *NMR tomograph* consisting of a magnet, a radio-frequency transmitter, receiver, a modulator for magnetic *gradient fields*, and a computer
- Measurements of transport parameters: NMR tomograph
- Well logging: NMR spectrometer incl. magnet in a tube, shock resistant, and temperature resistant up to 170° C
- Process and quality control: PC spectrometer or *mobile NMR spectrometer* with dedicated NMR sensors

NMR spectrometer for spectroscopy and imaging

transmitter, receiver, signal timer

magnet 11.6 T

4.7 T

7 T

Magnetic Resonance Center MARC, RWTH Aachen

PC spectrometer

NMR-MOUSE

NMR tomograph for medical diagnostics
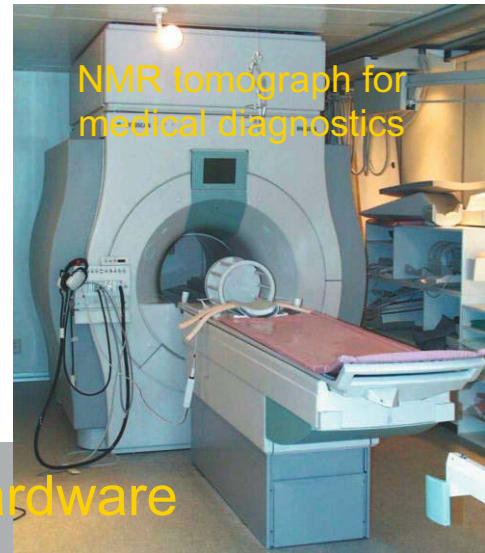
NMR Hardware

History of NMR

1945: First successful detection of an NMR signal by Felix Bloch (Stanford)
and Edward Purcell (Harvard): Nobel prize in Physics 1952

1949: Discovery of the *NMR echo* by Erwin Hahn

1951: Discovery of the *chemical shift* by J. T. Arnold and F. C. Yu

1951: Discovery of the *indirect spin-spin coupling* by W. G. Proctor

1953: *Earth field NMR* for well logging by Schlumberger-Doll

1966: Introduction of *Fourier NMR* by Richard Ernst,
Nobel Prize in Chemistry 1991

1971: *Two-dimensional NMR* by Jean Jeener, later multi-dimensional NMR
by Richard Ernst

1972: *NMR imaging* by Paul Lauterbur and Peter Mansfield, Nobel prize in
Medicine 2003

1975: *Multi-quantum NMR* and spectroscopy by T. Hashi, later by Alex Pines
and Richard Ernst

1977: *High-resolution solid-state NMR* spectroscopy by John Waugh,
Ed Stejskal, and Jack Schaefer

1979: 2D *Exchange NMR* by Jean Jeener. Application to protein analysis in
molecular Biology by Kurt Wüthrich, Nobel prize in Chemistry 2002

1980: *Unilateral NMR* in process control and medicine by Jasper Jackson

1984: Hyper polarization of xenon by William Happer
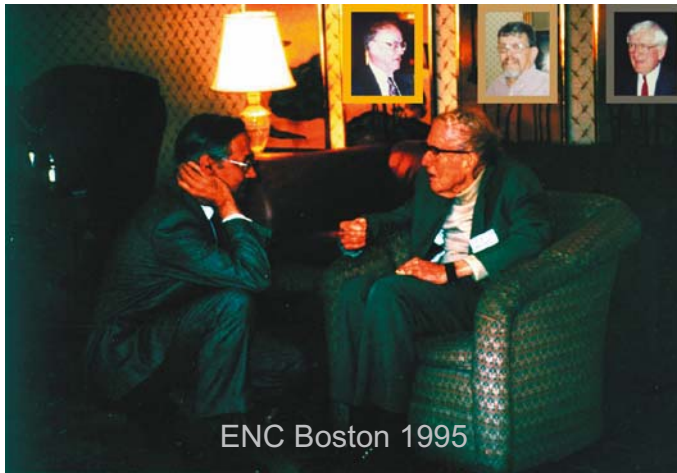
1995: Commercialization of *well logging* NMR by NUMAR

Some Nobel Prizes for NMR

Kurt Wüthrich, 1938.
Nobel Prize in
Chemistry 2002

Sir Peter
Mansfield, 1933.
Nobel Prize in
Medicine 2003

ENC Boston 1995

Richard R. Ernst, 1933.
Nobel Prize in
Chemistry 1991

Edward Mills Purcell,
1912 - 1997.
Nobel Prize in
Physics 1952

Felix Bloch,
1905 - 1983.
Nobel Prize in
Physics 1952

Paul Lauterbur, 1929.
Nobel Prize in
Medicine 2003

The Cost of NMR

Equipment:
- spectroscopy: € 250.000 to € 4.000.000
- imaging: € 250.000 to € 2.000.000
- measurements of transport parameters: € 250.000 to € 1.000.000
- well logging: € 250.000
- NMR for process and quality control: € 25.000 to € 100.000

Measurements:
- NMR spectrum: € 100 to € 500
- NMR image, flow NMR: € 500
- measurement day: € 1.500
- diploma thesis: € 20.000
- PhD thesis incl. equipment cost: € 200.000

Literature: General

- R. Freeman, Magnetic Resonance in Chemistry and Medicine, Oxford University Press, Oxford, 2003
- D. M. Grant, R. K. Harris, Eds., Encyclopedia of Nuclear Magnetic Resonance, Wiley-Liss, New York, 1996
- C. P. Slichter, Principles of Magnetic Resonance, 3. edition, Springer, Berlin, 1990
- R. R. Ernst, G. Bodenhausen, A. Wokaun, Principles of Nuclear Magnetic Resonance in One and Two Dimensions, Clarendon Press, Oxford, 1987
- F. A. Bovey, Nulear Magnetic Resonance Spectroscopy, Academic Press, New York, 1987
- E. Fukushima, S. B. W. Roeder, Experimental Pulse NMR: A Nuts and Bolts Approach, Addison Wesley, New York, 1986
- A. Abragam, The Principles of Nuclear Magnetism, Clarendon Press, Oxford, 1961

Literature: Liquid-State Spectroscopy

- E. T. Becker, High Resolution NMR: Theory and Chemical Applications, 3. edition, Academic Press, New York, 1999
- S. Braun, H.-O. Kalinowski, S. Berger, 150 And More Basic NMR Experiments: A Practical Course, VCH-Wiley, Weinheim, 1998
- H. Friebolin, Basic One- and Two-Dimensional NMR Spectroscopy, Wiley, New York, 1998
- R. S. Macomber, A Complete Inroduction to Modern NMR Spectroscopy, Wiley-Interscience, New York, 1998
- W. R. Croasmun, R. M. K. Carlson, Two-Dimensional NMR Spectroscopy, VCH, Weinheim, 1994
- A. E. Tonelli, NMR Spectroscopy and Polymer Microstructure, VCH Publishers, New York, 1989

Literature: Solid-State Spectroscopy

- M. H. Levitt, Spin Dynamics, Wiley, Chichester, 2001
- E. O. Stejskal, J. D. Memory, High Resolution NMR in the Solid State: Fundamentals of CP/MAS, Oxford University Press, New York, 1994
- K. Schmidt-Rohr and H. W. Spiess, Multidimensional Solid-State NMR and Polymers, Academic Press, London, 1994
- V. J. McBrierty and K. J. Packer, Nuclear Magnetic Resonance in Solid Polymers, Cambridge University Press, Cambridge, 1993
- W. Engelhardt, D. Michel, High-Resolution Solid-State NMR of Silicates and Zeolites, Wiley, New York, 1987
- B. C. Gerstein, C. Dybowski, Transient Techniques in NMR of Solids, Academic Press, New York, 1985
- M. Mehring, Principles of High-Resolution NMR in Solids, 2nd Edition, Springer-Verlag, Heidelberg, 1980
- U. Haeberlen, High-Resolution NMR in Solids: Selective Averaging, Adv. Magn. Reson. Suppl. 1, Academic Press, New York, 1976

Literature: Imaging

- B. Blümich, NMR Imaging of Materials, Clarendon Press, Oxford, 2000
- E. M. Haacke, R. W. Brown, M. R. Thompson, R. Venkatesan, Magnetic Resonance Imaging, Physical Principles and Sequence Design, Wiley-Liss, New York, 1999
- W. S. Price, NMR Imaging, Annual Reports on NMR Spectroscopy 35, (1998) 139 - 216
- J. B. Miller, NMR Imaging of Materials, Progr. Nucl. Magn. Reson. Spectrosc. 33 (1998) 273 – 308
- P. Blümler, B. Blümich, R. Botto, E. Fukushima, Eds., Spatially Resolved Magnetic Resonance, Wiley-VCH, Weinheim, 1998
- R. Kimmich, NMR Tomography, Diffusometry, Relaxometry, Springer, Berlin, 1997
- M. T. Vlaardingerbroek, J. A. den Boer, Magnetic Resonance Imaging, Springer, Berlin, 1996
- B. Blümich, W. Kuhn, Eds., Magnetic Resonance Microscopy, VCH, Weinheim, 1992
- P. T. Callaghan, Principles of Nuclear Magnetic Resonance Microscopy, Clarendon Press, Oxford, 1991

Literature: Flow

- P. T. Callaghan, Rheo-NMR: Nuclear Magnetic Resonance and the Rheology of Complex Fluids, Rep. Prog. Phys. 62 (1999) 599 – 668
- D. Traficante, Ed., Well Logging, Concepts of Magnetic Resonance, vol. 13, Wiley, New York, 2001
- G. R. Coates, L. Xiao, M. G. Prammer, NMR Logging: Principles and Applications, Halliburton Energy Services, Houston, 1999
- E. Fukushima, Nuclear Magnetic Resonance as a Tool to Study Flow, Annu. Rev. Fluid Mech. 31 (1999) 95 - 123
- A. Caprihan, E. Fukushima, Flow Measurements by NMR, Physics Reports 4 (1990) 195 - 235

2. Basic Principles

NMR spectrum
Nuclear magnetism
Rotating coordinate frame
NMR spectrometer
Pulse NMR
Fourier transformation
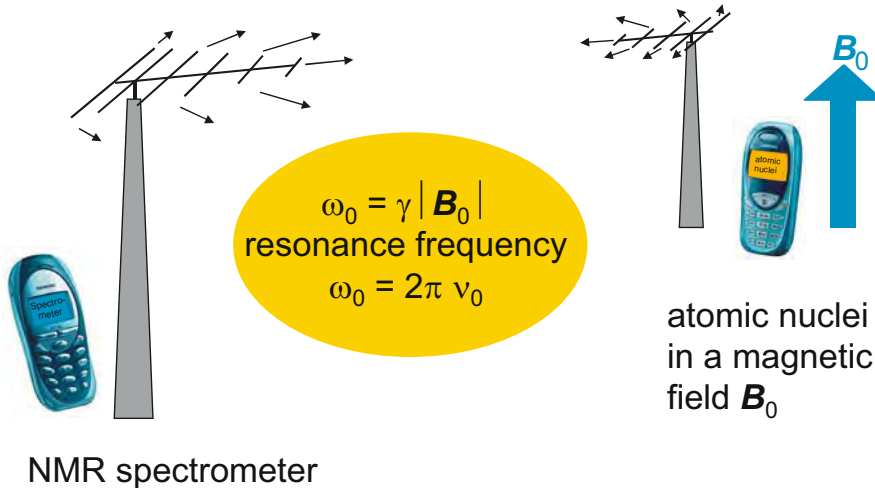Phase correction
Relaxation
Spin echo
Measurement methods
Spatial resolution

Properties of Atomic Nuclei

- When exposed to magnetic fields, magnetic nuclei can receive and emit radio waves. Their *frequency* ν_0 is proportional to the strength B_0 of the magnetic field: $\omega_0 = 2 \pi \nu_0 = \gamma B_0$
- The constant of proportionality is the *gyro-magnetic ratio* γ. It is a characteristic constant of the nuclear isotope
- Examples of isotope abundance and radio frequencies are:

nuclear isotope	nat. abundance	ν_0 at B_0 = 1.0 T
^{1}H	99.98 %	42.57 MHz
^{14}N	99.63 %	3.08 MHz
^{19}F	100.00 %	40.05 MHz
^{13}C	1.108 %	10.71 MHz
^{129}Xe	26.44 %	11.78 MHz

NMR is a Form of Telecommunication in a Magnetic Field

$$\omega_0 = \gamma \left| B_0 \right|$$
resonance frequency
$$\omega_0 = 2\pi \, \nu_0$$

B_0

atomic nuclei

NMR spectrometer

atomic nuclei
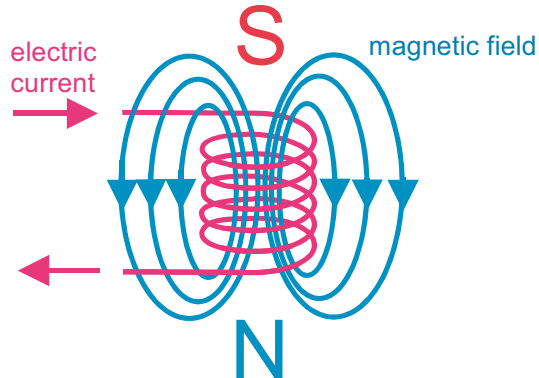in a magnetic
field B_0

Magnetic Shielding

- The NMR frequency is determined by the magnetic field at the site of the nucleus
- Atomic nuclei are surrounded by electrons
- In molecules, the electrons of the chemical bond are shared by different nuclei
- Electrons of atoms and molecules move in orbitals which are studied in quantum mechanics
- The orbitals of the binding electrons are characteristic of the *chemical structure* of the molecule
- Electrons carry an electric charge
- Electric charges in motion induce a magnetic field
- The internal magnetic field induced by the electrons moving in the external magnetic field B_0 is usually opposed to B_0. It shields the nucleus from B_0.

Electrons in Motion

double bond
C = C

single bond
C - C
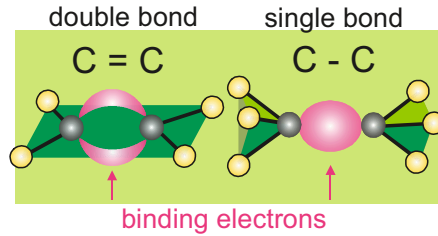
binding electrons

distribution of
binding electrons
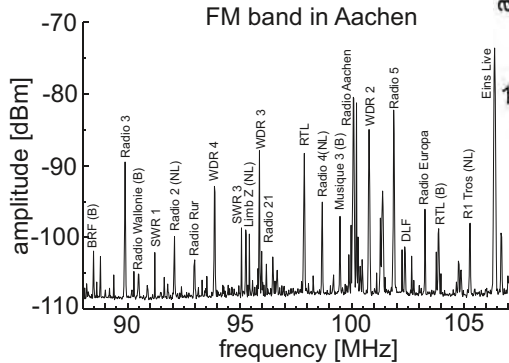
electric
current

S

magnetic field

N

moving charges induce
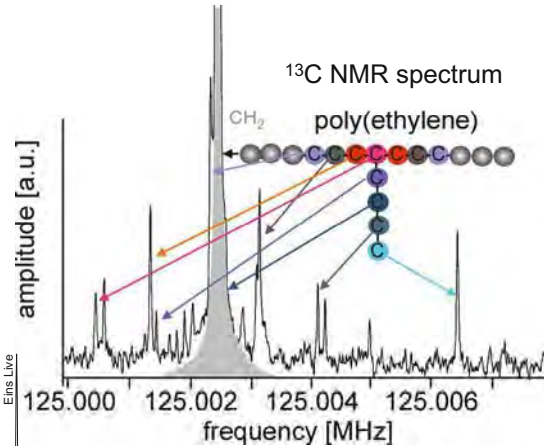a magnetic field

example: coil

Chemical Shift

- The induced magnetic field shifts the resonance frequency:
$$\omega_L = 2\pi \, \nu_L = \gamma \, (1 - \sigma) \, B_0$$
- The quantity σ is the *magnetic shielding* for a given chemical group
- The quantity $\delta = (\nu_L - \nu_{ref}) / \nu_{ref}$ is the *chemical shift* of a chemical group. It is independent of the magnetic field strength B_0.
- The chemical shift can be calculated from tabulated chemical shift increments as well as *ab initio* from quantum mechanics
- The quantity ν_{ref} is the reference frequency, for example, the resonance frequency of tetramethyl silane (TMS) for ^{1}H and ^{13}C NMR
- Magnetically inequivalent chemical groups possess different chemical shifts
- In liquids narrow resonance signals are observed with typical widths of 0.1 Hz
- The distribution of resonance frequencies forms the *NMR spectrum*
- The NMR spectrum is a fingerprint of the molecular structure similar to a distribution of FM signals at a given location which is a fingerprint of the geographical position
- The acquisition of NMR spectra of molecules in solution is a standard method of analysis in following chemical synthesis

Frequency Distributions of Radio Waves

^{13}C NMR spectrum

poly(ethylene)

CH$_2$

amplitude [a.u.]

125.000   125.002   125.004   125.006
frequency [MHz]

chemical structure

FM band in Aachen

amplitude [dBm]

-70

-80

-90

-100

-110

BRF (B)
Radio Walonie (B)
Radio 3
SWR 1
Radio 2 (NL)
Radio Rur
WDR 4
SWR 3
Limb Z (NL)
Radio 21
WDR 3
RTL
Radio 4(NL)
Musique 3 (B)
Radio Aachen
WDR 2
Radio 5
DLF
Radio Europa
RTL (B)
R1 Tros (NL)
Eins Live

90   95   100   105
frequency [MHz]

geographic position

Nuclear Magnetism

- In a sample of material there are roughly 10^{23} atomic nuclei per mole
- Some atomic nuclei have the properties of a *magnetic dipole*
- Examples: ^{1}H, ^{2}H, ^{13}C, ^{14}N, ^{19}F, ^{31}P, ^{129}Xe
- Because atomic nuclei consist of a small number of elementary particles, the laws of classical physics do not apply. Instead the laws of *quantum mechanics* do
- According to quantum mechanics an elementary magnetic dipole with a dipole moment μ also possesses an *angular momentum* $\hbar\,\textbf{I}$ or *spin I.*
- In the laws of physics involving elementary particles Planck`s constant h or $\hbar = h\,/\,(2\pi)$ appears
- A classical object with angular momentum is the *spinning top*
- A top spinning in a gravitational field formally follows the same laws as a spin in a magnetic field: it precesses around the direction of the field
- In NMR the precession frequency is called the *Larmor frequency*

Arnold Sommerfeld, 1868 – 1951, Heisenberg's teacher, described the spinning top

Paul Adrien Maurice Dirac, 1902 – 1984, 1933 Nobel prize in Physics, postulated the existence of the spin

Otto Stern 1888 – 1963, 1943 Nobel prize in Physics, experimental discovery of the spin

Nuclear Spin

precession frequency

graviation mg

ν_t

angular momentum

magnetic moment $\mu = \gamma \hbar I$

magnetic field $B_0 = \begin{pmatrix} 0 \\ 0 \\ B_0 \end{pmatrix}$

Larmor frequency ν_0

spin I

atomic nucleus
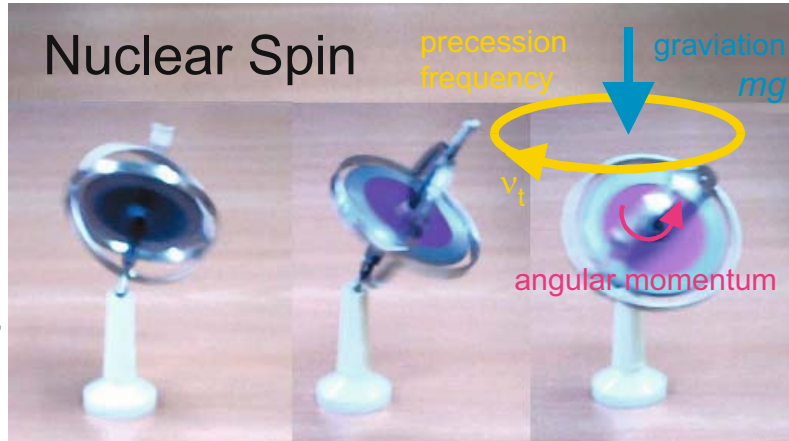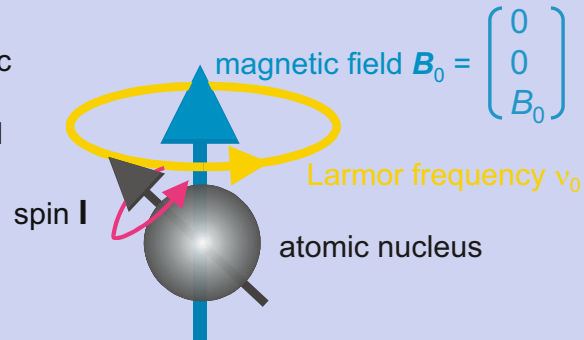
Properties of Nuclear Spins

- Following Heisenberg's uncertainty principle, only the component of the spin in the direction of the magnetic field can be measured
- From quantum mechanics it is known that a spin with the *spin quantum number I* can assume $2I + 1$ stable orientations in a magnetic field
- The projection of the spin angular momentum along the direction of the magnetic field is proportional to the *magnetic quantum number m*, where $m = I, I-1, ..., -I$
- $I = \frac{1}{2}$ is valid for the nuclei ^1H, ^{13}C, ^{19}F, ^{31}P, ^{129}Xe and $I = 1$ for ^2H, ^{14}N
- For nuclei with spin $I = \frac{1}{2}$ there are two possible orientations of it's projection along the axis of the magnetic field: $\uparrow$ und $\downarrow$
- Both orientations differ in the interaction energy $E_m = -\hbar \gamma m B_0$ of the nuclear magnetic dipoles with the magnetic field
- According to Bohr's formula $\Delta E = h \nu_0$ the energy difference $\Delta E = E_{-1/2} - E_{+1/2} = \hbar \gamma B_0$ associated with both orientations corresponds to the frequency $\omega_0 = 2\pi \nu_0 = \gamma B_0$
- Here ν_0 is the precession frequency of the nuclear spins in the magnetic field

Quantum Mechanics

Niels Henrik David Bohr 1885 - 1962, 1922 Nobel prize in Physics: $\Delta E = h \nu$

Felix Bloch, scholar of Heisenberg: 1905 – 1983, 1952 Nobel prize in Physics: NMR

Edward Mills Purcell 1912 – 1997, 1952 Nobel prize in

energy $E = -\mu_z B_0$

$\downarrow$ $\mu_z = -\hbar \gamma / 2$

$E_{-1/2}$

$\Delta E = h \nu_0$

$\uparrow$ $\mu_z = +\hbar \gamma / 2$

$E_{+1/2}$

$2\pi \nu_0 = \gamma B_0$

magnetic field B_0

magnetic field B_0

frequencies at $B_0 = 7$ T:
$\nu_0 = 300.5$ MHz for ^{1}H
$\nu_0 = 75.0$ MHz for ^{13}C
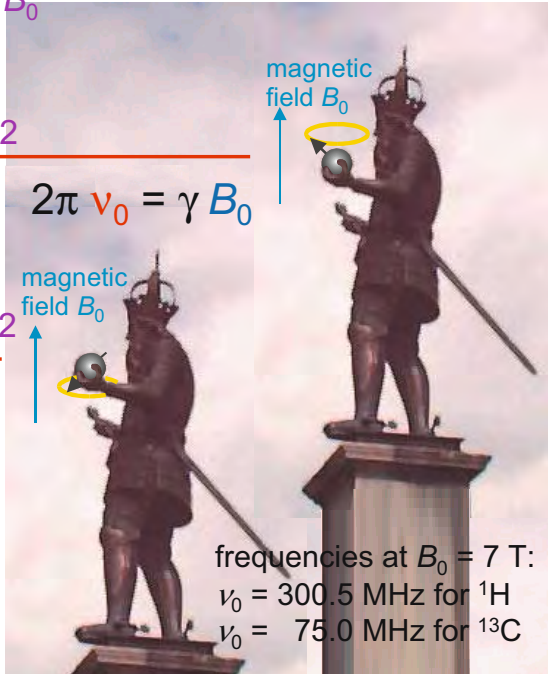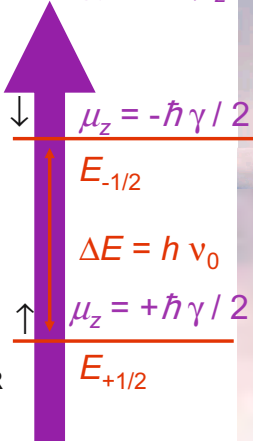
Nuclear Magnetization in Thermodynamic Equilibrium

- All magnetic dipole moments are added as vectors; their components in each space direction are additive
- The sum of transverse components (if observable) vanishes
- The sum of longitudinal components constitutes the *longitudinal magnetization*
- This component is referred to as the *magnetic polarization* of the nuclei or the *nuclear magnetization*
- At room temperature only about 10^{18} spins of all 10^{23} spins contribute to the macroscopic nuclear magnetization of the sample
- In the thermodynamic equilibrium state, the nuclear magnetization is oriented parallel to the direction of the magnetic field
- The direction of the magnetic field is referred to as the *z* direction of the *laboratory coordinate frame* LCF (index L)

Macroscopic Magnetization

macroscopic sample:
10^{23} nuclear spins

$n_-/n_+ = \exp\{-\Delta E/k_B T\}$

vector sum:
macroscopic
magnetization $\mathbf{M}$
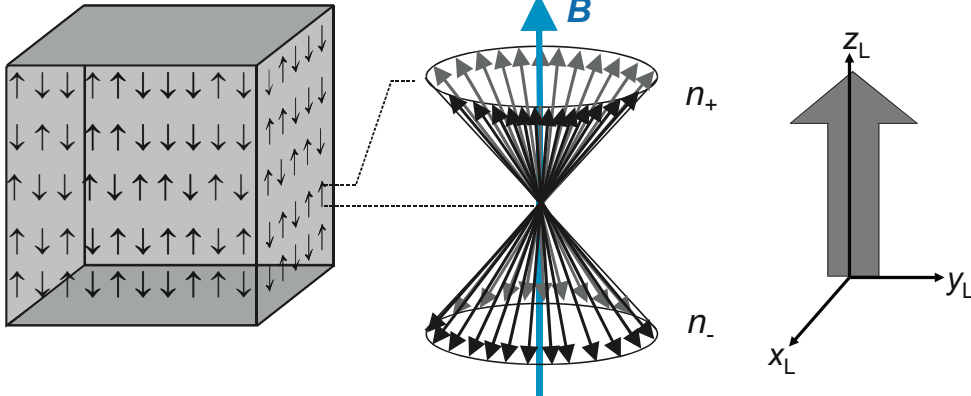
Bloch's Equation

- When the magnetization M is not aligned with the z_L direction, it precesses around z_L with the frequency ν_0 in complete analogy with the precession of a top spinning in a gravitational field g
- The precession is described by the equation for the magnetic *spinning top*:

$$\frac{\mathrm{d}}{\mathrm{d}t} M = \gamma\, M \times B$$

- This equation states that any change dM of the magnetization M is perpendicular to M and B; therefore M precesses
- In general any macroscopic precessional motion is attenuated. This is why Felix Bloch introduced phenomenological attenuation terms:

$$\mathbf{R} = \begin{pmatrix} 1/T_2 & 0 & 0 \\ 0 & 1/T_2 & 0 \\ 0 & 0 & 1/T_1 \end{pmatrix}$$

- The resultant equation is the *Bloch equation*,

$$\frac{\mathrm{d}}{\mathrm{d}t} M = \gamma\, M \times B - \mathbf{R}\,(M - M_0)$$

  where M_0: initial magnetization, T_1: longitudinal relaxation time, T_2: transverse relaxation time
- Note: The Bloch equation formulates a left-handed rotation of the transverse magnetization. But for convenience sake a right handed one is followed throughout this text and many others in the literature

Precession of Nuclear Magnetization

spinning top in a
gravitational field

g

L

L **g**

precession
frequency

$\omega_t = 2\pi\,\nu_t$

macroscopic nuclear
magnetization

$\mathbf{B}_0 \parallel z_L$

M

$\mathbf{B}_0 \parallel z_L$

Larmor
frequency ω_0
$= 2\pi\,\nu_0 = \gamma\,B_0$

M
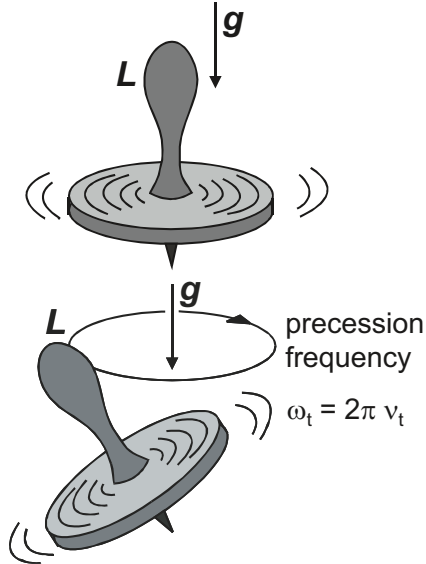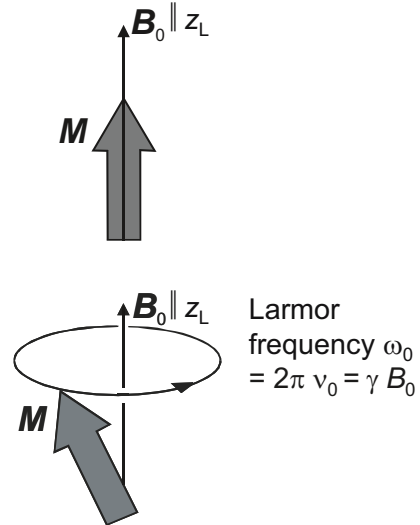
Contacting Nuclear Magnetization

- Nuclear magnetization can be rotated away from the direction z_L of the magnetic polarization field $\boldsymbol{B}_0$ by radio-frequency (rf) irradiation
- To this end one generates a magnetic field which rotates around $\boldsymbol{B}_0$ with frequency ω_{rf}
- For maximum interaction of the rotating field with the nuclear magnetization the *resonance condition* $\omega_{rf} = \omega_0$ is chosen
- Because $\nu_0 = \omega_0/2\pi$ is a frequency in the radio-frequency regime, the rotating magnetic field is an electromagnetic *radio-frequency wave*
- High frequency electromagnetic waves are emitted from transmission antennas or oscillating electronic rf circuits
- An *electronic oscillator* consists of a *coil* with inductance L, a capacitor with capacitance C, and a resistor with resistance R
- The coil generates a linearly polarized, oscillating magnetic field $2B_1 \sin\omega_{rf}t$
- Two orthogonal, linearly polarized waves $\cos\omega_{rf}t$ und $\sin\omega_{rf}t$ generate a rotating wave
- A linearly polarized wave $\sin\omega_{rf}t$ can be decomposed into a right rotating wave $\frac{1}{2}\exp\{i\omega_{rf}t\}$ and a left rotating wave $\frac{1}{2}\exp\{-i\omega_{rf}t\}$
- For optimum use of the oscillating magnetic field, the sample to be investigated is placed inside the coil

Magnetic Fields in an Oscillator Circuit

C

R

L

sample
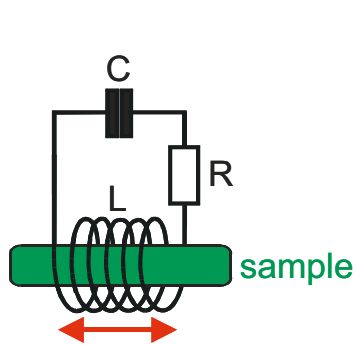
$2\,B_1\,\sin(\omega_{rf}\,t)$

magnetic field B_1 oscillating with frequency ω_{rf}

t

$\cos(\omega_{rf})t$

y_L

ω_{rf}

x_L

$\sin(\omega_{rf})t$

t
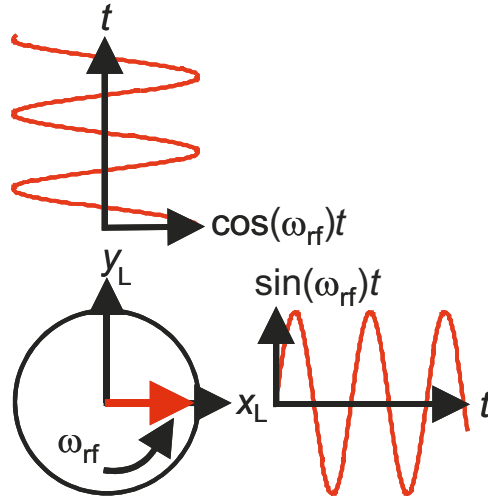
$\exp\{i\omega_{rf}\,t\} = \cos(\omega_{rf}\,t)$
$+ i\,\sin(\omega_{rf}\,t)$

$2\,B_1\,\sin(\omega_{rf}\,t) = -i\,B_1\,[\exp\{i\omega_{rf}\,t\} - \exp\{-i\omega_{rf}\,t\}]$

Rotating Coordinate Frame

- Transformations from one coordinate frame into another change the point of view, i. e. they change the mathematics but not the physics
- As the precession of nuclear magnetization is a rotational motion and the rf excitation is a rotating wave, the magnetization is conveniently studied in a *rotating coordinate frame* (RCF)
- The dog at the traffic circuit is positioned in the *laboratory coordinate frame* (LCF): For him the bicycles are driving in the traffic circuit with angular velocities ω_{rf} and $\omega_{rf} + \Omega$
- The cyclists on the bicycles are viewing the world from the RCF. They are at rest in their respective RCF
- For the red cyclist the world is rotating against the direction of his bicycle with angular velocity $-\omega_{rf}$
- For the red cyclist the yellow bicycle rides with angular velocity Ω in his RCF
- The connecting vectors from the center of the traffic circle to the bicycles correspond to the magnetization vectors in the transverse *xy* plane
- The angular velocity of the RCF as seen in the LCF corresponds to the frequency ω_{rf} of the rf wave

Coordinate Transformation
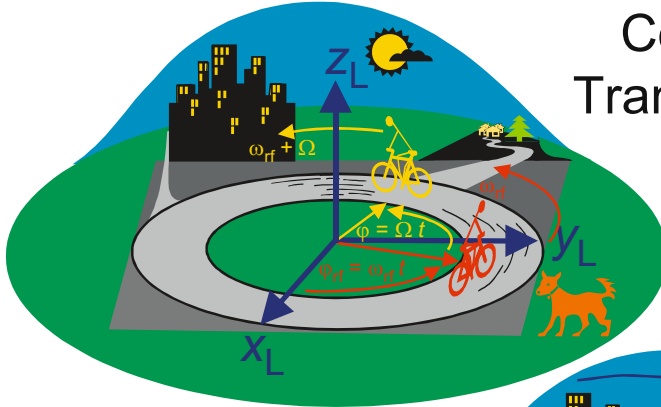
laboratory coordinate frame x_L, y_L, z_L: the dog looks at the bicycle riders

rotating coordinate frame x, y, z: the red bicycle rider looks at the dog
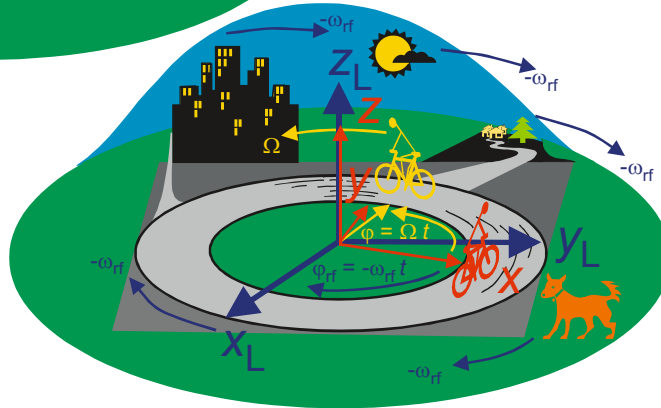
Radio-Frequency Pulses

- In a coordinate system, which rotates with frequency ω_0 around the *z* axis the magnetization **M** appears at rest even if it is not parallel to the magnetic field **B**$_0$
- When the magnetization is not rotating, there is no magnetic field active in that frame which produces a torque on the magnetization
- On resonance $\omega_{rf} = \omega_0$, and the rf field **B**$_1$ is time independent and appears static in the RCF when turned on
- In the RCF, which rotates in the LCF with $\omega_{rf} = \omega_0$ around **B**$_0$, the magnetization rotates around the **B**$_1$ field with frequency $\omega_1 = \gamma\,|\textbf{B}_1|$ in analogy to the rotation with frequency $\omega_0 = \gamma\,|\textbf{B}_0|$ around the **B**$_0$ field in the LCF
- If B_1 is turned on in a pulsed fashion for a time t_P, a 90° pulse is defined for $\omega_1 t_P = 90°$ and a 180° pulse for $\omega_1 t_P = 180°$
- The phase φ_0 of the *rotating rf field $B_1\exp\{i\omega_{rf}t + i\,\varphi_0\}$* defines the direction of the B_1 field in the *xy* plane of the RCF
- Using this phase the magnetization can be rotated in the RCF around different axes, e. g. 90°$_y$ denotes a positive 90° rotation around the *y* axis of the RCF and 180°$_x$ a positive 180° rotation around the *x* axis

Action of rf Pulses

laboratory coordinate frame

$\omega_0 = \gamma B_0$

M precesses around **B₀**

rotating coordinate frame

rf field **B₁** is off: **M** appears static

$-\omega_0 = -\gamma B_0$
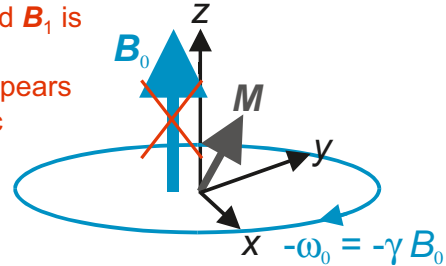
rf field **B₁** is on: **M** precesses around **B₁**

$\omega_1 = \gamma B_1$

$-\omega_0 = -\gamma B_0$

90° pulse: $\omega_1 \, t_p = \pi/2$
180° pulse: $\omega_1 \, t_p = \pi$
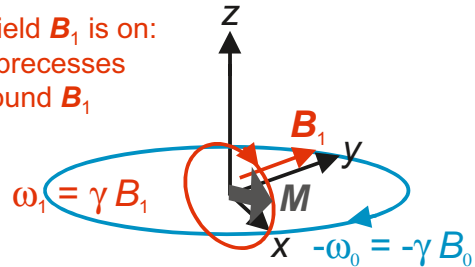
NMR Spectrometer

- The sample is positioned in a magnetic field B_0 inside a rf coil which is part of a *rf oscillator* tuned to the frequency ω_{rf}
- The oscillator is connected under computer control either to the rf *transmitter* (TX) or to the *receiver* (RX)
- A 90° rf pulse from the transmitter rotates the magnetization from the z_L direction of the B_0 field into the transverse plane
- Following the pulse, the transverse magnetization components precess around the z_L axis of the LCF with frequency ω_0
- According to the dynamo principle, the precessing magnetization induces a voltage in the coil which oscillates at frequency ω_0
- In the receiver, this signal is mixed with a reference wave at frequency ω_{rf}, and the audio signal at the difference frequency is filtered for acquisition
- This step is the transition into the *rotating coordinate frame*
- Depending on the phase $\phi_0 = 0°$ and $90°$ of the reference wave $\sin(\omega_{rf}t + \phi_0)$ the *quadrature components* $\sin(\omega_0 - \omega_{rf})t$ and $\cos(\omega_0 - \omega_{rf})t$ of the transverse magnetization are measured in the RCF, respectively
- Usually both quadrature components are measured simultaneously
- For imaging and flow measurements the spectrometer is equipped with switchable *gradient fields* in x_L, y_L, and z_L directions of the LCF

Spectrometer Hardware
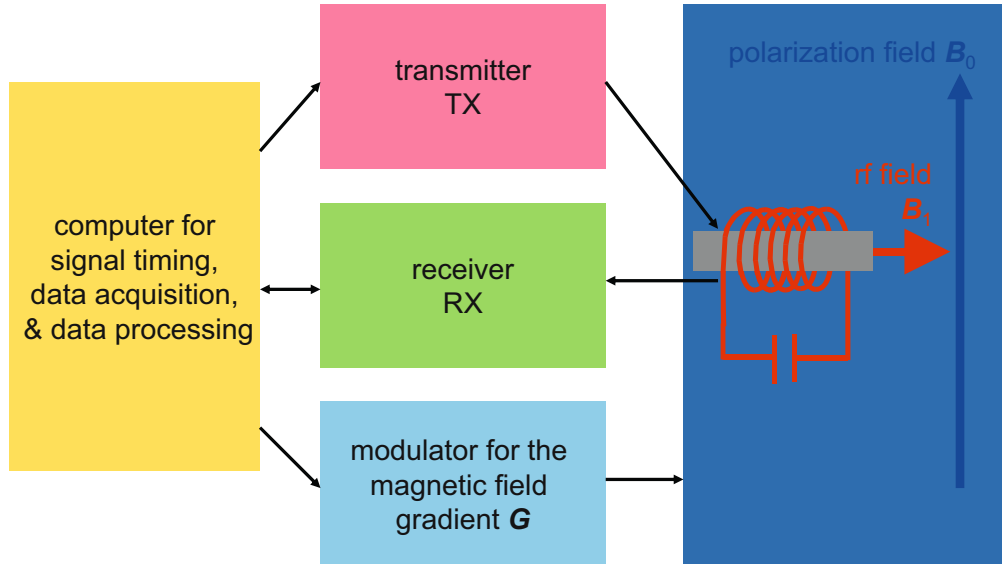
Pulse Excitation

- Outside a magnetic field the nuclear magnetic dipole moments are oriented in random directions in space
- When introducing the sample into the magnetic field $\boldsymbol{B}_0$, the *longitudinal magnetization* $\boldsymbol{M}_0$ is formed parallel to $\boldsymbol{B}_0$ with the time constant T_1 by aligning the nuclear magnetic moments according to the Boltzmann distribution: $M_z(t) = M_0 (1 - \exp\{-t/T_1\})$
- A $90°$ rf pulse from the transmitter rotates the magnetization from the z direction of the magnetic field $\boldsymbol{B}_0$ into the transverse plane of the RCF
- After the rf pulse the transverse components M_i of the magnetization precess around the z axis of the RCF with the difference frequencies $\Omega_i = \omega_{Li} - \omega_{rf}$
- Each component M_i corresponds to a different chemical shift or another position in the sample with a different magnetic polarization field
- The vector sum of the *transverse magnetization* components decays with the time constant T_2^* due to interference of the components with different precession frequencies Ω_i
- T_2^* is the *transverse relaxation time* due to time-invariant and time-dependent local magnetic fields
- The signal decay is often exponential: $M_{xy}(t) = M_z(0) \exp\{-t/T_2^*\}$
- The signal induced in the coil after pulse excitation is the *free induction decay* (*FID*)
- The frequency analysis of the FID by *Fourier transformation* produces the *NMR spectrum* with a *linewidth* $\Delta\Omega = 1/(\pi T_2^*)$

Fourier NMR
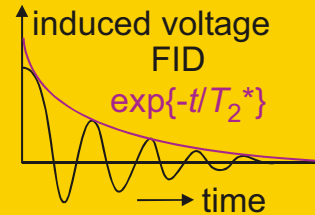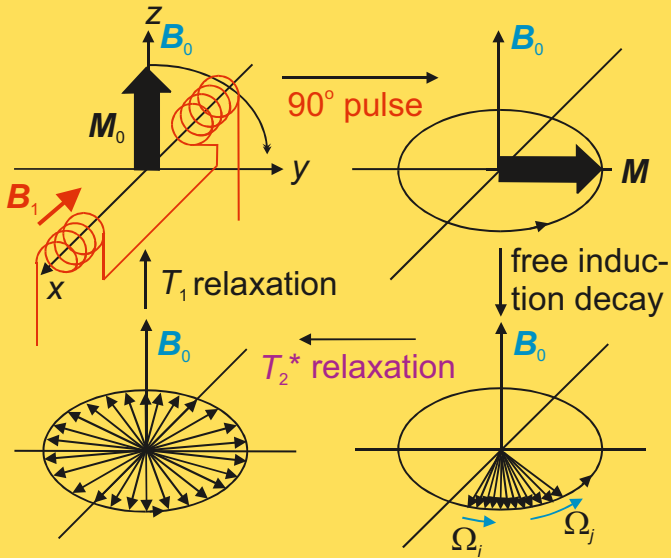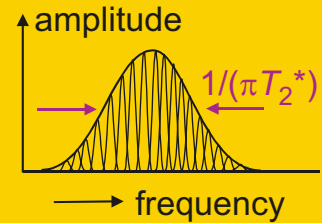
Fourier Transformation

- Fourier introduced the transformation named after him when studying thermal conductivity
- The *Fourier transformation* (FT) is a decomposition of a function $s(t)$ into harmonic waves $\exp\{i\,\omega t\} = \cos\omega t + i\,\sin\omega t$ with variable frequency ω
- In NMR the *FID* $s(t)$ is transformed to the spectrum $S(\omega)$ of cosine and sine waves: $S(\omega) = \int s(t)\exp\{-i\omega t\}dt$
- The *spectrum* $S(\omega) = U(\omega) + i\,V(\omega)$ consists of a real part $U(\omega)$ and an imaginary part $V(\omega)$
- Often, only the magnitude spectrum $|S(\omega)| = [U(\omega)^2 + V(\omega)^2]^{1/2}$ is employed
- The Fourier transformation corresponds to the transformation of an acoustic signal into the colors of sound when listening to it
- For the discrete Fourier transformation there is a fast algortithm which was rediscovered in 1965 by J. W. Cooley and J. W. Tukey
- The algorithm requires the discrete representation of the time function $s(t)$ and the spectrum $S(\omega)$ in steps Δt and $\Delta\omega$ of the variables t and ω
- The abscissa of the discrete spectrum corresponds to the keys of a piano
- The spectral amplitude corresponds to the volume of a given tone
- In NMR with pulsed excitation the Fourier transformation is part of processing the data
- *Pulsed NMR* is also called *Fourier NMR*
- The product of two Fourier conjugated variables, e. g. t and ω, is always an angle. It is referred to as *phase*

Frequency Analysis
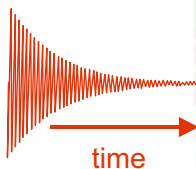
Jean Baptiste
Joseph Fourier
1768 - 1830

time
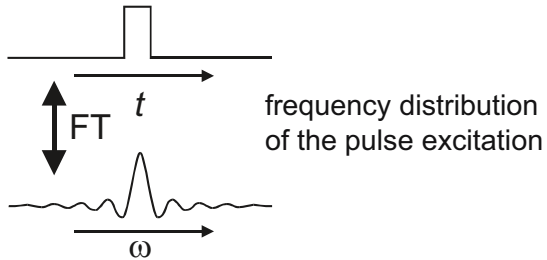
Fourier transformation

frequency
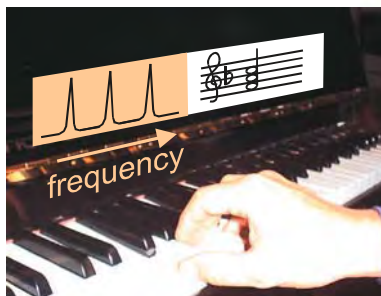
Signal Processing

- Depending on the phase ϕ_0 of the *rotating coordinate frame*, the *FID* is measured as the sum of impulse responses $s(t) = s(0) \exp\{-[1/T_2 - i\Omega]\,t + i\,\phi_0\}$ for each magnetization component with different Ω in the RCF
- For $\phi_0 = 0$ the real part $U(\omega)$ of the *Fourier transform* $S(\omega)$ is an *absorption signal* $A(\omega)$ and the imaginary part $V(\omega)$ a *dispersion signal* $D(\omega)$
- For $\phi_0 \neq 0$ the absorptive and dispersive components are mixed in $U(\omega)$ and $V(\omega)$, and the associated complex *spectrum* $S(\omega) = U(\omega) + i\,V(\omega) = [A(\omega) + i\,D(\omega)]\exp\{i\,\phi_0\}$ has to be corrected in phase by multiplication with $\exp\{-i\,\phi_0\}$
- The correction phase ϕ_0 consists of a frequency dependent and a frequency independent part
- The frequency-independent part can be adjusted by software before data acquisition via the rf reference phase of the spectrometer
- The frequency dependent part is determined by time the signals take to pass through the spectrometer and by the receiver *deadtime* following an excitation pulse
- For optimum resolution the spectrum is needed in pure absorptive mode
- A frequency dependent *phase correction* of the spectrum is a routine step in data processing of high-resolution NMR spectroscopy

$s(t)$ $\phi_0 = 45.9°$

$s(t)$ $\phi_0 = 0$

t

t

FT

FT

Phase Correction

$U(\omega)$ $U(\omega) \neq A(\omega)$

ω

$U(\omega)$ $U(\omega) = A(\omega)$

ω

$V(\omega)$ $V(\omega) \neq D(\omega)$

ω

$V(\omega)$ $V(\omega) = D(\omega)$

ω
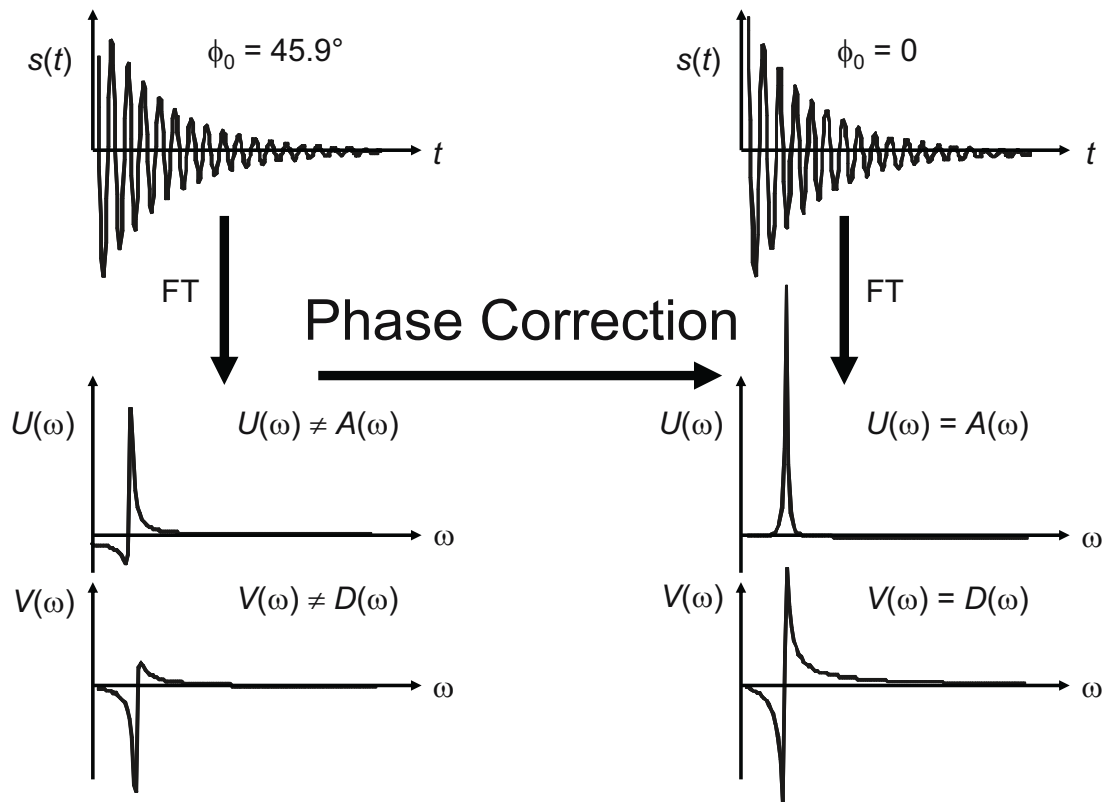
Frequency Distributions

- The rotating coordinate frame rotates with the rf frequency ω_{rf}
- In the laboratory frame the magnetization components M_i rotate with frequencies ω_{Li}
- The *rf pulse* with frequency ω_{rf} has to couple to several frequencies ω_{Li}
- The *bandwidth of the excitation* pulse is determined in approximation by the inverse of the pulse width t_p
- A better measure for the frequency dependence of the excitation is the *Fourier transform* of the excitation pulse
- For a rectangular pulse the Fourier transform is the *sinc function*
- Vice versa, the excitation can be made frequency selective by excitation with a rf pulse having a sinc shape in the time domain
- This simple Fourier relationship is a convenient approximation valid for small flip angles only
- In the RCF the magnetization components rotate with frequencies $\Omega_i = \omega_{Li} - \omega_{rf}$
- For a given component the offset frequency Ω corresponds to a magnetic *off-set field* Ω/γ along the z axis of the RCF
- The magnetization always rotates around the *effective field* $\boldsymbol{B}_{eff}$, which is the vector sum of the offset field Ω/γ and the rf field $\boldsymbol{B}_1$
- The *rotation angle of a pulse* is then given by $\gamma\, B_{eff}\, t_p = \omega_{eff}\, t_p$
- The rotation axis is in the *xy* plane if $|B_1| >> |\Omega/\gamma|$
- If $|B_1| << |\Omega/\gamma|$, longitudinal magnetization cannot be rotated into the *xy* plane

RF Excitation and Effective Field

frequency distribution
of the pulse excitation

B_{eff}
$= (B_{\text{RCF}}^2 + B_1^2)^{1/2}$

B_{RCF}
$= \Omega/\gamma$

ω_{eff}

B_1

selective
excitation
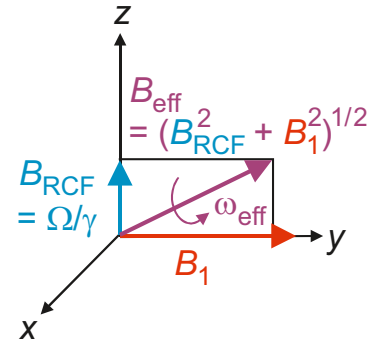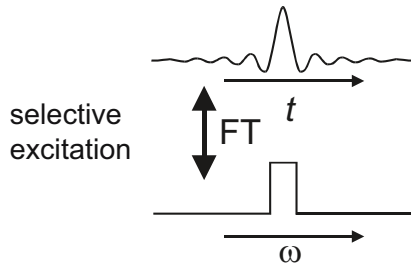
effective field in the rotating
coordinate frame

Relaxation

- *Relaxation* denotes the loss of *transverse magnetization* with the time constant T_2 and build-up of *longitudinal magnetization* with T_1
- The loss of transverse magnetization due to different time-invariant local magnetic fields can stroboscopically be reversed by formation of *echoes*
- For formation of a *racetrack echo* all bicyclists start at the same time but ride with different speeds. At a certain time all go back and meet at the starting line forming the *echo* after twice that time
- Their total riding time is the *echo time* t_E
- The NMR *echo* has accidentally been discovered in 1949 by Erwin Hahn
- For formation of a *Hahn echo* all transverse magnetization components are rotated by 180° around an axis in the *xy* plane
- The direction of precession is maintained with this change of positions on the circle, and all magnetization components refocus at time t_E
- If some components randomly change their precession frequencies, the *echo amplitude* is irreversibly reduced
- Random frequency changes arise from fluctuating local magnetic fields associated with molecules in motion
- T_2 relaxation denotes the irreversible loss of the echo amplitude
- Both *relaxation times* T_1 and T_2 are determined by the type and time scale of molecular motion
- By splitting the 180° pulse of the Hahn echo sequence into two 90° pulses separated by a time delay, one obtains the *stimulated echo* sequence

Echoes

racetrack echo

Hahn echo

stimulated echo

primary echo

stimulated echo
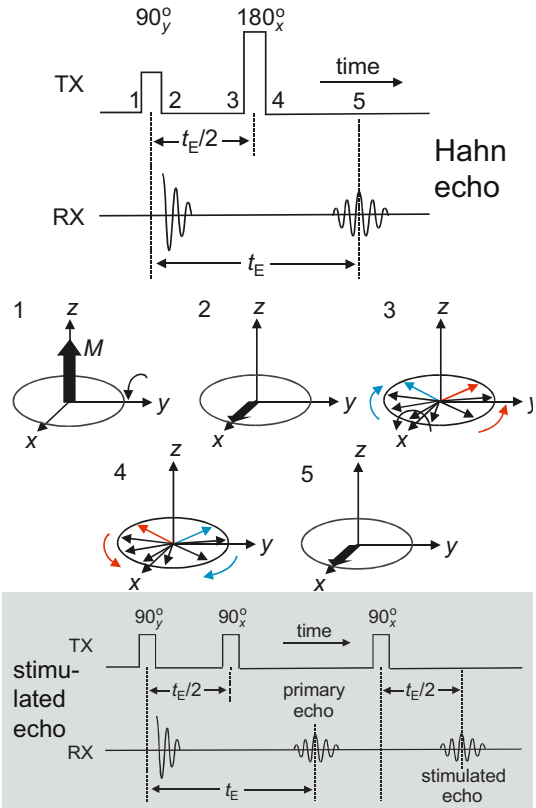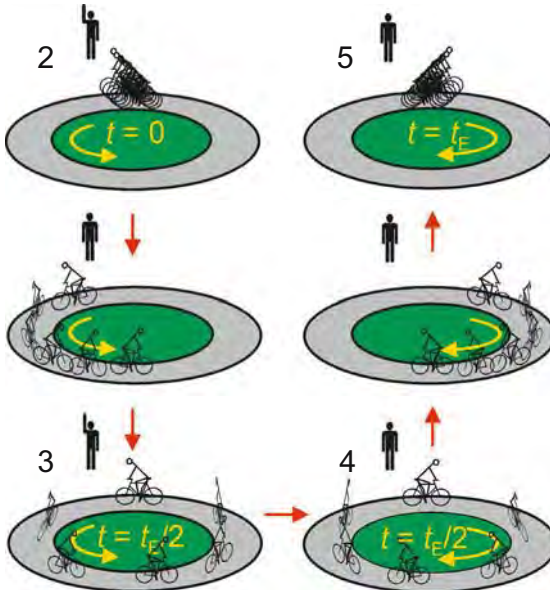
Multiple Echoes

- Transverse relaxation is often exponential with the time constant T_2
- In *inhomogeneous magnetic fields*, the FID decays faster with $T_2^* < T_2$
- The resonance signal in inhomogeneous magnetic fields is broad and small
- The envelope of the *FID* in homogeneous fields can be observed stroboscopically in inhomogeneous fields via the amplitude of many time shifted echoes
- Instead of many Hahn echoes with different echo times the echo envelope can be observed by a single train of multiple Hahn echoes
- The rf pulse scheme for excitation of multiple Hahn echoes is the *CPMG sequence* named after their discoverers Carr, Purcell, Meiboom, and Gill
- The repetition times of $5T_1$ for regeneration of longitudinal magnetization between generation of different Hahn echoes are eliminated
- $5T_1$ are needed to regain 99% of the thermodynamic equilibrium magnetization, because $\exp\{-5\} = 0.007$
- Besides the Hahn echo and the CPMG echo train there are many more echoes and multiple-echo schemes to partially recover signal loss caused by the influence of different nuclear spin interactions on the resonance frequencies
- In the *Hahn echo* maximum, inhomogeneities in the B_0 field and the spread in chemical shifts do not affect the NMR signal

Echoes and Inhomogeneous Magnetic Fields

$s(t)$ FID

amplitude

homogeneous magnetic field
$\exp\{-t/T_2\}$

$\exp\{-t/T_2^*\}$
inhomogeneous magnetic field

time

FT

$\mathrm{Re}\{S(\omega)\}$ spectrum

amplitude

frequency
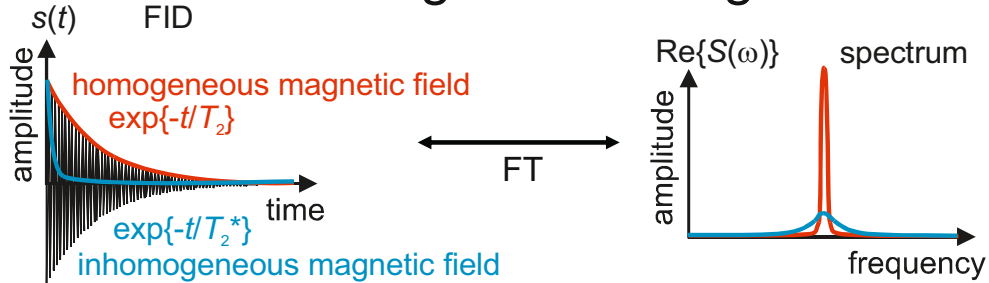
multiple Hahn echoes following Carr, Purcell, Meiboom, and Gill (CPMG):

90_y^o 180_x^o 180_x^o 180_x^o

time

transmitter
TX

$t_E/2$

receiver
RX

$\exp\{-t/T_2^*\}$ $\exp\{-t/T_2\}$

t_E t_E t_E
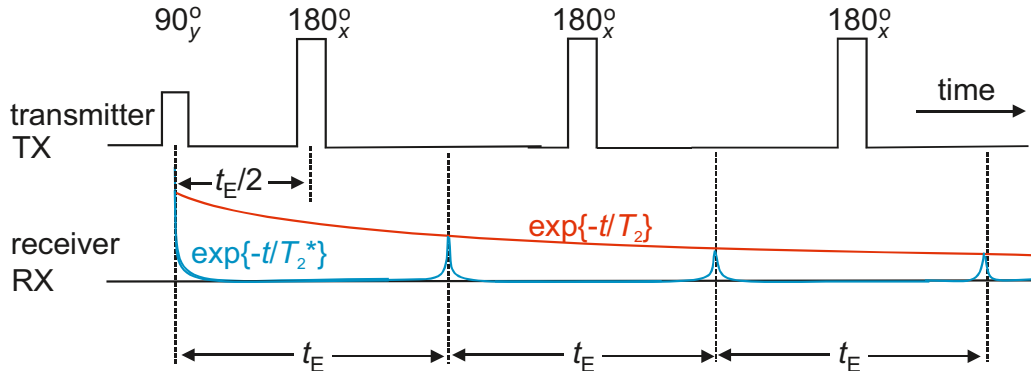
Determination of T_1

- *Longitudinal magnetization* cannot be directly observed
- Its momentary value can be interrogated via the amplitude of the FID following a 90° pulse
- There are two methods to measure the build-up of longitudinal magnetization: the recovery following saturation (*saturation recovery*) and the recovery following inversion of the magnetization (*inversion recovery*)
- For saturation, the spin system is irradiated with an aperiodic sequence of 90° pulses which destroys all magnetization
- Inversion of longitudinal magnetization is achieved by a 180° pulse following the establishment of equilibrium magnetization after a waiting time of $5T_1$
- After such preparation of the initial magnetization a variable evolution time t_0 follows for partial recovery of the *thermodynamic equilibrium* state
- Following the waiting time t_0, the momentary value of the longitudinal magnetization is converted into the amplitude of the *transverse magnetization* by a 90° pulse
- The transverse magnetization is measured and evaluated for different values of t_0
- In homogeneous spin systems, the longitudinal relaxation follows an exponential law

Pulse Sequences for Measurement of T_1

build-up of longitudinal
magnetization following
saturation
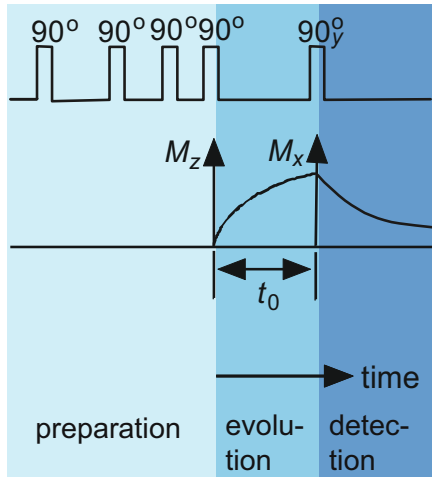
build-up of longitudinal
magnetization following
inversion
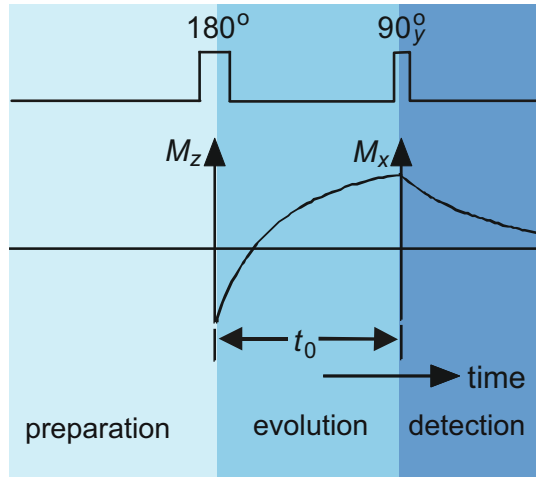
Measuring Methods

- *Pulsed excitation* and acquisition of an impulse response or an echo constitute the most successful class of methods to acquire NMR data
- In pulsed NMR, the signal measured can be conditioned by manipulating the initial magnetization in preceding preparation and evolution periods
- Pulsed NMR is uniquely suited for extension to *multi-dimensional NMR*
- With short pulses large spectral widths can be excited, and many frequency components can be simultaneously measured (*multiplex advantage*)
- When exciting the spins with *continuous waves* (CW), the frequency of the excitation wave is slowly scanned through the spectrum
- CW NMR is slow, because the frequency components of the spectrum are measured successively
- With *noise excitation* large bandwidths are excited and can be measured simultaneously (*stochastic NMR*)
- A division of the experiment into different periods such as preparation, evolution, and detection is not possible
- Such a partitioning of the time axis can be achieved during data processing by means of *cross-correlation* of excitation and response signals
- The *excitation power* in CW NMR and stochastic NMR is several orders of magnitude lower compared to that of pulsed NMR

CW-, Fourier, and Stochastic NMR

B. Blümich, *Prog. Nucl. Magn. Reson. Spectr. 19* (1987) 331 - 417
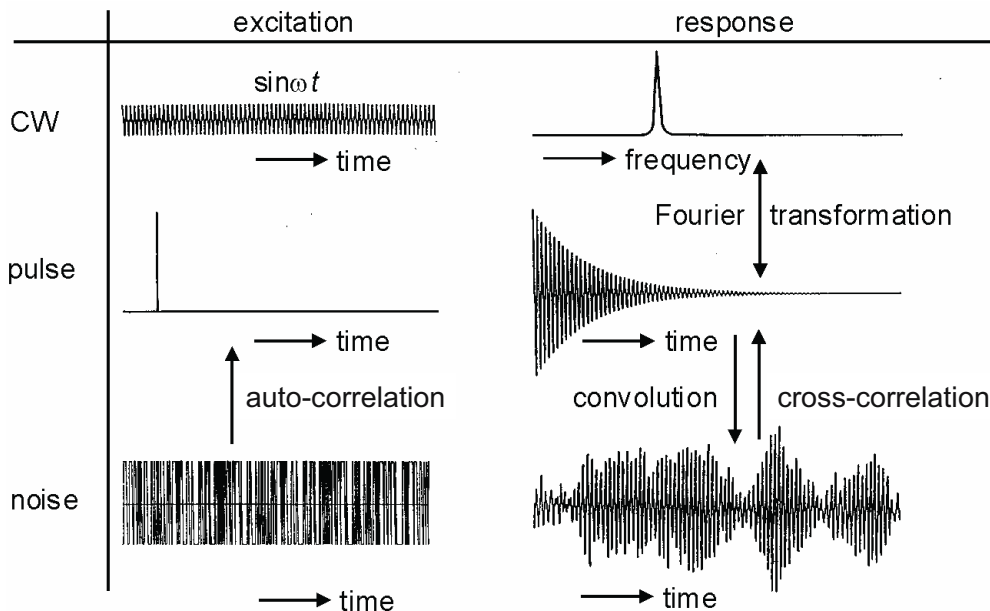
Spatial Resolution

- By exploring the proportionality of the NMR frequency ω and the applied magnetic field B, signals from different positions in the sample can be discriminated if the magnetic field changes with position
- For a linear change of B with position, the NMR frequency ω is directly proportional to position
- Then, the magnetic field B is characterized by a space-invariant *gradient G*
- In such a gradient field, the linear frequency axis of an NMR spectrum can be directly replaced by a linear space axis
- The signal amplitude is determined by the number of nuclear spins at a particular position along the gradient direction
- This number is obtained by summation over all nuclei in the other two space directions
- Due to the large number of nuclei, the sum is written as an integral
- This integral over the spatially resolved magnetization $M_z(x,y,z)$ is called a *projection*
- $M_z(x,y,z)$ is also referred to as *spin density*
- From a set of projections acquired for different gradient directions an image of the object can be reconstructed in analogy to X-ray tomography

Space Encoding
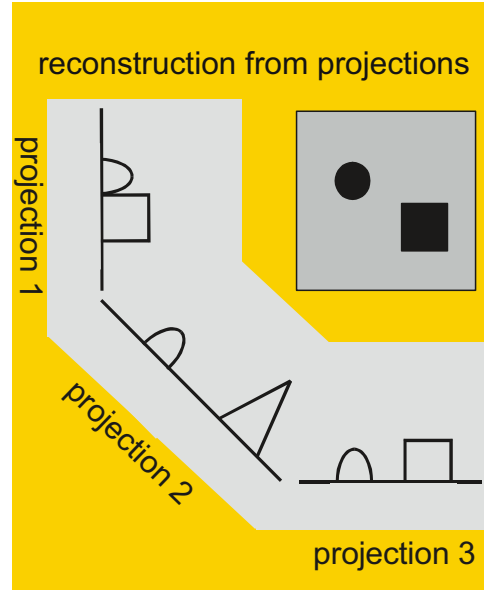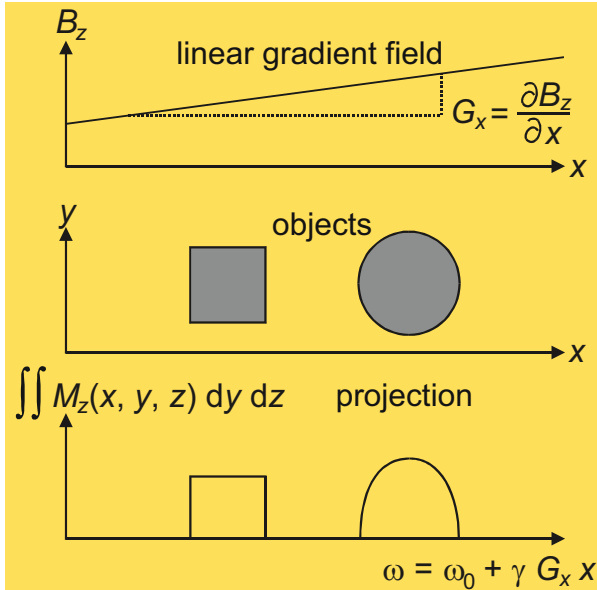
3. Spectroscopy

Dipole-dipole interaction
Anisotropy
Further spin interactions
Hidden information: multi-quantum NMR
Multi-dimensional NMR

Interactions Between Spins

- The magnetic *dipole moment* μ of a nucleus is proportional to its spin *I*
- The dipole moment and the spin are vectors with a magnitude and a direction
- In addition, the magnetic field *B* is a vector quantity
- The strength of an interaction is measured by the *interaction energy E*. This is a quantity without direction. It is, therefore, a scalar
- An interaction is formally described by the product of two quantities
- For the product of the spin vector *I* and its coupling partner to be a scalar, the coupling partner must be a vector *V*
- The coupling partners can be the magnetic fields $\boldsymbol{B}_0$ and $\boldsymbol{B}_1$, the magnetic field induced by the shielding electrons, and a further spin *I'*
- In the simplest case, the interaction is described by the scalar product of two vectors, for example, by $E \propto I^\dagger\ V$, where † denotes the transpose
- To describe orientation dependent interactions, a *coupling tensor* **P** must be introduced, so that $E = I^\dagger\ \mathbf{P}\ V$
- The significance of **P** is elaborated below by example of the *dipole-dipole interaction*
- Interactions of a spin with a magnetic field $\boldsymbol{B}_0$ or $\boldsymbol{B}_1$ are distinguished from interactions of one spin with another spin. In addition to the interactions between two spins, the latter formally includes the nuclear *quadrupole interaction*

General Formalism

$\mu = \gamma \, p = \gamma \, \hbar \, I$

μ: nuclear magnetic dipole moment
γ: gyro-magnetic ratio
p: vector of the angular momentum
$\hbar = h/2\pi$, h: Planck's constant
I: nuclear spin vector operator

$E = I \, P \, V$

E: interaction energy
I: nuclear spin vector
P: coupling tensor
V: coupling vector partner

$$E = \begin{bmatrix} I_x \\ I_y \\ I_z \end{bmatrix}^{\dagger} \begin{bmatrix} P_{xx} & P_{xy} & P_{xz} \\ P_{yx} & P_{yy} & P_{yz} \\ P_{zx} & P_{zy} & P_{zz} \end{bmatrix} \begin{bmatrix} V_x \\ V_y \\ V_z \end{bmatrix} \qquad \nu = \Delta E/h$$

Zeeman interaction	B_0	100 MHz
chemical shift	$-\sigma B_0$	10 kHz
rf excitation	B_1	100 kHz
quadrupole coupling	I	10 MHz
dipole-dipole interaction	I^r	50 kHz
indirect coupling	I^r	5 Hz

Two Interacting Dipoles

- Interactions of nuclear spins are interactions of elementary quantities for which the laws of quantum mechanics apply
- The classical treatment of nuclear interactions is at best an approximation which provides some intuitive insights
- The orientation dependence of the interaction energy can be understood by considering two classical bar magnets or compass needles
- For a parallel orientation, the magnets repel each other when they are side by side, and they attract each other when one is above the other
- With the magnetic dipole being the simplest distortion of an isotropic sphere, the *orientation dependence* of the *dipole-dipole interaction* can be described by the difference between a sphere and a simply deformed sphere, i. e. a rotational ellipsoid
- This difference is quantified by the *second Legendre polynomial* $P_2(\cos\beta) = (3 \cos^2\beta -1)/2$
- Deformations of lower symmetry are described by the *spherical harmonic functions*, which also describe the electron orbitals of the hydrogen atom
- The angle β denotes the angle between the magnetic field vector $\boldsymbol{B}_0$ and the vector $\boldsymbol{r}$ which connects the two point dipoles

Dipole-Dipole Interaction

$E \propto 1/r^3 \, (3\cos^2\beta - 1)/2$
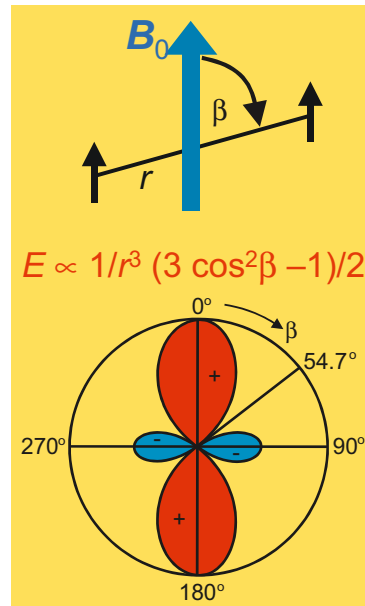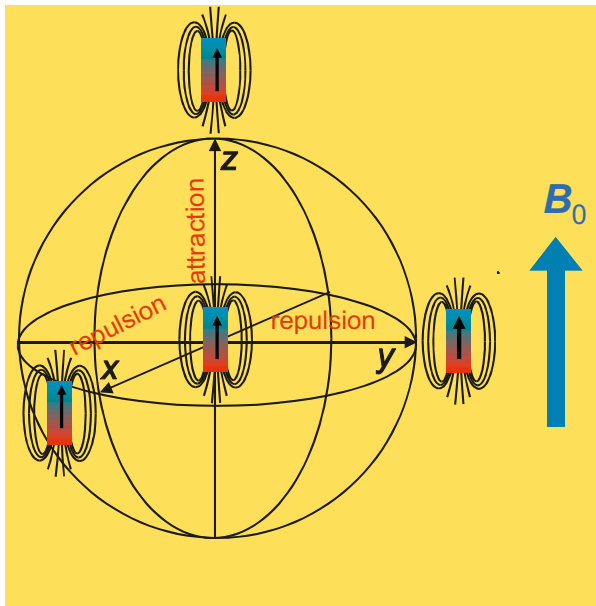
Second Legendre Polynomial

- The *second Legendre polynomial P_2* describes the geometrically most simple deformation of a circle
- It quantifies the quadratic deviation of a circle from an *ellipse*, where both figures are generated by a thread of length $2r$ corresponding to the diameter of the circle and the long axis of the ellipse
- The difference between the circle and the ellipse is only in the direction of the small axis of the ellipse
- The average of this difference is subtracted to obtain a function with a mean value of zero
- The resultant function is normalized to 1 for the angle 0°
- The result is proportional to the second Legendre polynomial $P_2 = (3\cos^2\beta - 1)/2$
- The *principal value* is obtained for the angle 0°. Its value amounts to 2/3 of the *anisotropy parameter*
- The values of P_2 for 0° and 90° can be defined as the half axes $P_{anisoZZ}$ and $P_{anisoXX} = P_{anisoYY}$ of a *rotational ellipsoid*
- Without transverse symmetry $P_{anisoXX} \neq P_{anisoYY}$, and the *asymmetry parameter* is defined as $\eta = (P_{anisoYY} - P_{anisoXX})/\delta$

Deformation of a Circle
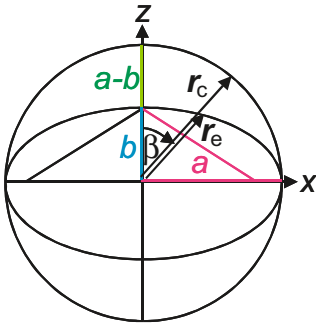
circle: $\mathbf{r_c} = \begin{pmatrix} a\sin\beta \\ 0 \\ a\cos\beta \end{pmatrix}$

ellipse: $\mathbf{r_e} = \begin{pmatrix} a\sin\beta \\ 0 \\ b\cos\beta \end{pmatrix}$

deviation from a circle in z direction:

$$(\mathbf{r_c} - \mathbf{r_e})^2 = (a - b)^2 \cos^2\beta$$

subtraction of the mean along z:

$$P_{aniso} = \frac{1}{3}(a - b)^2 (3\cos^2\beta - 1)$$

normalization of the angle-dependent part along z:

$$P_{aniso} = \frac{2}{3}(a - b)^2 \frac{1}{2}(3\cos^2\beta - 1)$$

$\beta = 0°$: principal value $\delta = (2/3)(a - b)^2$

anisotropy parameter $\Delta = (a - b)^2$

axially symmetric deformation of a sphere
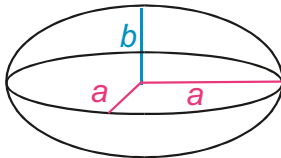
deformation ellipsoid

$$P_{anisoZZ} = \frac{2}{3}(a - b)^2$$
$$P_{anisoXX} =$$
$$P_{anisoYY} = \frac{-1}{3}(a - b)^2$$

Anisotropy of the Interaction

- The ellipsoid defined by $P_{anisoXX}$, $P_{anisoYY}$, and $P_{anisoZZ}$ describes the *anisotropy of the spin interactions* in the limit of coupling energies that are weak compared to the spin interaction with the polarization field $\boldsymbol{B}_0$ (Zeeman interaction)
- For the *dipole-dipole interaction* $P_{anisoXX} = P_{anisoYY}$, for the *chemical (magnetic) shielding*, and the *quadrupole interaction* $P_{anisoXX} \neq P_{anisoYY}$
- The interaction of a spin with the magnetic fields $\boldsymbol{B}_0$ und $\boldsymbol{B}_1$ is isotropic, i. e. $P_{anisoXX} = P_{anisoYY} = P_{anisoZZ} = 0$.
- For *anisotropic couplings* the orientation of the interaction ellipsoid within the molecule is determined by the chemical structure
- In case of the dipole-dipole interaction, the long axis of the interaction ellipsoid is aligned along the direction of the internuclear vector
- Also the chemical shielding is anisotropic. Here, the orientation of the interaction ellipsoid can be obtained by means of quantum-mechanical calculations of the electron orbitals
- For a description of the interaction ellipsoid, three values are sufficient within the coordinate frame of the ellipsoid. These are the *eigenvalues*
- In an arbitrary coordinate frame, the LCF for example, the orientation of the interaction ellipsoid has to be specified as well. One needs 6 values

Orientation Dependence

magnetic shielding

dipole-dipole interaction

$\sigma B_0 < 0$

$\sigma B_0 > 0$

$\sigma B_0 > 0$

$\boldsymbol{B}_0$

$\sigma B_0 = 0$

$\boldsymbol{B}_0$

β

coupling tensor
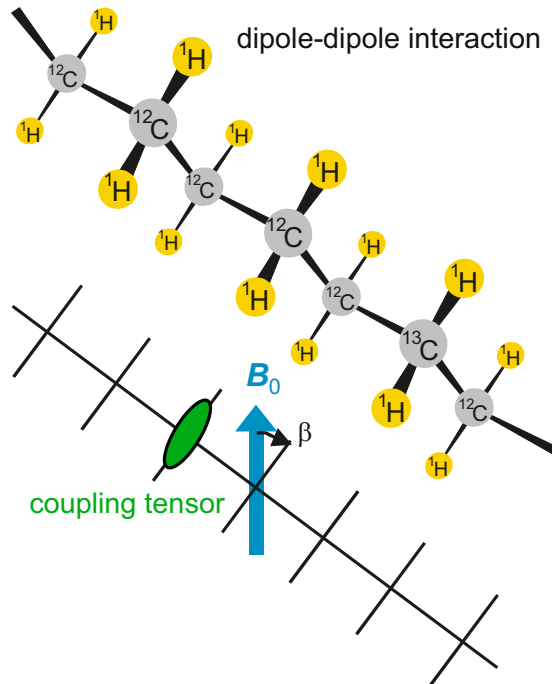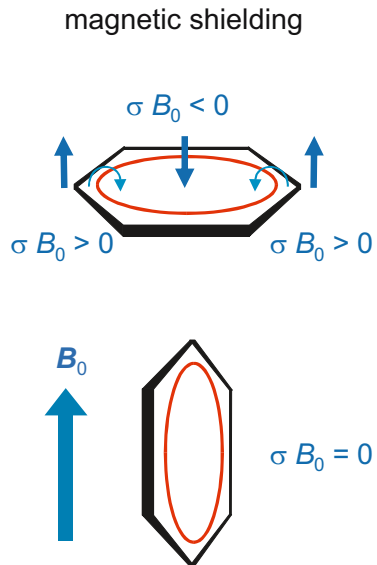
Anisotropic and Asymmetric Couplings

- The *anisotropy* described by the *second Legendre polynomial* $P_2 = (3 \cos^2\beta - 1)/2$ is represented by a rotational ellipsoid with the half axis $P_{anisoZZ}$ for $\beta = 0°$ and the half axes $P_{anisoXX} = P_{anisoYY}$ for $\beta = 90°$
- For an *asymmetry* in the transverse plane $P_{anisoXX} \neq P_{anisoYY}$
- To describe this asymmetry in spherical coordinates, another angle α needs to be introduced
- The ellipsoid which, in this case, describes the interaction, has the shape of an American football pressed flat, $P_{ansio} = \delta[3 \cos^2\beta - 1 - \eta \sin^2\beta \cos(2\alpha)]/2$
- It possesses the half axes $P_{anisoZZ} = \delta$, $P_{anisoXX} = -\delta(1 + \eta)/2$, and $P_{anisoYY} = -\delta(1 - \eta)/2$
- Examples for *asymmetric spin couplings* with asymmetry are the *chemical shielding* and the electric *quadrupole interaction*
- In liquids, the angles α and β change rapidly and isotropically in a random fashion. In the time average the anisotropy of the interaction vanishes
- For *symmetric interactions* like the *dipole-dipole interaction* $\eta = 0$, and the interaction vanishes at the *magic angle* $\beta_m = \arccos\{1/3\} = 54.7°$

Anisotropy and Asymmetry

symmetric anisotropy:
$P_{aniso} = \delta(3\cos^2\beta-1)/2$

$P_{anisoZZ} = \delta$

$P_{anisoXX} = -\delta/2$ $P_{anisoYY} = -\delta/2$

asymmetric anisotropy:
$P_{aniso} = \delta\,[3\cos^2\beta - 1 - \eta\,\sin^2\beta\,\cos(2\alpha)]/2$
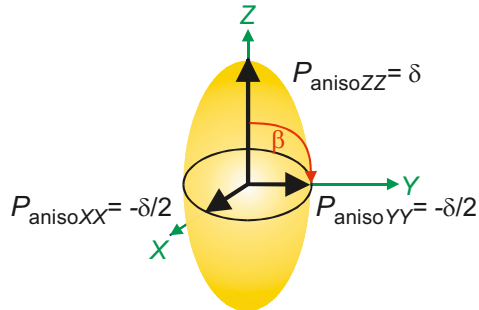
$P_{anisoZZ} = \delta$

$P_{anisoXX} = -\delta(1 + \eta)/2$ $P_{anisoYY} = -\delta(1 - \eta)/2$
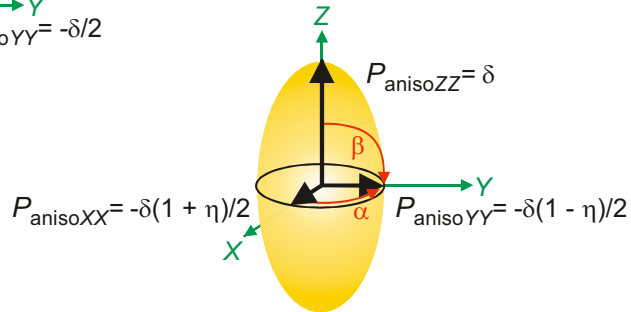
Vectors, Matrices, and Tensors

- The half axes of the *interaction ellipsoid* define orthogonal vectors in a Cartesian coordinate frame, which is called the *principal axes frame*
- These three vectors are grouped into a 3×3 matrix
- A matrix with physical significance is called a *tensor*
- In the principal axes frame, the interaction tensor is diagonal
- The numbers on the diagonal of this tensor are called *eigenvalues*
- In a different coordinate frame, the interaction tensor appears rotated
- Then, the interaction tensor is no longer diagonal
- The tensor can be returned to diagonal form by a *rotation*
- A vector r is rotated by a *rotation matrix* $\mathbf{R}(\gamma)$ according to $r' = \mathbf{R}(\gamma)\, r$
- A matrix or a tensor $\mathbf{P}_{aniso}$ is rotated according to $\mathbf{P}_{aniso}' = \mathbf{R}(\gamma)\, \mathbf{P}_{aniso}\, \mathbf{R}^{-1}(\gamma)$, because, for example, $r'' = \mathbf{P}_{aniso}\, r$: $r' = \mathbf{R}\, r'' = \mathbf{R}\, \mathbf{P}_{aniso}\, r = \mathbf{R}\, \mathbf{P}_{aniso}\, \mathbf{R}^{-1}\, \mathbf{R}\, r$, where $\mathbf{P}_{aniso}' = \mathbf{R}\, \mathbf{P}_{aniso}\, \mathbf{R}^{-1}$ is valid in the rotated frame
- A rotation matrix is specified by the rotation axis and the rotation angle. For example, $\mathbf{R}_z(\gamma)$ describes a rotation around the z axis by the angle γ
- An arbitrary rotation $\mathbf{R}$ of an arbitrary object is described by rotations around orthogonal axes through the three *Euler angles* α, β, γ
- One successively performs the rotations $\mathbf{R}_z(\alpha)$, $\mathbf{R}_x(\beta)$, $\mathbf{R}_z(\gamma)$
- The row vectors of the rotation matrix which diagonalizes the matrix $\mathbf{P}_{aniso}$ are called *eigenvectors* of the matrix $\mathbf{P}_{aniso}$
- The eigenvectors are the unit vectors in the directions of the principal axes of the interaction ellipsoid

Rotation of Tensors

laboratory coordinate frame
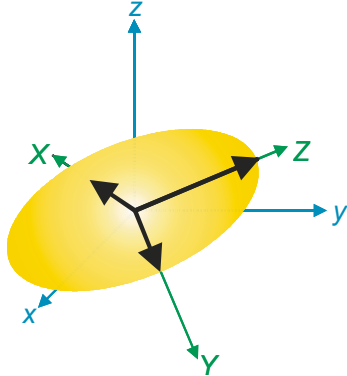
principal axes frame
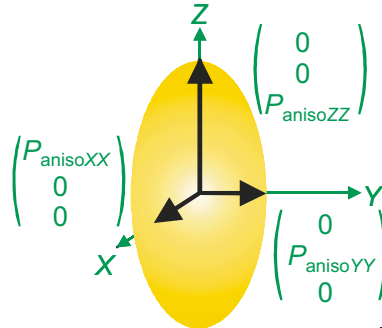
$$\begin{pmatrix} 0 \\ 0 \\ P_{anisoZZ} \end{pmatrix}$$

$$\begin{pmatrix} P_{anisoXX} \\ 0 \\ 0 \end{pmatrix}$$

$$\begin{pmatrix} 0 \\ P_{anisoYY} \\ 0 \end{pmatrix}$$

$$\begin{bmatrix} P_{anisoxx} & P_{anisoxy} & P_{anisoxz} \\ P_{anisoyx} & P_{anisoyy} & P_{anisoyz} \\ P_{anisozx} & P_{anisozy} & P_{anisozz} \end{bmatrix} = \mathbf{R}(\alpha,\beta,\gamma) \begin{bmatrix} P_{anisoXX} & 0 & 0 \\ 0 & P_{anisoYY} & 0 \\ 0 & 0 & P_{anisoZZ} \end{bmatrix} \mathbf{R}^{-1}(\alpha,\beta,\gamma)$$

interaction tensor $\mathbf{P}_{aniso}$ interaction tensor $\mathbf{P}_{aniso}$

right-hand rule

rotation matrix $\mathbf{R}(\alpha,\beta,\gamma)$. Example: $\mathbf{R}_z(\gamma) = \begin{bmatrix} \cos\gamma & -\sin\gamma & 0 \\ \sin\gamma & \cos\gamma & 0 \\ 0 & 0 & 1 \end{bmatrix}$
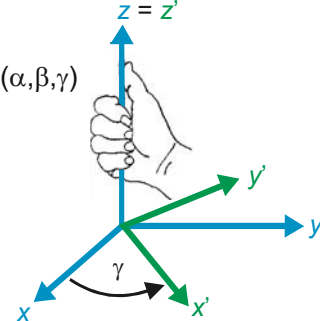
Interaction Tensors

- In addition to the orientation dependent part of a *spin interaction*, there can be an orientation independent part. Examples are the *indirect spin-spin coupling* and the *chemical shielding*
- The interaction tensor is then the sum of the isotropic part $\mathbf{P}_{iso}$ and the anisotropic part $\mathbf{P}_{aniso}$
- The isotropic part of the interaction tensor $\mathbf{P} = \mathbf{P}_{iso} + \mathbf{P}_{aniso}$ is given by the *trace of the tensor*, independent of the coordinate system
- For symmetric interactions, which are weak compared to the *Zeeman interaction*, the anisotropic part is described by the *second Legendre polynomial*
- It is the convention in NMR to measure interaction energies in frequency units according to $E = h\nu = \hbar\omega$
- Usually, several spin interactions act simultaneously and the respective coupling energies are added
- Many NMR methods have been developed with the goal to isolate the effects of one interaction from all the other interactions and to correlate the frequency shifts from different interactions with each other

Spin Interactions

	coupling partner	isotropic part	anisotropy parameter Δ	asymmetry parameter η
Zeeman interaction	$\mathbf{B}_0$	ω_0	0	0
chemical shielding	$\mathbf{B}_0$	$-\gamma\sigma\,B_0$	✓	✓
rf excitation	$\mathbf{B}_1$	ω_1	0	0
quadrupole interaction	$\mathbf{I}$	0	✓	✓
dipole-dipole interaction	$\mathbf{I}^r$	0	✓	0
indirect coupling	$\mathbf{I}^r$	J	✓	✓

general interaction tensor: $\mathbf{P} = \mathbf{P}_{iso} + \mathbf{P}_{aniso}$

principal axes frame:

$$\mathbf{P} = P_{iso}\begin{bmatrix}1 & 0 & 0 \\ 0 & 1 & 0 \\ 0 & 0 & 1\end{bmatrix} + \begin{bmatrix}P_{anisoXX} & 0 & 0 \\ 0 & P_{anisoYY} & 0 \\ 0 & 0 & P_{anisoZZ}\end{bmatrix}$$

laboratory coordinate frame:

$$\mathbf{P} = P_{iso}\begin{bmatrix}1 & 0 & 0 \\ 0 & 1 & 0 \\ 0 & 0 & 1\end{bmatrix} + \begin{bmatrix}P_{anisoxx} & P_{anisoxy} & P_{anisoxz} \\ P_{anisoyx} & P_{anisoyy} & P_{anisoyz} \\ P_{anisozx} & P_{anisozy} & P_{anisozz}\end{bmatrix}$$

rules:

$P_{anisoXX} + P_{anisoYY} + P_{anisoZZ} = \mathrm{Tr}\{\mathbf{P}_{aniso}\} = 0$

$\mathrm{Tr}\{\mathbf{P}\} = 3\,P_{iso}$

anisotropy: $\Delta = P_{ZZ} - (P_{XX} + P_{YY})/2$

asymmetry: $\eta = (P_{YY} - P_{XX})/(P_{ZZ} - P_{iso})$

Interaction Energies

- The *interaction energies* of coupling nuclei are calculated using *quantum mechanics*
- In a first approximation, the interaction energy is proportional to the total spin of the coupled spins
- Depending on the *magnetic quantum numbers* of the interacting partners, a different total spin is obtained and with it a different interaction energy
- The number of nearly equal interaction energies is obtained by combinatorial arguments
- According to quantum mechanics, only those transitions can directly be observed, for which the magnetic quantum number m changes by ± 1
- They correspond to *transverse magnetization* and are called *single-quantum coherences*
- There, one of the interacting spins changes its orientation in the magnetic field by absorption or stimulated emission of one rf quantum or photon
- For two coupling spins ½, the observable interaction energy differences $\Delta E = \hbar \omega$ are proportional to $P_{iso} \pm \delta [3 \cos^2\beta - 1 - \eta \sin^2\beta \cos(2\alpha)]/2$ and lead to *orientation-dependent splittings*
- The absorption or stimulated emission of more than one rf quantum cannot directly be observed
- *Multi-quantum coherences* (0Q, 2Q) can indirectly be observed by *multi-dimensional NMR*

Energy Levels and Transitions

energy level diagram
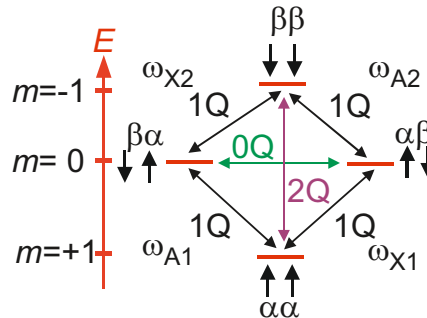
NMR spectrum for
two coupling spins at
resonance frequencies
ω_A and ω_X and
orientation-dependent
splittings
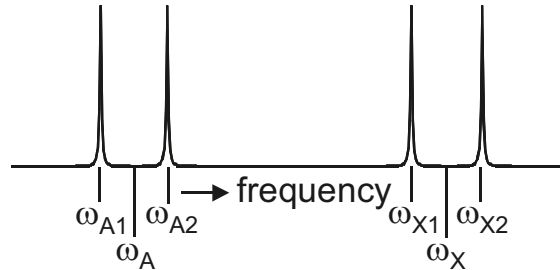
Indirect Spin-Spin Coupling

- Nuclear spins can interact with each other in two ways: one is the *dipole-dipole interaction* through space, the other is the indirect or *J coupling*
- The *indirect coupling* is mediated by the electrons of the chemical bonds between the coupling spins
- The nuclear spin polarizes the magnetic field of the electron orbits. This distortion is seen by the coupling partner spin
- The direct dipole-dipole interaction is described by a traceless coupling tensor **D**; therefore, the coupling vanishes in the fast motion limit
- The indirect spin-spin coupling is described by a coupling tensor **J** with trace *J*; therefore, the trace is preserved in the fast motion limit, and the *J* coupling leads to a *multiplet splitting* of the resonance of the coupling spins
- The sign of the coupling constant *J* alternates with the number of chemical bonds between the coupling spins
- The *J* multiplets bear important information for structural analysis
- The multiplet structure is determined by the number of different combinations of orientations of the coupling spins
- Hetero-nuclear *J* couplings are often exploited for *hetero-nuclear polarization transfer* and chemical *editing of spectra* from molecules in solution
- In contrast to the chemical shift dispersion, the splitting from direct and indirect spin-spin couplings is not removed in the *Hahn echo* maximum

Multiplet Structure in ^{1}H Spectra

3-bond *J* coupling of protons

binding electrons

^{1}H NMR spectrum of ethyl alcohol CH_3-CH_2-OH

OH CH$_2$ CH$_3$

δ [ppm]

6 5 4 3 2 1 0
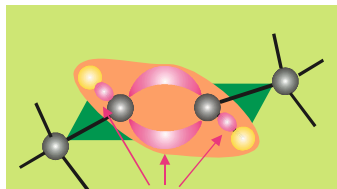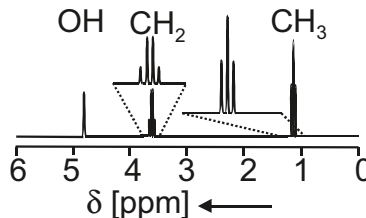
polarizations of spins

CH$_2$ group

↑↑ ↑↓ ↓↓
↓↑

signal of coupling partner
splits into a triplet with
rel. amplitudes 1:2:1

CH$_3$ group

↑↑↑ ↑↑↓ ↑↓↓ ↓↓↓
↑↓↑ ↓↑↓
↓↑↑ ↓↓↑

signal of coupling partner
splits into a quartet with
rel. amplitudes 1:3:3:1

Quantum Mechanics

- The energies E and the *transition frequencies* ω of interacting nuclei are calculated using *quantum mechanics* and exploring the relation $\Delta E = \hbar\,\omega$
- Depending on the orientation in the magnetic field, a spin is found in a state of different energy E
- A spin ½ can be oriented parallel ($\uparrow$, state α) or antiparallel ($\downarrow$, state β) to the polarization field B_0
- Two coupled spins ½ can assume the four states $\uparrow\uparrow$, $\downarrow\uparrow$, $\uparrow\downarrow$, $\downarrow\downarrow$
- *States of spins* are described in quantum mechanics by *wave functions*
- The wave functions are the *eigenfunctions* of operators similar to the *eigenvectors* associated with matrices
- The interaction energies are the *eigenvalues* of the *Hamilton operator*
- Quantum mechanical operators can be expressed in matrix form
- The *Schrödinger equation* describes the energy balance of a quantum mechanical system by means of the Hamilton operator and wave functions
- The wave function of an ensemble of coupled spins is often expressed as a linear combination of the eigenfunctions of a suitable Hamilton operator
- Accessible by measurement are usually only the ensemble averages of the bilinear products of the complex expansion coefficients
- These averages are written in matrix form and constitute the so-called *density matrix*
- In the eigenbasis of the Hamilton operator the elements of the density matrix are of the general form $A_{kl}\exp\{-(1/T_{kl} - \mathrm{i}\,\omega_{kl})t\}$

Density Matrix for Two Spins ½

wave function: $\Psi = a_1(\uparrow\uparrow) + a_2(\downarrow\uparrow) + a_3(\uparrow\downarrow) + a_4(\downarrow\downarrow)$
$\qquad\qquad = a_1(\alpha\alpha) + a_2(\beta\alpha) + a_3(\alpha\beta) + a_4(\beta\beta)$
$\qquad\qquad = a_1\psi_1 \;+\; a_2\psi_2 \;+\; a_3\psi_3 \;+\; a_4\psi_4$

density matrix:

$$
\rho =
\begin{array}{c|cccc}
 & \alpha\alpha & \beta\alpha & \alpha\beta & \beta\beta \\
\hline
\alpha\alpha & \langle a_1 a_1{}^*\rangle & \langle a_1 a_2{}^*\rangle & \langle a_1 a_3{}^*\rangle & \langle a_1 a_4{}^*\rangle \\
\beta\alpha & \langle a_2 a_1{}^*\rangle & \langle a_2 a_2{}^*\rangle & \langle a_2 a_3{}^*\rangle & \langle a_2 a_4{}^*\rangle \\
\alpha\beta & \langle a_3 a_1{}^*\rangle & \langle a_3 a_2{}^*\rangle & \langle a_3 a_3{}^*\rangle & \langle a_3 a_4{}^*\rangle \\
\beta\beta & \langle a_4 a_1{}^*\rangle & \langle a_4 a_2{}^*\rangle & \langle a_4 a_3{}^*\rangle & \langle a_4 a_4{}^*\rangle
\end{array}
\;\hat{=}\;
\begin{pmatrix}
P & 1Q & 1Q & 2Q \\
1Q & P & 0Q & 1Q \\
1Q & 0Q & P & 1Q \\
2Q & 1Q & 1Q & P
\end{pmatrix}
$$

P: populations, $\omega_{ij} \propto \Delta m = 0$
1Q: single-quantum coherences, $\omega_{kl} \propto |\Delta m| = 1$, directly observable
0Q: zero-quantum coherences, $\omega_{kl} \approx 0 = |\Delta m|$, indirectly observable
2Q: double-quantum coherences, $\omega_{kl} \propto |\Delta m| = 2$, indirectly observable

description of NMR with the density matrix $\rho(t) = \mathbf{U}(t - t_0)\, \rho(t_0)\, \mathbf{U}^{-1}(t - t_0)$,
the evolution operator $\mathbf{U}(t - t_0) = \exp\{i\mathbf{H}(t-t_0)/\hbar\}$, and the Hamilton operator $\mathbf{H}$

Wideline Spectroscopy

- The *NMR frequency* depends on the orientation of the *interaction tensor* ellipsoid in the laboratory frame
- Consequently, also the separation of the lines or the *line splitting* depends on the *molecular orientation*
- For vanishing isotropy and vanishing asymmetry (*dipole-dipole interaction*) $P_{iso} = 0$ and $\eta = 0$. The NMR frequency is then determined by the *second Legendre polynomial*, $\Omega_{\pm} = \omega_{\pm} - \omega_{L} = \pm\delta\,(3\cos^2\beta - 1)/2$
- In this case, $\Omega_{\pm} = 0$ at the *magic angle* $\beta = \arccos(3^{-1/2}) = 54.7°$, and only one line is observed at one and the same position $\Omega_{\pm} = 0$ for both nuclear spins A and X
- At other angles, one separate line is observed for each spin with a frequency separation $\Delta\Omega = \omega_{+} - \omega_{-} = \delta\,(3\cos^2\beta - 1)$
- In *powders* with a statistical distribution of the angles, one obtains the so-called *wideline spectrum*
- For an *isotropic distribution* with $P_{iso} = 0$, $\eta = 0$, and $I = 1$, the wideline spectrum is called *powder spectrum* or *Pake spectrum*
- It is often observed for deuterons and pairs of coupled spins 1/2
- The Pake spectrum consists of a sum of two wide lines with mirror symmetry, which are centered at the isotropic chemical shift

Pake Spectrum

$P_{iso} = 0, \quad \eta = 0$:

$\Omega_{+} = +\delta\,[3\cos^2\beta - 1]/2$

$\Omega_{-} = -\delta\,[3\cos^2\beta - 1]/2$

$-\delta \quad -\delta/2 \quad 0 \quad +\delta/2 \quad +\delta$

Ω

$\beta = 90°$ \qquad $\beta = 0°$

$-\delta \quad -\delta/2 \quad 0 \quad +\delta/2 \quad +\delta$

Ω
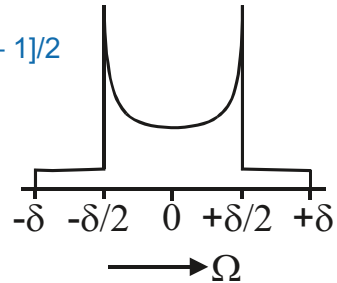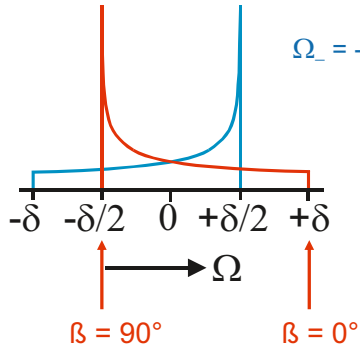
Molecular Order and Dynamics

- The position of a line or the splitting of lines in orientation dependent spectra can be used to measure *molecular orientations*
- The frequency axis belonging to each of the overlapping wings of a *Pake spectrum* relates to the orientation angle through the *second Legendre polynomial $P_2(\cos\beta)$*
- The angle β is the angle enclosed by the principal axis Z of the interaction tensor ellipsoid and the magnetic field $\boldsymbol{B}_0$
- For *partially oriented solids*, information about the distribution of orientations of the interaction tensors is obtained from the lineshape of the powder spectrum
- The lineshape depends on the orientation angle β_0 of the sample in the field $\boldsymbol{B}_0$
- In case of molecular motions with correlation times on the time scale of the NMR experiment, the lineshape is altered in a specific way depending on the geometry of the motion
- *Wideline NMR* is used for analysis of timescale and geometry of *slow molecular motion* in the solid state
- Particularly successful is *deuteron wideline NMR spectroscopy* for investigations of the *molecular dynamics* of chemical groups labeled site selectively by ^2H

Wideline-NMR Spectra

^{13}C-NMR spectra of an oriented photo-LC polymer

30 %

H_2C
  |
$HC-C-O-(CH_2)_6-O-$⬡$-N=N-$⬡$-CN$

70%

H_2C
  |
$HC-C-O-(CH_2)_6-O-$⬡$-C-O-$⬡$-^{13}CN$

before irradiation with light

$\beta = 90°$

$\beta = 0°$

after irradiation with light

$\beta_o = 0°$

$\beta = 90°$

$\beta_o = 30°$

$\beta_o = 90°$ $\beta = 0°$

ppm 200 0 -200

ppm 200 0 -200
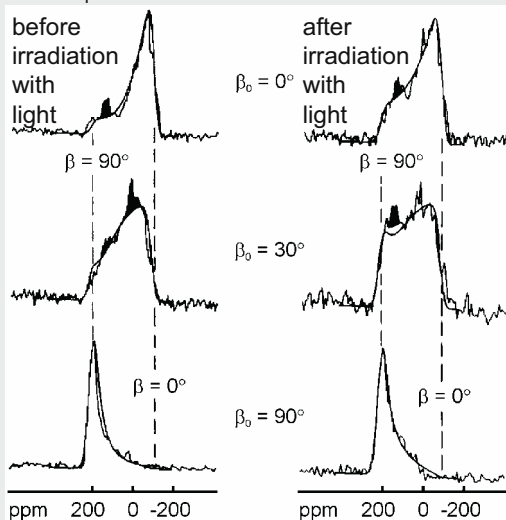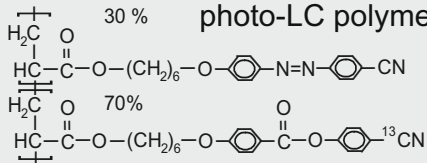
simulation of dynamic ^{2}H spectra

$\tau_c = 10^{-5}$ s $\tau_c = 10^{-6}$ s $\tau_c = 5\times10^{-8}$ s

180° jump of a p-phenylene ring

triple jump of a methyl group
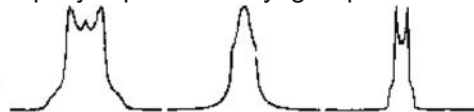
isotropic rotational diffusion
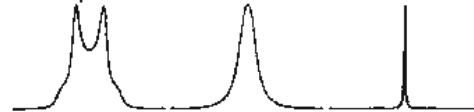
100 kHz

K. Müller, K.-H. Wassmer, G. Kothe, **Adv. Polym. Sci. 17** (1990) 1

Echoes in Solid Samples

- *Wideline-NMR spectra* are favorably acquired by measuring their Fourier transforms in the time domain in terms of *echoes*
- Because the linewidth is broad, the echo signal is narrow
- The time lag between the last rf pulse and the echo serves to overcome the receiver *deadtime* (ca. 5 μs)
- For a system with total spin $I = 1$ (^{2}H or two dipolar coupled spins $\frac{1}{2}$), maximum echo amplitudes are obtained for the *solid echo* and for the *alignment echo*
- These *solid-state echoes* correspond to the *Hahn echo* and the *stimulated echo* of non-interacting spins $\frac{1}{2}$
- The flip angles of the refocusing pulses are reduced to half the values in their liquid-state counterparts, and the pulses are shifted by 90° in their phase with respect to the first rf pulse
- For spin systems with a total spin $I > 1/2$, the *magic echo* leads to maximum echo amplitude
- One example is the dipolar interaction between the three protons of a methyl group
- In the echo maximum, the precession phases of the magnetization components assume their initial values as a result of their interaction during the echo time
- It is said, that the interaction is refocused in the echo maximum

Pulse Sequences for Echoes from Solid-State Samples

90°_y 90°_x solid echo

t_1 $t_2 = t_1$ t_2
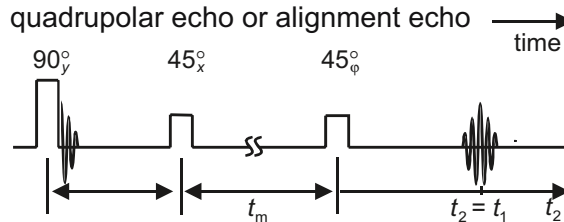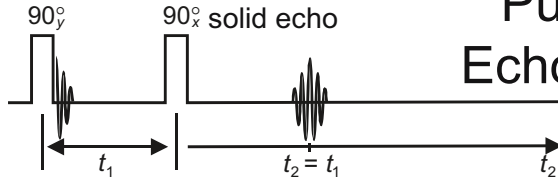
in the echo maxima the dipole-dipole interaction between two spins ½ is refocused

quadrupolar echo or alignment echo → time

90°_y 45°_x 45°_φ

t_m $t_2 = t_1$ t_2

magic echo

90°_y 90°_x 90°_{-x}

x $-x$

0 τ 3τ 5τ 6τ t
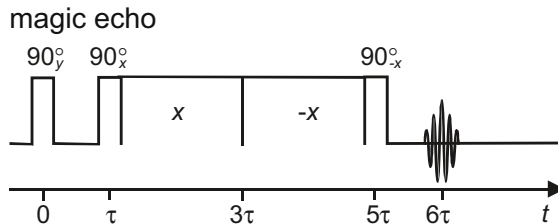
in the echo maximum the dipole-dipole-interaction between several spins ½ is refocused

Sample Rotation at the Magic Angle

- The *angular dependence of the NMR frequency* resulting from an *anisotropic interaction* is given by $\omega_{aniso} = \delta\,[3\cos^2\beta - 1 - \eta\,\sin^2\beta\,\cos(2\alpha)]/2$
- *Sample rotation* in the laboratory at an axis inclined about the angle θ with respect to $\boldsymbol{B}_0$ modulates ω_{aniso} by $P_2(\cos\theta) = (3\cos^2\theta - 1)/2$
- The angular dependent part can be eliminated on the time average by rotating the interaction tensors rapidly around the *magic angle* θ_m = arcos$\{1/3^{1/2}\}$ = 54.7° where $P_2(\cos\theta_m) = 0$
- 'Rapid' means that the angular rotation speed $\omega_R = 2\pi\,\nu_R$ is larger than the principal value δ of the interaction tensor
- For slower rotation speeds, *spinning sidebands* are observed in the NMR spectrum. These are separated from the isotropic resonance frequency by multiples $n\,\omega_R$ of the spinning speed
- In the limit of vanishing spinning speed, the envelope of the sideband spectrum assumes the shape of the *powder spectrum*
- Rotation of the sample at the magic angle is called *magic angle spinning* (*MAS*)
- One of the most important applications of MAS is the measurement of high-resolution ^{13}C-NMR spectra of solid samples
- In such samples, the *hetero-nuclear dipole-dipole-interaction* between ^{13}C and ^{1}H must be eliminated as well

MAS NMR (Magic Angle Spinning)
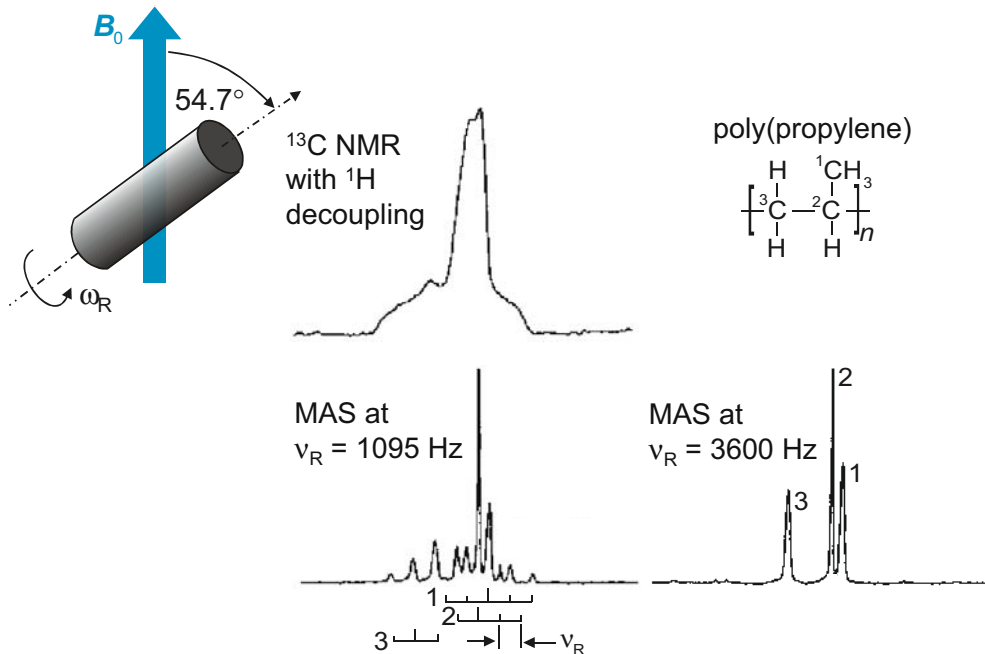
Cross-Polarization, MAS, and Hetero-Nuclear Dipolar Decoupling

- The measurement of *high-resolution solid-state NMR* spectra of rare nuclei such as ^{13}C and ^{29}Si requires *MAS* for elimination of the *anisotropy of the chemical shift* as well as the *hetero-nuclear dipolar decoupling* of the protons
- *Dipolar decoupling* (DD) is usually achieved by irradiating ^{1}H with a strong B_1 field while observing the rare nucleus (^{13}C)
- Due to the fact that ^{13}C arises with a natural abundance of only 1%, the nuclear magnetization of ^{13}C is much lower than that of ^{1}H
- Furthermore, the T_1 relaxation time of ^{13}C is often longer than that of ^{1}H
- Both disadvantages can be alleviated by transfer of magnetization from ^{1}H to ^{13}C with a method called *cross polarization*
- To this end, one simultaneously irradiates resonant B_1 fields to ^{1}H and ^{13}C with an amplitude critically chosen, so that the ^{1}H spins as well as the ^{13}C spins rotate around their individual B_1 fields with the same frequency
- This adjustment fulfills the *Hartmann-Hahn condition*: $\gamma_H \omega_{1H} = \gamma_C \omega_{1C}$
- Then, along the *z* axis the magnetization of each nuclear species oscillates with the same frequency
- By this resonance effect, transverse ^{1}H magnetization can be converted directly into transverse ^{13}C magnetization

CPMAS
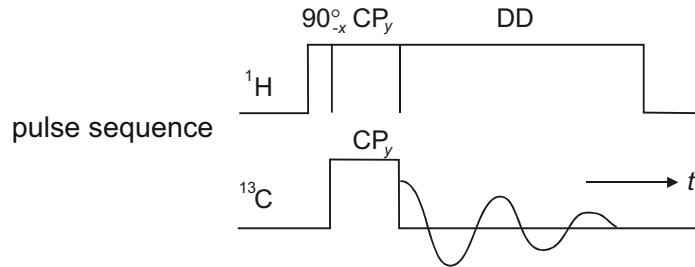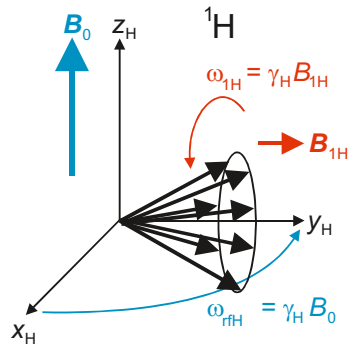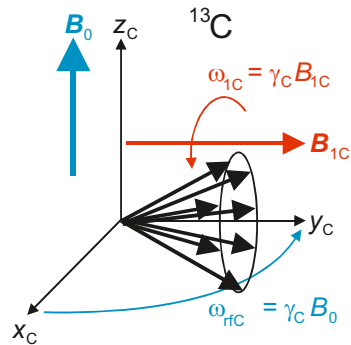
Solid-State Multi-Pulse NMR

- *Energy levels* and *NMR frequencies* are calculated with the *Hamilton operator* and the *density matrix* following the rules of *quantum mechanics*
- Accordingly, the expression for the Hamilton operator consists of a space and a spin dependent part
- The space dependent part describes the *anisotropy of an interaction*
- The spin dependent part determines the constitution of the energy level diagram and the allowed transitions
- The *orientation dependence of the NMR frequency* can be eliminated by manipulation of the space dependent part using *MAS*, but also by manipulation of the spin dependent part using *multi-pulse NMR*
- The most simple *multi-pulse sequence* for elimination of the *dipole-dipole interaction* is the *WAHUHA sequence* named after Waugh, Huber, and Haeberlen
- It consists of four 90° pulses and is cyclically repeated
- In each cycle, one data point is acquired stroboscopically
- The pulse cycle is designed in such a way, that the quantization axis of the Hamilton operator is aligned along the space diagonal on the time average
- This axis encloses the *magic angle* with the *z* axis of the RCF
- Improved homo-nuclear dipolar decoupling at slow MAS is achieved by combining multi-pulse NMR (e. g. BR-24) and MAS (*CRAMPS*: combined rotation and multi-pulse spectroscopy)
- With fast MAS frequencies of 70 kHz being available today, the most important use of homo-nuclear multi-pulse NMR is as a *dipolar filter*

Homo-Nuclear Dipolar Decoupling

WAHUHA pulse sequence

z_{rcf}

y_{rcf}

x_{rcf}

90°_x 90°_{-y} 90°_y 90°_{-x}

t

0 τ 2τ 3τ 4τ 5τ 6τ

n
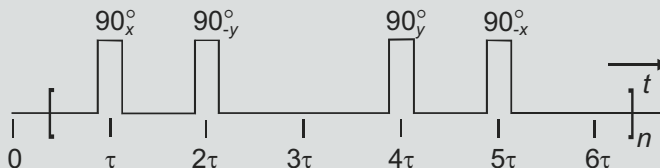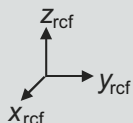
orientation of the toggling coordinate frame in the rcf

z_t y_t x_t y_t z_t

y_t z_t y_t z_t z_t y_t

x_t x_t x_t x_t
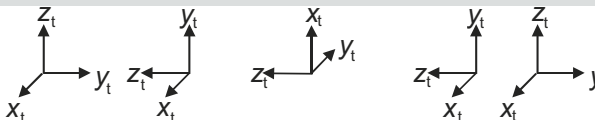
average orientation of the quantization axis z_{rcf} in the toggling frame during the cycle period 6τ

z_t β_m

z_{rcf}

y_t

x_t
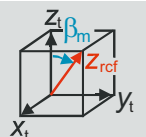
time sharing of excitation and detection

data acquisition $\longrightarrow$ t

^1H-NMR spectra

CRAMPS

BR24

MAS

FT

30 20 10 0 -10 -20
ppm
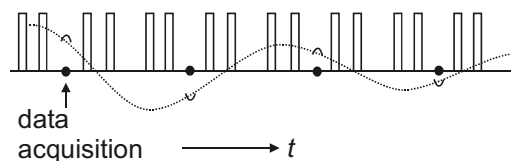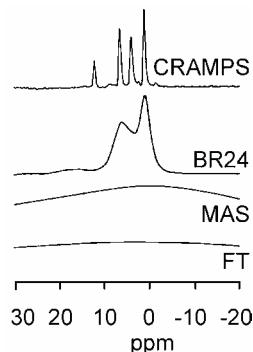
C. E. Bronniman, B. L. Hawkins, M. Zhang, G. E. Maciel, **Anal. Chem. 60** (1988) 1743

Multi-Quantum NMR

- *Multi-quantum coherences* are superposition states with $|\Delta m| \neq 1$, where, for example, two or more interacting spins ½ flip simultaneously
- Multi-quantum coherences can be detected only indirectly via the modulation of directly detectable *single-quantum coherences* (*transverse magnetization*)
- To generate them in the density matrix, usually two rf pulses are required
- To suppress the chemical shift evolution between the pulses, a 180° pulse is centered the *preparation period* to form a *Hahn echo* at the end
- The resultant sequence of three rf pulses and two precession intervals is called the *preparation propagator* $\mathbf{U}_p$ of duration τ_p
- In the subsequent *multi-quantum evolution period* t_1 the multi-quantum coherences precess and relax similar to transverse magnetization
- For observation, they are converted into directly observable single-quantum coherences or into *longitudinal magnetization* by the mixing propagator $\mathbf{U}_m$
- The *mixing propagator* $\mathbf{U}_m$ for longitudinal magnetization is a time inverse copy of the *preparation propagator* $\mathbf{U}_p$
- The *multi-quantum coherence order* can be selected by the pulse phases in combination with suitable phase cycling during signal accumulation
- The *build-up curves* of *multi-quantum coherences* (signal amplitude versus $\tau_p = \tau_m$) are steep in the initial part for strong *dipole-dipole interactions*
- Multi-quantum pulse sequences can serve as *filters* to select magnetization from rigid domains of dynamically heterogeneous solids, and multi-pulse line-narrowing sequences to select magnetization from mobile domains
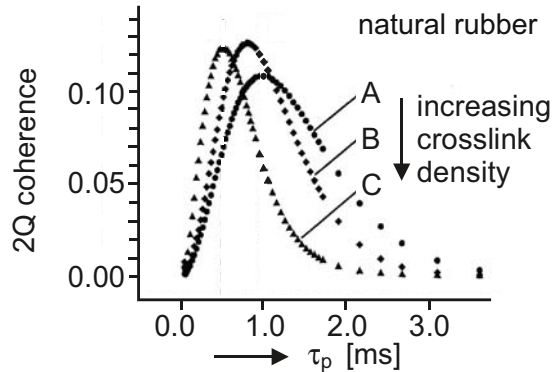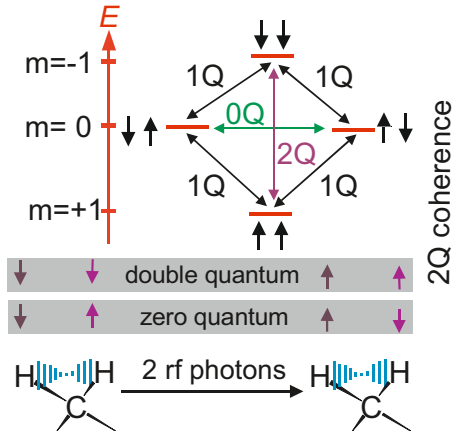
Double-Quantum NMR

Introduction to Multi-Dimensional NMR Spectroscopy

- *Multi-dimensional NMR* denotes the generation of NMR spectra with more than one frequency axis
- Multi-dimensional Fourier spectra are generated by measuring FIDs following several pulses with systematic variation of parameters before the last pulse, for example, by variation of *evolution times* like pulse separations
- In 2D NMR, successive FIDs acquired for increasing evolution times are stored in the rows of a data matrix
- The *2D spectrum* is obtained by *2D Fourier transformation* of the data matrix
- A 2D FT consists of 1D FTs for all rows and columns of the data matrix
- Straight forward 2D FT leads to phase twisted 2D peaks which cannot be phase corrected
- Purely absorptive 2D peaks are obtained by suitable phase cycling and data manipulation
- Depending on the pulse sequence, correlations between different peaks in 1D spectra can be revealed, or complicated 1D spectra can be simplified by spreading them into two or more dimensions

Principle of 2D NMR

preparation | detection

90°

1D NMR

t_0 → t →

repeat for signal averaging

$s(t)$ FID

t

Re$\{S(\omega)\}$

1D FT

ω

spectrum

preparation | evolution | detection

90°   90°

2D NMR

t_0 → t_1 → t_2 →

$t_1 := t_1 + \Delta t_1$

Re$\{s(t_1, t_2)\}$

t_2

t_1

20
10
0
-10
-4
-2
0
2
4

Re$\{S(\omega_1, \omega_2)\}$

ω_2

ω_1

5
0
-4
-2
0
2
4

2D FT
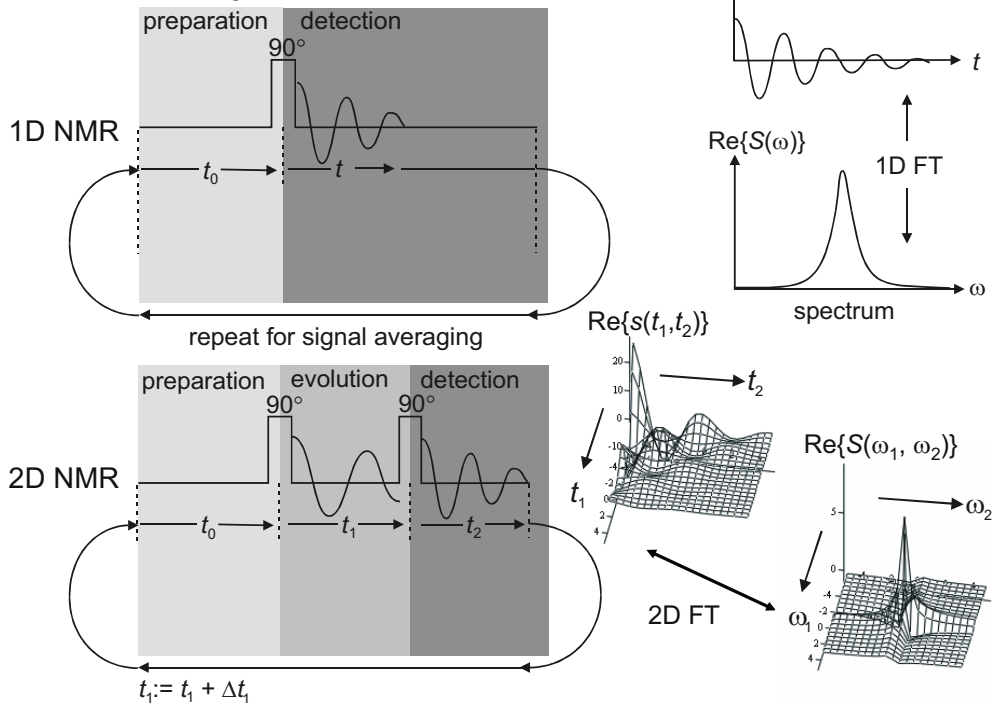
A Simple Example

- The most simple example of *2D NMR* is *2D J-resolved spectroscopy*
- In 2D *J*-resolved NMR spectra, the *J* multiplets appear in one dimension and the *chemical shift* δ in the other
- The basic pulse sequence is the *spin echo* sequence
- In the echo maximum, the evolution of the spin system due chemical shift dispersion is refocused, while the phase evolution of magnetization during the FID is governed by the chemical shift and the *J* coupling
- Choosing the echo time as the evolution time t_1, and acquiring the decay of the echo during the detection time t_2 lead to a 2D data matrix. After subsequent *Fourier transformation*, the spin multiplets are centered in the second dimension at *J* = 0 and are rotated by 45°
- A shear transformation aligns the *J* multiplets along one axis, so that *J* coupling and chemical shift are separated in both dimensions of the spectrum
- 2D *J* spectroscopy is an example for *2D separation NMR*. The 1D spectrum is simplified, but no correlations between lines are revealed
- A *projection* of the sheared 2D *J* spectrum onto the chemical shift axis yields a 1D spectrum with homo-nuclear decoupling
- Due to the *phase twist*, a 1D projection of the unsheared 2D spectrum onto one axis always results in zero signal amplitude

2D J-Resolved Spectroscopy

90° 180°

t_0 t_1 t_2

preparation	evolution	detection
T_1 relaxation	no chem. shift but J coupling	chemical shift and J coupling

$t_1 := t_1 + \Delta t_1$
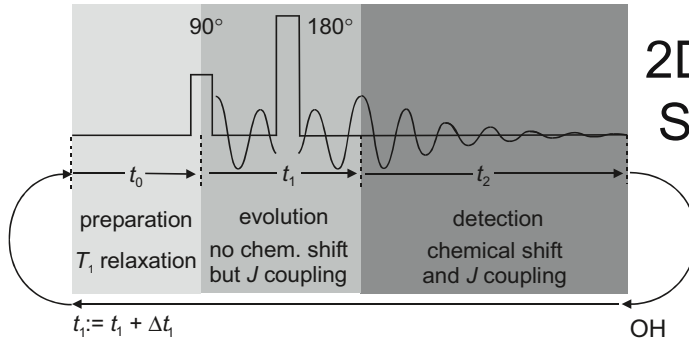
pulse sequence: spin echo
with variable echo time

OH CH$_2$ CH$_3$

6 5 4 3 2 1 0
δ [ppm] ←
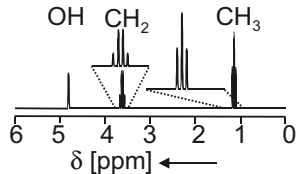
example: ^{1}H NMR
of ethyl alcohol

OH   CH$_2$ CH$_3$

J
0-

2D J spectra $\delta + J$ ←

shear
transfor-
mation

J
0-

δ ←
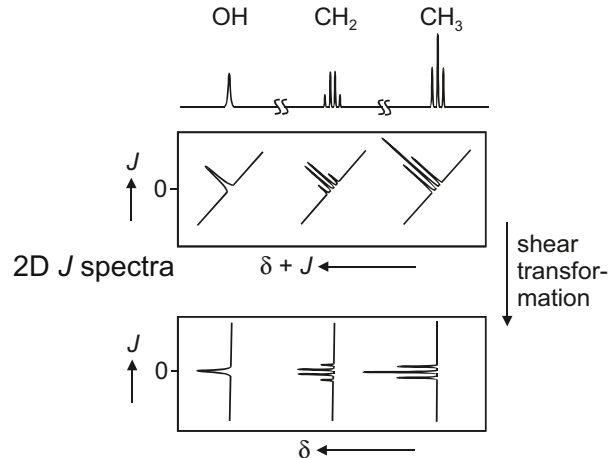
Multi-Dimensional Correlation-NMR

- The most simple pulse sequence for uncovering correlations between lines in 1D spectra is the double-pulse experiment with two 90° pulses
- It generates correlation spectra (*COSY*: *correlation spectroscopy*), in which lines coupled in 1D spectra are identified by cross-peaks
- Depending on the connectivity, progressive or regressive, in the energy level diagram the phase of the cross-peaks is positive and negative, respectively
- By preparation of the initial state of the spin system with two pulses, *multi-quantum coherences* are excited. These can be explored to modulate detectable single-quantum coherences by means of applying a third pulse for mixing of coherences
- The multi-quantum pulse sequence shown before is obtained from this two-pulse sequence by insertion of 180° pulses in the middle of the evolution and detection periods, and by terminating the detection period with a 90° pulse to generate longitudinal instead of transverse magnetization at the end of the sequence
- There a many more pulse sequences for the generation of various other *multi-dimensional NMR* spectra

2D COSY and Multi-Quantum NMR
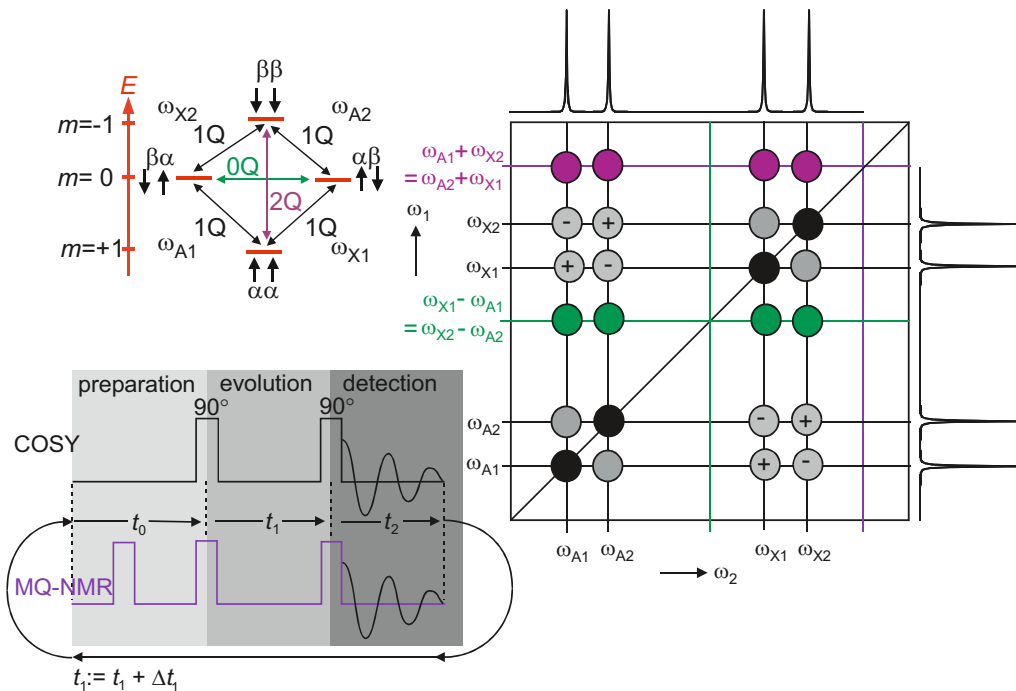
Coherent Hetero-Nuclear Polarization Transfer by *J* Coupling

- Hetero-nuclear experiments explore the *transfer of polarization* (*longitudinal magnetization*) between different spins, for example spins I and S or ^{1}H and ^{13}C
- Polarization can be transferred *coherently* by making use of spin couplings or *incoherently* by making use of relaxation
- In liquids the *J coupling* is often used for coherent polarization transfer
- Transverse magnetization is generated for the I spins, and the doublet components are allowed to precess for a time $t_1 = 1/2J$ to align in opposite directions along one of the axes in the transverse plane
- These anti-phase components are converted to longitudinal magnetization by a 90° pulse resulting in a redistribution of populations of the energy levels
- The new distribution shows greatly enhanced *population differences* but with changing signs
- This distribution is interrogated by a 90° pulse applied to the S spins
- The resultant transverse anti-phase S-spin magnetization focuses into an *echo* after time $t_2 = 1/2J$
- Recording of the signal beginning in the echo maximum produces an in-phase doublet

Illustration for the *J*-Coupled IS System
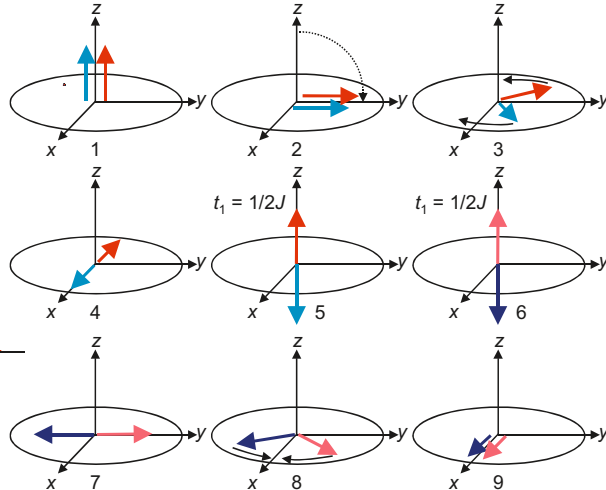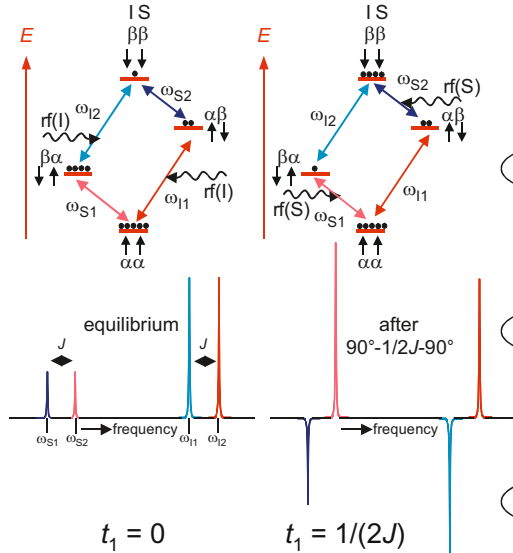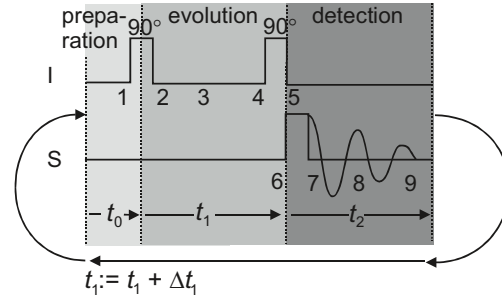
2D NMR Correlation NMR

- *2D NMR methods* are classified into separation and correlation methods
- *Separation methods* simplify a complicated 1D spectrum by spreading it into a second frequency dimension without generating additional peaks
- *Correlation methods* generate additional peaks which reveal connectivities of lines in the 1D spectrum
- Depending on the type of connectivity, different NMR methods are used
- For an understanding of most 2D NMR methods, the use of quantum mechanics is required to study the evolution of the *density matrix* under the action of different rf pulses
- Connectivities of resonance frequencies in 1D spectra can arise from spin coupling and from cross relaxation
- The spin-spin coupling dominant in liquids is usually the *indirect coupling*; in solids it is the *dipole-dipole interaction*
- Spin coupling leads to line splittings and *multi-quantum coherences*
- They can be explored for *coherent transfer* and mixing *of* longitudinal and transverse *magnetization* in homo- and hetero-nuclear schemes (*COSY*, *HETCOR*, *TOCSY*, *INADEQUATE*)
- Connectivities due to *incoherent polarization transfer* arise from *chemical exchange* and *cross-relaxation* (*EXSY, NOESY*)
- The generic scheme of 2D NMR consists of four periods: preparation, evolution, mixing, and detection with a systematic variation of the evolution time
- *Multi-dimensional NMR* with *n* dimensions has *n* evolution times

Elementary Pulse Sequences for 2D Correlation NMR

- correlation spectroscopy: COSY
- incredible natural abundance double-quantum transfer: INADEQUATE
- hetero-nuclear correlation: HETCOR
- total coherence transfer spectroscopy: TOCSY
- exchange spectroscopy: EXSY
- nuclear Overhauser spectroscopy: NOESY
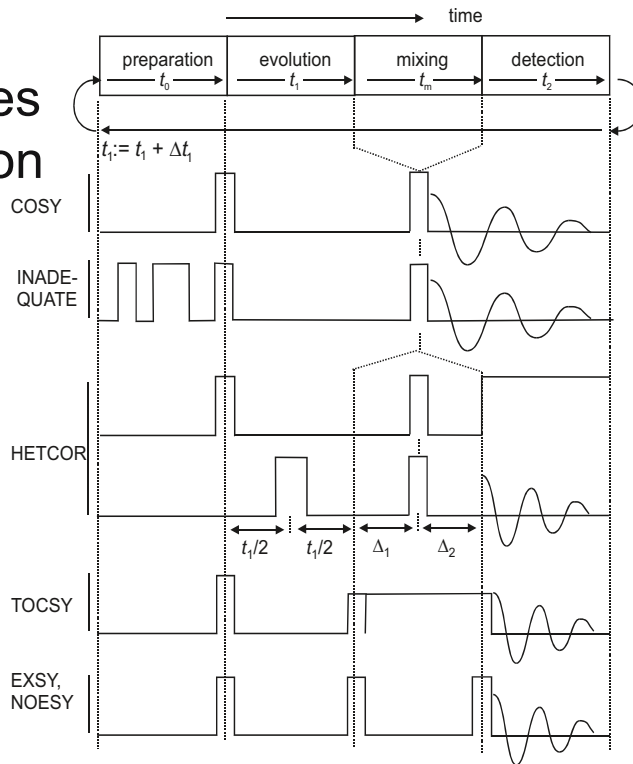
2D Correlation Spectroscopy: COSY

- The 2D *COSY* (COrrelation SpectroscopY) experiment is the 2D NMR experiment originally proposed by J. Jeener in 1971
- It is generated by applying two 90° rf pulses instead of just one which are separated by a variable *evolution time t_1*
- The first pulse and the subsequent evolution time t_1 prepare the spin system in a non-equilibrium state, which is probed by recording the *impulse response (FID)* after the second pulse during the detection time t_2 as a function t_1
- The Fourier transform of the time domain data set $s(t_1, t_2)$ is a *2D spectrum*
- Both its axes bear the same information of the homo-nuclear 1D spectrum
- The 1D spectrum also appears along the diagonal
- Off-diagonal peaks identify lines which belong to the same spin system
- Their *connectivities* can be automatically identified and displayed in a connectivity table for a first analysis
- Spins are said to belong to the same system when they are coupled
- In liquid-state NMR the most significant coupling is the *indirect* or *J coupling*
- To resolve the *multiplet splitting*, the evolution and detection times have to be at least as long as the inverse coupling constant
- The detection of small couplings requires long evolution times resulting in large data sets unless fixed time off-sets are employed in sampling the data
- Often, magnitude spectra are displayed and the line-shapes are artificially adjusted from star to circularly shaped 2D peaks by shaping the time domain signal prior to *2D Fourier transformation*

COSY of Menthol

K	J	I	H	G	F	E	D	C	B	A		ppm	automated
	J										A	0.81	COSY
	J		H		F						B	0.91	analysis
K											C	0.94	
		I									D	0.94	
K				G							E	1.10	
									B		F	1.41	
						E					G	1.60	
									B		H	1.62	
K					D						I	1.96	
								B	A		J	2.16	
		I			E		C				K	3.40	

regular COSY for identification of coupled spins

the long-range COSY with 0.2 s fixed delays after pulses reveals cross-peaks for small *J* couplings

W. R. Croasmun, R. M. K. Carlson, eds., **Two-Dimensional NMR Spectroscopy**, VCH, Weinheim, 1994

$J_{H9,H10}$
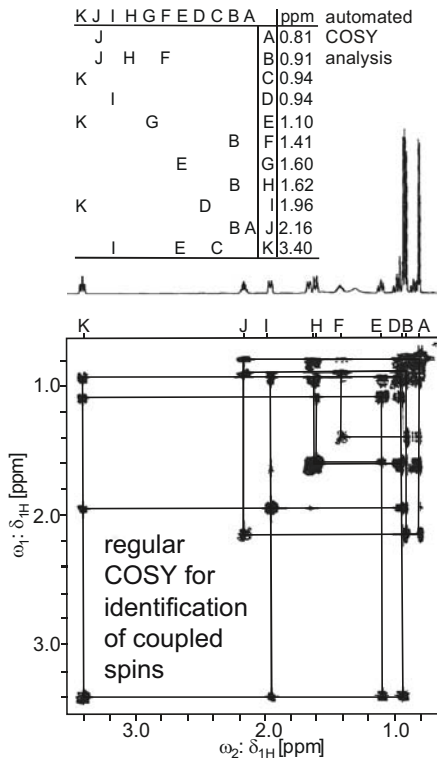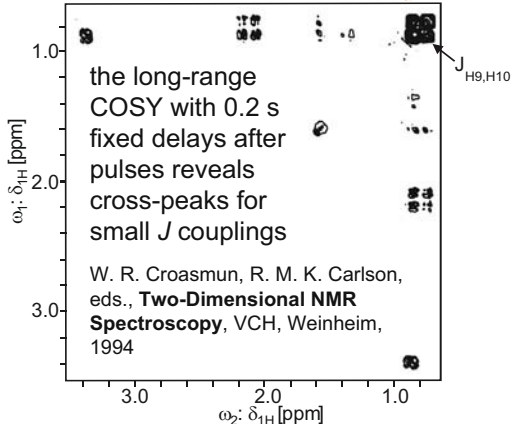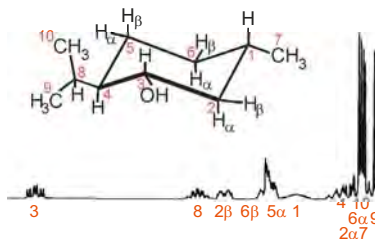
2D Double-Quantum NMR Spectroscopy

- The acquisition of a *COSY* spectrum often does not provide sufficient information for an unambiguous assignment of a chemical structure to the lines in a 1D spectrum
- ^{13}C NMR provides better *chemical shift resolution* than ^1H NMR but is less sensitive due to the low natural abundance of ^{13}C (1 %) and the lower gyro-magnetic ratio
- *J*-coupled ^{13}C spin pairs arise with a probability of 0.0001 (1% of 1%)
- Nevertheless, they can be detected, and *double-quantum coherences* can be generated in such spin pairs
- *INADEQUATE* is the 2D version of the double-quantum ^{13}C NMR experiment
- The indirectly detected frequency ω_1 is a double-quantum frequency corresponding to the sum frequency of the coupling spins; the directly detected frequency ω_2 corresponds to the chemical shift in the 1D spectrum
- Along ω_2, pairs of doublets are observed, centered at the chemical shifts of the directly bonded ^{13}C spins in the carbon backbone of the molecule
- The frequencies ω_1 of a particular carbon lead to its different neighbors
- With 2D INADEQUATE NMR the complete carbon skeleton of a molecule can be traced
- The large spread of ^{13}C chemical shifts facilitates the assignment of the ^{13}C resonance lines
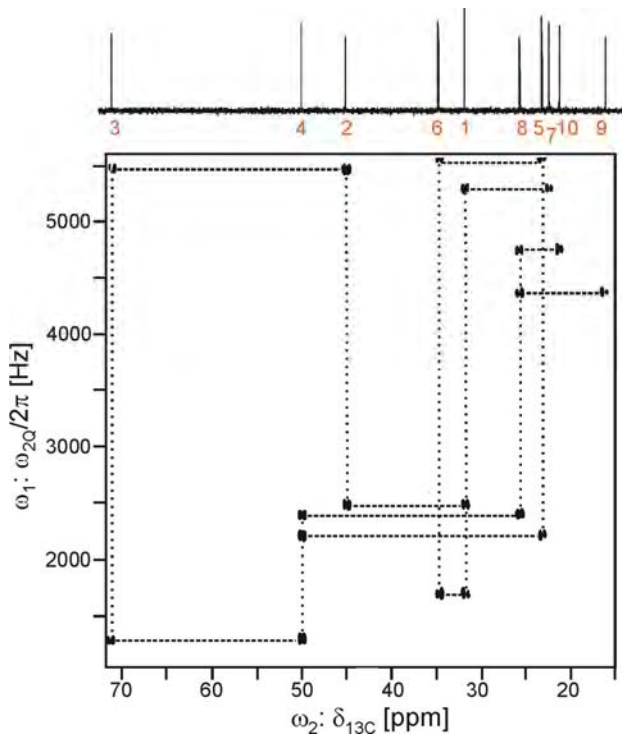
INADEQUATE of Menthol

direct carbon-carbon connectivities through double-quantum NMR of ^{13}C
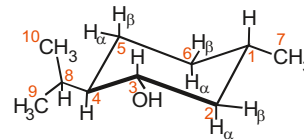
W. R. Croasmun, R. M. K. Carlson, eds., *Two-Dimensional NMR Spectroscopy*, VCH, Weinheim, 1994

2D Hetero-Nuclear Correlation NMR

- To interpret the lines of the ^{1}H NMR spectrum it is helpful to make use of the large *chemical shift* dispersion of the ^{13}C resonances which may be assigned with the help of the 2D *INADEQUATE* spectrum
- To this end, the hetero-nuclear variant *HETCOR* of the *COSY* experiment is performed which makes use of the *hetero-nuclear indirect coupling* between ^{1}H and ^{13}C
- Following an evolution time t_1 the transverse ^{1}H magnetization is transferred to the ^{13}C spins, and the ^{13}C FID is detected during t_2
- During the evolution time, the ^{13}C spins are decoupled from the ^{1}H spins by a 180° pulse in the ^{13}C channel, and during detection of the ^{13}C signal both nuclei are decoupled by irradiating the protons
- The transfer of ^{1}H magnetization to ^{13}C is achieved by *coherent hetero-nuclear polarization transfer*
- Approximate anti-phase magnetization of the ^{1}H doublet is established during a waiting time Δ_1 before irradiation of the coupled ^{1}H and ^{13}C spins with 90° pulses, and subsequently, in-phase magnetization of the ^{13}C doublet forms during the waiting time Δ_2 before sampling the ^{13}C FID
- As Δ_1 and Δ_2 are of the order of $1/(2\,J_{CH})$ and appreciable signal may be lost by T_2 relaxation during these times, the delays, and the particular transfer pulse sequence are optimized for maximum transfer efficiency and minimum signal loss
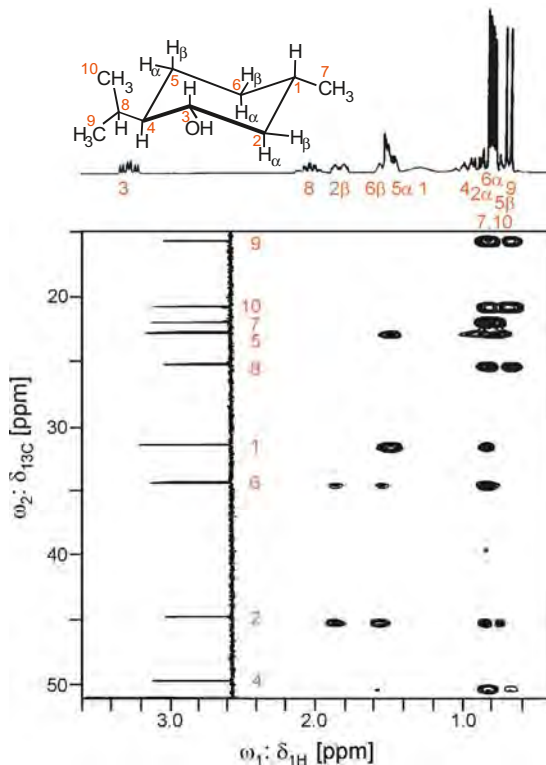
Hetero-Nuclear Correlations of Menthol

correlations of ^1H and ^{13}C chemical shifts

W. R. Croasmun, R. M. K. Carlson, eds., *Two-Dimensional NMR Spectroscopy*, VCH, Weinheim, 1994

Total Correlation Spectroscopy

- In the regular *COSY* spectrum, coupled spins like A and B as well as B and C are identified by cross-peaks
- If the coupling between A and C is too weak, no cross-peak is observed although all three spins A, B, and C belong to the same network of spins
- To identify different networks of spins in crowded spectra, it is helpful to generate a COSY-type spectrum which shows cross-peaks between all spins of a network by relaying the magnetization of spin A to spin C and vice versa via spin B
- Experiments of this type are called *TOCSY* (TOtal Coherence transfer SpectroscopY) experiments
- In the simple form of TOCSY the 90° mixing pulse of the COSY experiment is replaced by a spin-lock period of 50 to 75 ms duration, in which all spins share their initial magnetization
- The TOCSY experiment is a standard tool in the structural analysis of biological macromolecules by multi-dimensional high-resolution NMR spectroscopy
- The TOCSY spectrum of menthol shows many more cross-peaks than the corresponding COSY spectrum
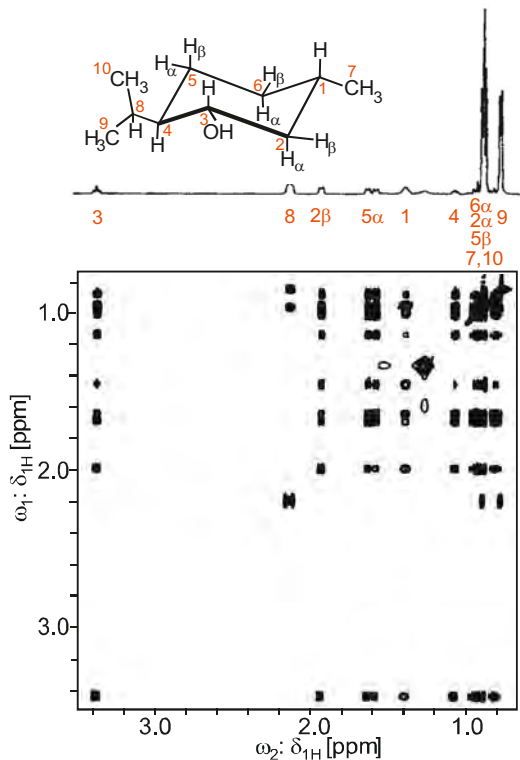
TOCSY of Menthol

total coherence transfer between all spins of a molecule can be achieved in different ways. TOCSY uses a spin-lock pulse of 50 to 75 ms after the mixing pulse to achieve this goal

W. R. Croasmun, R. M. K. Carlson, eds., *Two-Dimensional NMR Spectroscopy*, VCH, Weinheim, 1994

Sensitivity Enhancement by ^{1}H Detection

- The *sensitivity* of the *hetero-nuclear experiments* is determined by the sensitivity of the directly detected nucleus
- To improve the sensitivity of the ^{1}H/^{13}C *HETCOR* experiment, ^{13}C magnetization should be detected via ^{1}H; this is referred to as *inverse detection* of ^{13}C
- The strong signal from ^{1}H bound to ^{12}C and not to ^{13}C is eliminated by addition of signals acquired with different phases of the rf pulses
- A further sensitivity gain is achieved by transferring ^{1}H magnetization to ^{13}C at the beginning of the evolution period t_1
- In the *HMQC* experiment transverse ^{1}H magnetization is excited by the first pulse, and its evolution from the chemical shift and from J_{CH} is refocused during t_1 by a 180° pulse on ^{1}H half-way through t_1
- For optimum transfer of magnetization, the delays Δ are adjusted to $2/J_{CH}$
- In the HMQC and HSQC experiments ^{1}H is detected with ^{13}C decoupling
- The *HMBC* experiment is a variant of the HMQC experiment for detection of long-range hetero-nuclear couplings. It has a higher signal-to-noise ratio than the refocused and ω_2-decoupled HMQC experiment
- The *HSQC* experiment is a variant of the HMQC experiment with elimination of chemical-shift dephasing during the magnetization transfer delays Δ and improved hetero-nuclear decoupling by forming longitudinal ^{1}H magnetization during t_1
- Experiments with inverse detection are employed for structural analysis of large molecules like peptides and proteins, where the spin systems are dilute

Hetero-Nuclear NMR with ^{1}H Detection

time

| preparation t_0 | evolution t_1 | mixing t_m | detection t_2 |

$t_1 := t_1 + \Delta t_1$

hetero-nuclear multi-quantum correlation

^{1}H
HMQC
^{13}C
Δ
Δ
decoupling
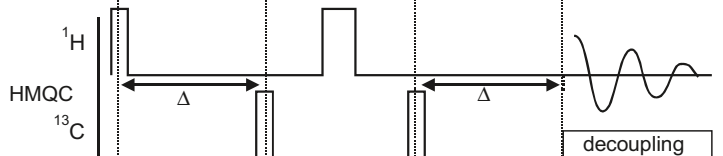
hetero-nuclear multi-bond correlation

^{1}H
HMBC
^{13}C
Δ
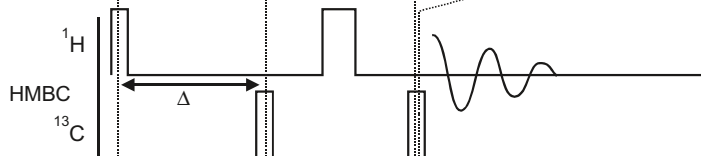
hetero-nuclear single-quantum correlation

^{1}H
HSQC
^{13}C
$\Delta/2$ $\Delta/2$
$\Delta/2$ $\Delta/2$
decoupling
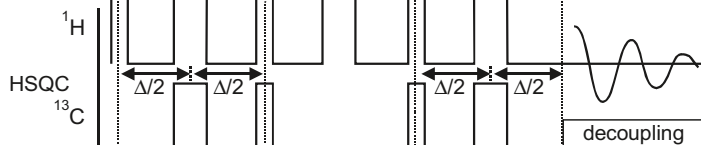
Dynamic 2D NMR

- *Dynamic multi-dimensional NMR* measures spectra which are combined probability densities corresponding to an initial NMR frequency for a spin packet and a final NMR frequency following a *mixing time t_m*
- Initial and final NMR frequencies are labeled in the evolution time t_1 and the detection time t_2, respectively. In the *slow motion limit*, these are so short compared to t_m, that no appreciable motion arises during these times
- Dynamic processes or motions relevant to NMR spectroscopy are rotations of chemical groups in liquids which are associated with a change in NMR frequency, reorientations of molecules in solids with an anisotropic chemical shift, and cross-relaxation corresponding to the nuclear *Overhauser effect* (*NOE*, see below)
- Dynamic multi-dimensional NMR or *exchange NMR* (*EXSY*) leads to cross-peaks at the cross-coordinates of initial and final frequencies
- In powders and partially oriented systems, *wideline exchange spectra* are observed: the off-diagonal signals provide detailed information about the geometry and timescale of the molecular motion
- By modeling the spectrum, one obtains the *distribution $P(\beta_3, t_m)$ of reorientation angles* β_3 which are accessed during the mixing time t_m

Segmental Dynamics in Polymers

pulse sequence
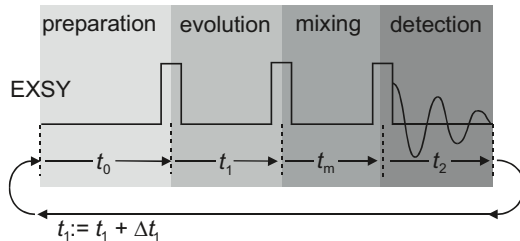
isotactic poly(propylene): threefold jump of the methyl group
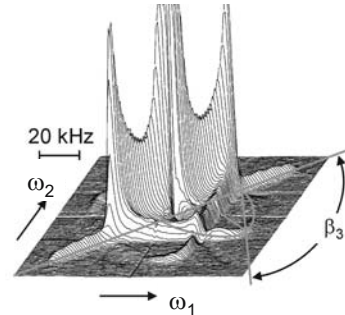
dynamic 2D spectrum
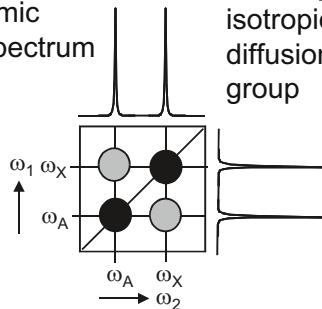
atactic poly(propylene): isotropic rotational diffusion of the methyl group
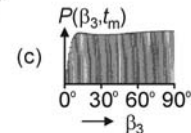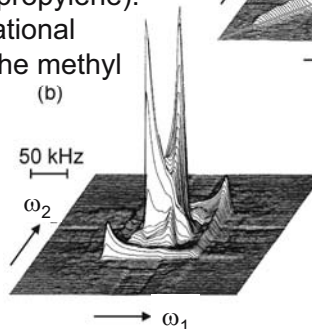
B. Blümich, A. Hagemeyer, D. Schaefer, K. Schmidt-Rohr, H. W. Spiess, **Advanced Materials 2** (1990) 72

Exchange NMR in Liquids

- For liquids *2D exchange cross peaks* often arise from hindered rotations around chemical bonds
- The classical examples are N,N-dimethylformamide (DMF) and dimethyl-acetamide (DMA), where the chemical groups rotate around the C-N bond, so that the *cis* and *trans* methyl groups exchange their positions
- The life times $\tau_c = k_{c \to t}^{-1}$ and $\tau_t = k_{t \to c}^{-1}$ depend on temperature, where $k = k_{c \to t} + k_{t \to c}$ is the rate of the exchange process
- Depending on the ratio R of exchange rate and frequency separation $\Delta \nu_0 = (\delta_c - \delta_t)\omega_0/2\pi$ of the resonances, one or two lines are observed in the spectrum (note: $\delta = 2.74$ and 2.91 ppm)
- In the fast exchange limit at $R > 50$, one line is observed
- Near $R = 5$, the lines coalesce and become small and broad
- For $R < 1$, two lines are observed in the 2D spectrum, and for mixing times $t_m > 1/R$, cross-peaks are observed in the *2D exchange spectrum*
- The exchange cross peaks exhibit the same phase as the auto peaks on the diagonal

Exchange, Coalescence, and Motional Narrowing
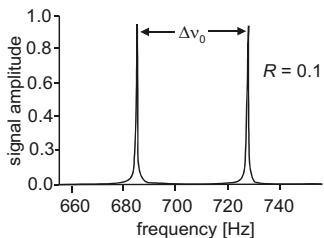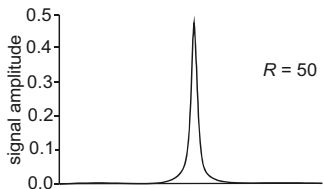
R. S. Macomber, *Modern NMR Spectroscopy*, Wiley, New York, 1998

J. Jeener, B. H. Meier, P. Bachmann, R. R. Ernst, **J. Chem. Phys. 71** (1979) 4546
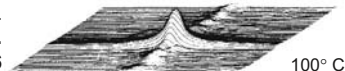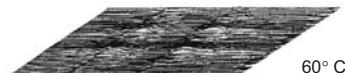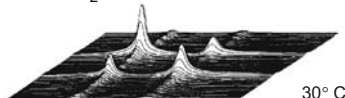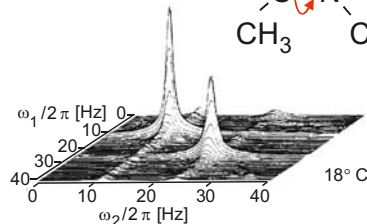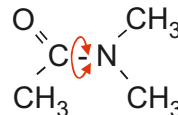
Dynamic Processes

- The decay of transverse magnetization and the build-up of longitudinal magnetization are determined by the *relaxation times T_1 und T_2* , respectively
- In homogeneous samples the build-up of longitudinal magnetization proceeds in an exponential fashion for liquids and solids
- *Transverse relaxation* is often Gaussian in solids and exponential in liquids in the limit of fast molecular motion
- The dominating relaxation mechanism is the *dipole-dipole interaction* between a spin and time-dependent magnetic dipoles such as paramagnetic centers on neighboring chemical groups or molecules
- A time-dependent modulation of the spin coupling is achieved primarily by *rotational motion* but also by *translational motion*
- In the *fast motion limit*, the motions at frequencies ω_0 and $2\omega_0$ determine the nuclear T_1 relaxation and those at frequencies 0, ω_0 and $2\omega_0$ the T_2 relaxation
- This is why T_1 und T_2 differ for slower motions
- Other than the dipole-dipole coupling, the *anisotropy of the chemical shift*, and in gases, the molecular rotation are active relaxation mechanisms
- *Longitudinal magnetization* moves towards spatial equilibrium by *spin diffusion*, which denotes energy conserving flip-flop transitions of coupled neighboring spins

Relaxation and Spin Diffusion

relaxation: molecular
reorientation with the
correlation time τ_c
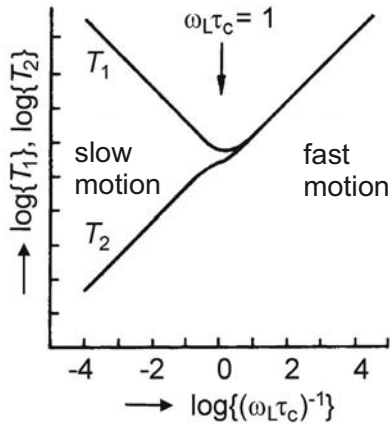
spin diffusion: spatial
magnetization transport
mediated by dipole-dipole
couplings
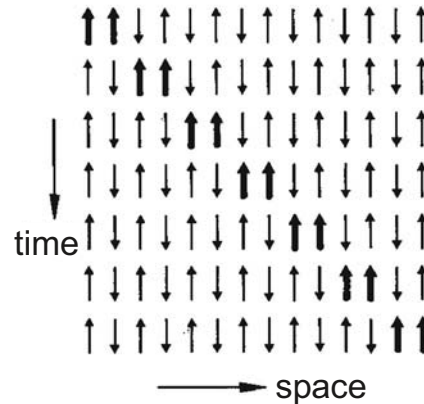
The Nuclear Overhauser Effect: NOE

- In 1955 A. W. Overhauser suggested to saturate the *electron spin resonance* of unpaired electrons to enhance the NMR signal of spins coupled to the electron
- If the T_1 relaxation is governed by the dipole-dipole interaction, and if there is appreciable *cross-relaxation* between coupling spins *S* and *I*, the *Overhauser effect* can be observed
- It can be used for modulating the signal of the low-abundance species *S* by cross-relaxation from the high-abundance species *I* following a perturbation of the thermodynamic equilibrium magnetizations
- A perturbation is achieved, e. g., by *selective population inversion* of the coupled spin S with a 180° pulse or in a systematic fashion in *2D NMR*
- The signal amplitudes are given by the population differences of the energy levels defining the transition frequency
- If the *cross-relaxation rate* W_2 is strong, the signal amplitude of the S spins changes by up to $S_z/S_0 = 1 + \eta$, where η is the *enhancement factor*
- η depends on the relaxation rates W_i, $\eta = \gamma_I(W_2 - W_0)/[\gamma_S(2W_S + W_2 + W_0)]$ and $W_2 - W_0 \propto \tau_c (r_{IS})^{-6}$. It is proportional to the correlation time τ_c of molecular motion and to $(r_{IS})^{-6}$, where r_{IS} is the distance of the cross-relaxing spins
- The maximum enhancement is given by $\eta = \gamma_I/(2\,\gamma_S)$
- The *NOE* is used for determining proximity of spins in isotropic fluids
- For partially oriented molecules, such as molecules in a liquid crystalline solvent, the *residual dipole-dipole coupling* can be exploited for the same purpose

Relaxation Paths in a Two-Spin IS System
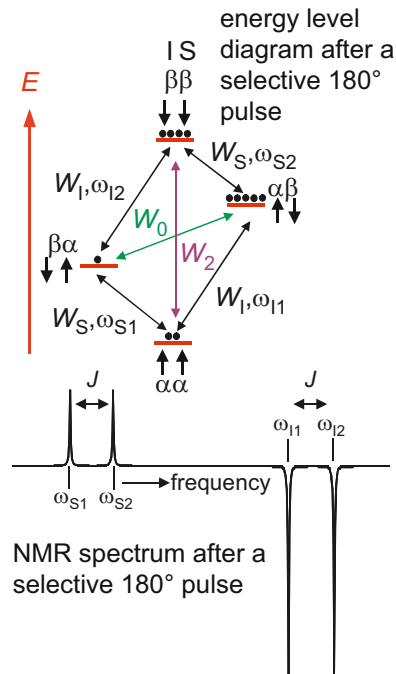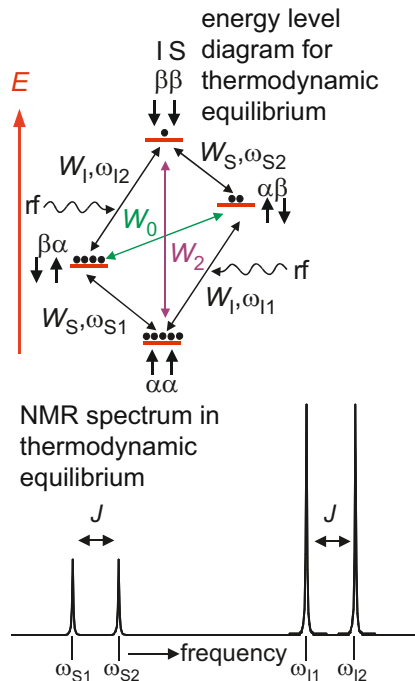
Through-Space Distance Information

- The *nuclear Overhauser effect* is conveniently studied by 2D NMR
- The pulse sequence equals that of the *EXSY* experiment but is referred to as *NOESY* for Nuclear Overhauser Effect SpectroscopY
- Compared to the EXSY experiment, the NOESY experiment uses longer *mixing periods* for *cross-relaxation* of *longitudinal magnetization* components and elimination of transverse magnetization components by T_2 relaxation
- The population differences prepared by the first two pulses and the *evolution time,* and modified in the *mixing time,* are detected as signal amplitudes by the *FID* recorded during the *detection time* following the third pulse
- The initial perturbation of the populations is systematically varied by incrementing the evolution time through a range of values
- A 2D FT leads to a 2D spectrum with cross peaks due to cross-relaxation
- The cross-peaks provide distance constraints to refine the *tertiary structure* of large molecules in solution, because cross-relaxation is determined by the through-space *dipole-dipole interaction* of spins 0.18 to 0.5 nm apart
- To interpret NOE spectra, all resonance lines need to be assigned to the *secondary structure* of the molecule
- This is achieved with a variety of different homo-and hetero-nuclear *multi-dimensional NMR spectra* typically involving ^{1}H, ^{13}C, and ^{15}N, often from molecules prepared with selective isotope labels
- For better sensitivity, experiments with *inverse detection* are frequently used
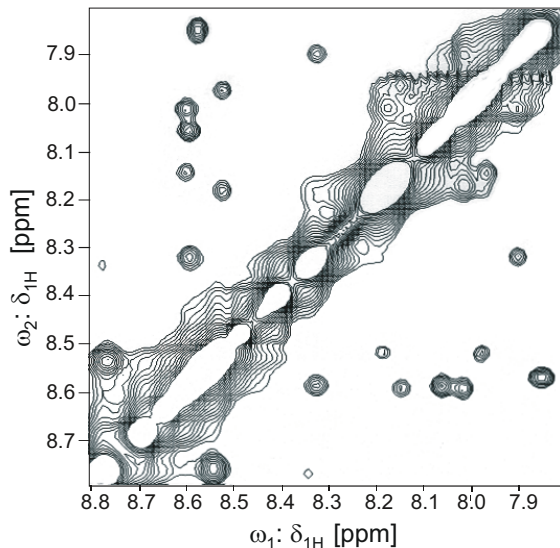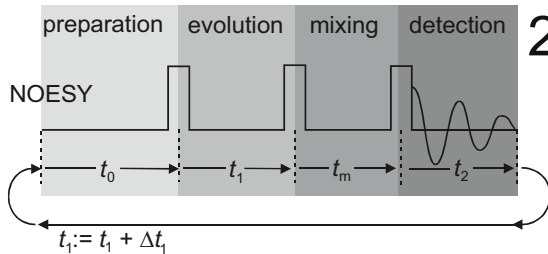
2D NOE Spectroscopy (NOESY)

tertiary structures of complex molecules in solution

example: ubiquitin, a linear protein from 76 amino acids in eukariotic organisms

http://bouman.chem.georgetown.edu/nmr/protein.htm
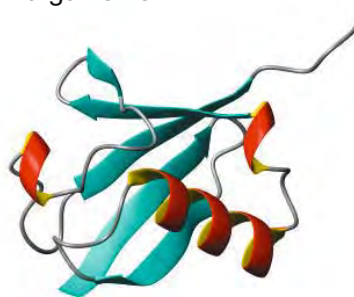
MET-GLN-ILE-PHE-VAL-LYS-THR-LEU-THR-GLY-LYS-THR-ILE-THR-LEU-GLU-VAL-GLU-PRO-SER-ASP-THR-ILE-GLU-ASN-VAL-LYS-ALA-LYS-ILE-GLN-ASP-LYS-GLU-GLY-ILE-PRO-PRO-ASP-GLN-GLN-ARG-LEU-ILE-PHE-ALA-GLY-LYS-GLN-LEU-GLU-ASP-GLY-ARG-THR-LEU-SER-ASP-TYR-ASN-ILE-GLN-LYS-GLU-SER-THR-LEU-HIS-LEU-VAL-LEU-ARG-LEU-ARG-GLY-GLY

4. Imaging and Mass-Transport

Precession phase
Scanning of *k* space
Slice and volume selection
Spin-echo imaging
Gradient-echo imaging
Spectroscopic imaging
Fast imaging
Imaging in the rotating frame
Imaging of solids
Velocity fields
Velocity distributions
Exchange NMR

The NMR Signal in a Volume Cell

- In heterogeneous objects, the *longitudinal magnetization M_z* and the transverse magnetization $M_{xy} = M_x + i\, M_y \equiv M$ generated by a 90° pulse depend on the position r within the sample
- In thermodynamic equilibrium, the longitudinal magnetization $M_{0z}(r)$ per volume element is often referred to as the *spin density*
- Following an excitation pulse, the transverse magnetization vector $M(t,r)$ of a volume cell or *voxel* precesses with frequency Ω around the z axis in the rotating frame, and the length of the vector decreases exponentially with T_2
- The *precession frequency* Ω is determined by the *off-set field* in the rotating frame which is approximated for a linear *gradient field* by $B_{\text{off}} = B_z - B_0 = G\, r$, where G is the *gradient vector* which collects the spatial derivatives of B_z
- Note, that in general the *gradient* is a *tensor* with nine elements G_{mn}
- For spins moving from one value B_z of the field to another, the precession frequency changes with time. So does the *precession phase*, so that the phase is written in integral form, $\varphi(t) = {}_0\!\int^t \Omega(t')\, dt'$
- To accommodate transverse relaxation decays other than of exponential from, a generalized signal *attenuation function $a(t,r)$* is introduced instead of $\exp\{-t/T_2(r)\}$

The Acquired Signal
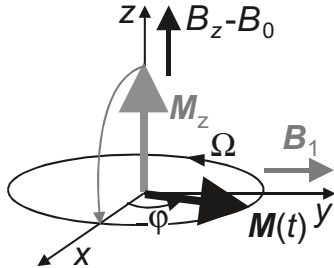
For each volume cell (voxel) at position r :

$M(t,r) = M_z(r) \exp\{-[1/T_2(r) - i \Omega(r)]\, t\}$, where

$\Omega = \gamma (B_z - B_0) = \gamma B_{off}$, and $M = M_x + i M_y$

In general, Ω depends on time. Then $\varphi = \Omega t$ becomes $\varphi(t) = {}_0\!\int^t \Omega(t')\, dt'$, and

$$M(t,r) = M_z(r) \exp\{-t/T_2(r) + i\, {}_0\!\int^t \Omega(t',r)\, dt'\}$$

For non-exponential relaxation, the relaxation decay $\exp\{-t/T_2\}$ assumes the general envelope $a(t)$, and

$$M(t,r) = M_z(r)\, a(t,r) \exp\{i\, \varphi(t)\} = M_z(r)\, a(t,r) \exp\{i\, {}_0\!\int^t \Omega(t',r)\, dt'\}$$

Dependence on Time and Position

- The fundamental quantity of importance for space encoding is the *phase* φ of the transverse magnetization *M*(*t*)
- The variation of the *magnetization phase* with position depends on the profile of the off-resonance field across the sample. For unknown profiles it is expanded into a *Taylor series*
- For conventional imaging only the linear term involving the *gradient* **G** of the field profile is important. The *curvature* **F** is usually made as small as possible in the design of the spectrometer hardware. However, it assumes significant values in unilateral NMR
- If the nuclear spins are moving through the sample by *diffusive motion* or *coherent flow*, their position depends on time
- For motions slow compared to the time scale of the NMR experiment the time-dependent position is expanded into a Taylor series as well, which involves initial *position* $\boldsymbol{r}_0$, initial *velocity* $\boldsymbol{v}_0$, and initial *acceleration* $\boldsymbol{a}_0$

The Precession Phase

z ↑ B_z-B_0

M_z

Ω B_1

φ $M(t)$ y

x
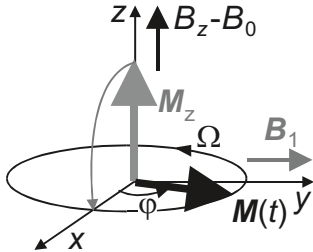
off-set field in the rotating frame:
$$B_{off} = B_z - B_0$$
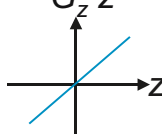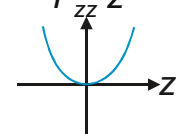
NMR phase
$$\varphi(t) = \gamma \int_0^t B_{off}(t)\, dt'$$

Taylor series expansion in space:

$$B_{off}(z, t) = \left.\frac{\partial B_z(z, t)}{\partial z}\right|_{z=0} z(t) + \frac{1}{2}\left.\frac{\partial^2 B_z(z, t)}{\partial z^2}\right|_{z=0} z(t)^2 + \ldots$$

$$= \quad G_z\, z \quad\quad + \quad\quad F_{zz}\, z^2 \quad\quad + \ldots$$

z

z

Taylor series expansion in time:

$$z(t) = z_0 + \left.\frac{\partial z}{\partial t}\right|_{t=0} t + \frac{1}{2}\left.\frac{\partial^2 z}{\partial t^2}\right|_{t=0} t^2 + \ldots = z_0 + v_{0z}\, t + \frac{1}{2}\, a_{0z} t^2 + \ldots$$

$$z^2(t) = z_0^2 + 2\, z_0 v_{0z}\, t + (v_{0z}^2 + z_0\, a_{0z})\, t^2 + \ldots$$

Truncated Phase Evolution

- The *Taylor expansions* in position and time are inserted into the expression for the *phase of the transverse magnetization*
- The resultant expression is valid for profiles of the polarization field B_0 with linear and quadratic parts, and for spins moving slowly through the inhomogeneous field during the NMR experiment
- *Linear field profiles* can readily be generated by most NMR hardware
- For *fast motions*, and for motions with a spectrum of correlation times, a frequency domain analysis can be developed
- The truncated expansion of the time- and position-dependent phase involves the integrals of the time-dependent gradients $G(t)$ and curvatures $F(t)$
- $G(t)$ and $F(t)$ can be manipulated during the NMR experiment. Typically $F(t) = 0$, and $G(t)$ is modulated in terms of positive and negative rectangular pulses of variable amplitude
- The gradient integrals are the different time *moments of the gradient modulation function*
- Including the gyro-magnetic ratio γ with the integrals, the products of the integrals and the associated kinetic variables r_0, v_0, and a_0 form individual phase contributions
- Thus, the integrals denoted by k, q_v, ε are *Fourier conjugated variables* to r_0, v_0, and a_0, i. e. together with their partner variables they form *Fourier pairs*
- From a systematic variation of k, q_v, and ε with measurements of the associated values of the phases φ, the quantities r_0, v_0, and a_0 can be determined

Moments and Fourier Pairs
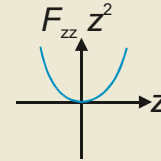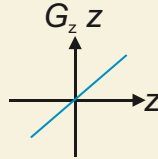
	$G_z\, z$	$F_{zz}\, z^2$
$\varphi(t) = \gamma \int\limits_0^t B_{off}(t')\, dt'$	$= \gamma\, [\int\limits_0^t G_z(t')\, dt'\, z_0$	$+[\int\limits_0^t F_{zz}(t')\, dt'\, z_0^2$
	$+ \int\limits_0^t G_z(t')\, t'\, dt'\, v_{0z}$	$+ \int\limits_0^t F_{zz}(t')\, t'\, dt'\, 2\, z_0\, v_{0z}$
	$+ \,^1/_2 \int\limits_0^t G_z(t')\, t'^2\, dt'\, a_{0z}$	$+ \,^1/_2 \int\limits_0^t F_{zz}(t')\, t'^2\, dt'\, (v_{0z}^2 + z_0\, a_{0z})$
	$+ \dots\,]$	$+ \dots\,]$
	$=\ k_z\, z_0$ $\quad + q_{vz}\, v_{0z}$ $\quad + \varepsilon_z\, a_{0z}$ $\quad + \dots$	$+ \kappa_{zz}\, z_0^2$ $+ \xi_{zz}\, 2\, z_0\, v_{0z}$ $+ \zeta_{zz}\, (v_{0z}^2 + z_0\, a_{0z})$ $+ \dots$

Manipulation of Gradient Moments

- *Gradient moments* are varied either by pulsing a gradient field, which is generated with additional coils surrounding the sample, or by means of rf pulses
- In *pulsed gradient field NMR* (*PFG NMR*: *pulsed field gradient NMR*) usually rectangular gradient pulses are generated with durations of 10 μs to 100 ms and gradients of 0.01 T/m to 10 T/m
- One gradient pulse generates a value for k; the same is true for several gradient pulses of the same sign
- One anti-phase gradient pulse pair generates a value for q_v while $k = 0$. It encodes velocity $v = R/\Delta_v$, where R is the *displacement* traveled by the spin during the time Δ_v of applying q_v
- Two anti-phase pairs of anti-phase gradient pulse pairs generate a value for ε, while $q_v = 0$ and $k = 0$

Pulsed Gradient Fields

$$k_z(t) = \gamma \int_0^t G_z(t')\, dt'$$

$$q_{vz}(t) = \gamma \int_0^t G_z(t')\, t'\, dt'$$

$$\varepsilon_z(t) = \gamma \int_0^t G_z(t')\, t'^2\, dt'$$

$$q_{vz} = q_z\, \Delta_v$$

$$q_z = k_z$$

$$\varphi = q_{vz} v_{0z} = q_z R_z$$
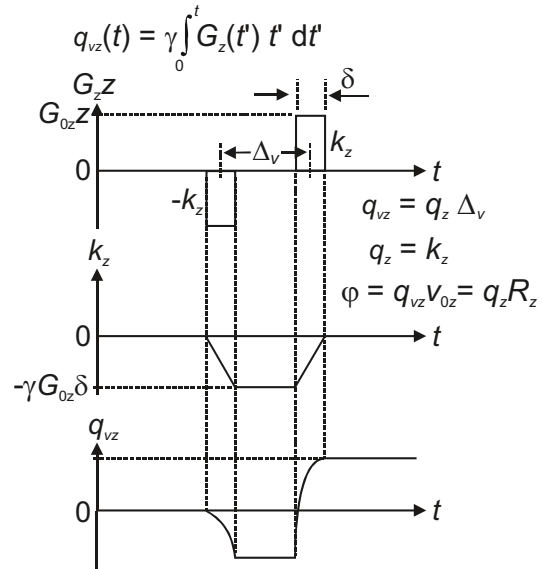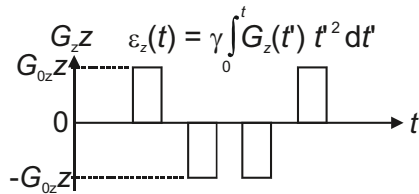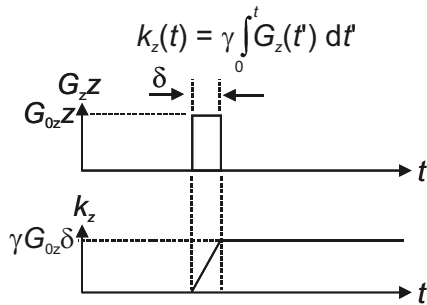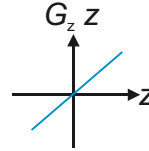
Encoding Time Derivatives of Position

- In *linear field profiles* a pulse of the offset field marks *position*
- In *quadratic field profiles* a pulse of the offset field marks position square
- An anti-phase pulse pair of a linear offset field marks negative initial and positive final positions of a moving spin at two times separated by the pulse spacing Δ_v
- By dividing the marked position difference by the encoding time Δ_v, *velocity* is measured in a *finite difference approximation*
- Similarly, *acceleration* can be measured in a finite difference approximation
- Other finite difference schemes known from numerical differentiation may be employed for encoding of kinetic variables of translational motion as well
- This finite difference approach applies to arbitrary profiles of the offset field including the quadratic field profile

Encoding Translational Motion

B_{off} — t_1 → time

B_{off} — Δ_v — t_1 — t_2 → time

B_{off} — Δ_a — Δ_v — Δ_v — t_1 — t_2 — t_3 — t_4 → time

B_{off} — t_1 — t_2 — t_3 — t_4 — t_5 — t_6 — t_7 — t_8 → time

$B_{off} = b\,z$

z
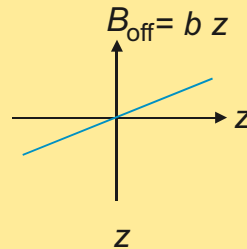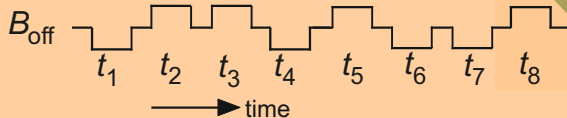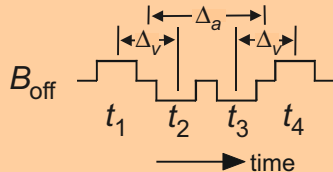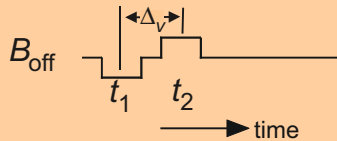
position z

$z_2 - z_1$
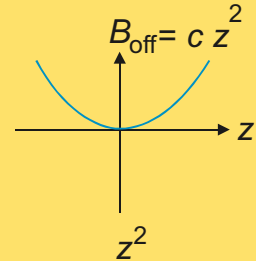
velocity v

$z_4 - z_3 - (z_2 - z_1)$

acceleration a

$B_{off} = c\,z^2$

z^2

z^2

$z_2^2 - z_1^2$

$2\,z\,v$

$z_4^2 - z_3^2 - (z_2^2 - z_1^2)$

$v^2 + za$

finite difference approximations in the slow motion limit

Static Inhomogeneous Polarization Fields

- A time modulation of the effect of the offset field on the phase of the transverse magnetization can also be achieved by rf pulses
- As soon as transverse magnetization is generated, the space dependent magnetization components accumulate a *phase* in the inhomogeneous field depending on their positions within the field
- Conversion of the transverse magnetization into longitudinal magnetization halts the accumulation of phase, but on average only half of the magnetization can be converted back to longitudinal magnetization; the other half is lost. This situation is identical to the one encountered with the *stimulated echo*
- The sign of the offset field can be changed by a 180° pulse. Actually, such a pulse apparently changes the sign of the precession frequencies in all evolution periods preceding the pulse
- While the effect of the offset field on the precession phase can be suspended and the sign of the effective offset field can be inverted, scaling of the time-invariant offset field by the use of rf pulses is a far more difficult task

Time-Invariant Off-Set Fields
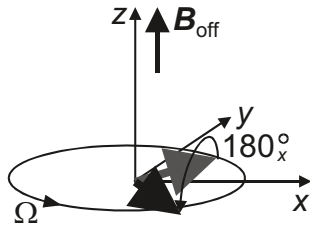
$\Omega = \gamma\, B_{off} = \gamma\, (B_z - B_0)$

before 180°_x pulse:

$s(t_-) = s_0 \exp\{i\, \Omega t_{0-}\}$

$\qquad = s_0\,(\cos \Omega t_{0-} + i \sin \Omega t_{0-})$

after 180°_x pulse:

$s(t_+) = s_0\,(\cos \Omega t_{0+} - i \sin \Omega t_{0+})$

$\qquad = s_0 \exp\{-i\, \Omega t_{0+}\}$

sign change of precession preceding
the 180° pulse:

t_E

CPMG $k = 0$ $k = 0$ $k = 0$ $k = 0$
TX $q = 0$ $q = 0$

0   0.5   1   1.5   2   2.5   3   3.5   4 t/t_E

$B_{off} = \Omega / \gamma$
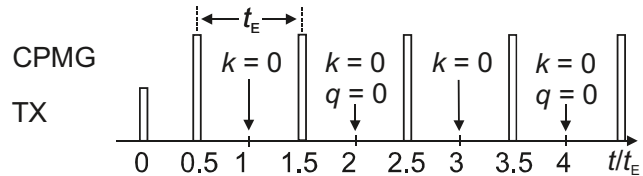
stimulated-echo
variant

0   0.5   1   1.5   2   2.5   3   3.5 t/t_E

$B_{off} = \Omega / \gamma$
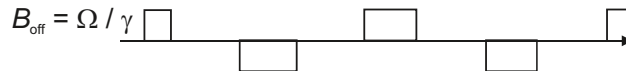
Interpretation of the Gradient Integral

- In a magnetic field which varies linearly with position z, the spins precess with linearly varying Larmor frequency
- For a given duration of the gradient the precession phase varies in a linear fashion as well
- The tips of the magnetization vectors lie on a helix which winds around the direction z of the magnetic field gradient
- The projection of magnetization vectors onto an axis perpendicular to the gradient direction produces a sinusoidal function with period $2\pi/k_z$ and phase $k_z z$
- Therefore, k is the *wave number* which denotes the spatial oscillation frequency corresponding to ω which denotes the oscillation frequency in time
- Similarly, $q = q_v \Delta$ denotes the wave number corresponding to *dynamic displacement* closely related to the spatial period in a crystal which is probed by X-ray and neutron scattering

Transverse Magnetization in a Gradient Field
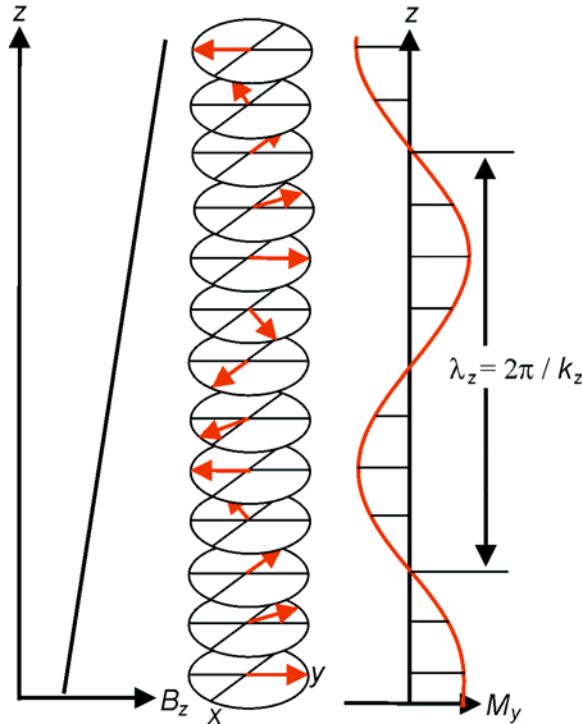
wave number: k_z
position: z_0

position and wave number form a Fourier pair:

$$\varphi(t) = \gamma \int_0^t G_z(t)\, dt\; z_0 = k_z\, z_0$$

Figure labels: z, B_z, x, y, M_y, $\lambda_z = 2\pi / k_z$

Examples of Information Accessible by Pulsed Gradient-Field NMR

- Gradient fields are applied to discriminate the NMR signal from different voxels along the gradient direction
- The signal acquired from a heterogeneous sample is the integral of the signal from all voxels at position r
- For spins in motion, one also needs to integrate over all velocities v
- In general the signal is acquired as a function of k and q, where both variables depend on time t
- The function of interest is the quantity $M_z(r_0,v_0)$ which, apart from the attenuation function $a(t,r_0)$, is the *Fourier transform of the measured signal*
- Therefore, the signal is acquired for a sufficiently large number of values k and q_v and subsequently Fourier transformed
- The *attenuation function $a(t,r_0)$* introduces a loss of image resolution, because the NMR image is the convolution of $M_z(r_0,v_0)$ with the Fourier transform of $a(t,r_0)$
- The Fourier transform of $a(t,r_0)$ is referred to as the *point spread function*
- When starting the imaging experiment from thermal equilibrium $M_z(r_0,v_0)$ is the *spin density* of the object

Transverse Magnetization with Space Encoding by Space-Invariant Gradients

Consider a single resonance at ω_0 in each voxel at the initial position $\boldsymbol{r}_0$:

$$M(t,\boldsymbol{r}_0,\boldsymbol{v}_0) = M_z(\boldsymbol{r}_0,\boldsymbol{v}_0)\, a(t,\boldsymbol{r}_0)\, \exp\{i\, \varphi(t)\}$$
$$= M_z(\boldsymbol{r}_0,\boldsymbol{v}_0)\, a(t,\boldsymbol{r}_0)\, \exp\{i\, [\omega_0(\boldsymbol{r}_0)t + \boldsymbol{k}(t)\boldsymbol{r}_0 + \boldsymbol{q}_v(t)\boldsymbol{v}_0(\boldsymbol{r}_0) + ...]\}$$

For the whole sample with a distribution of resonance frequencies ω_0:

$$M(t,\boldsymbol{k},\boldsymbol{q}_v) = \iiint M_z(\omega_0,\boldsymbol{r}_0,\boldsymbol{v}_0)\, a(t,\boldsymbol{r}_0)\, \exp\{i\, [\omega_0(\boldsymbol{r}_0)\, t + \boldsymbol{k}(t)\, \boldsymbol{r}_0 + \boldsymbol{q}_v(t)\, \boldsymbol{v}_0(\boldsymbol{r}_0) + ...]\}\, d\omega_0\, d\boldsymbol{r}_0\, d\boldsymbol{v}_0$$

Spectroscopy: $\boldsymbol{k} = \boldsymbol{0} = \boldsymbol{q}_v$

$$M(t) = \iiint M_z(\omega_0,\boldsymbol{r}_0,\boldsymbol{v}_0)\, a(t,\boldsymbol{r}_0)\, \exp\{i\, \omega_0(\boldsymbol{r}_0)\, t\}\, d\omega_0 d\boldsymbol{r}_0 d\boldsymbol{v}_0$$

Imaging and flow: t_G << correlation time of motion, neglect spread of ω_0, $\omega_0 = \omega_{rf}$

Imaging with phase encoding: $t = t_E$, $\boldsymbol{q}_v = \boldsymbol{0}$

$$M(\boldsymbol{k}) = \iint M_z(\boldsymbol{r}_0,\boldsymbol{v}_0)\, a(t_E,\boldsymbol{r}_0)\, \exp\{i\, \boldsymbol{k}(t_E)\, \boldsymbol{r}_0\}\, d\boldsymbol{r}_0 d\boldsymbol{v}_0$$

Imaging with frequency encoding: $\boldsymbol{k} = \gamma\, \boldsymbol{G}\, t$, $\boldsymbol{q}_v = \boldsymbol{0}$

$$M(t) = \iint M_z(\boldsymbol{r}_0,\boldsymbol{v}_0)\, a(t,\boldsymbol{r}_0)\, \exp\{i\, \gamma\, \boldsymbol{G}\, \boldsymbol{r}_0\, t\}\, d\boldsymbol{r}_0 d\boldsymbol{v}_0$$

Velocity distributions by phase encoding: $t = t_E$, $\boldsymbol{k} = \boldsymbol{0}$

$$M(\boldsymbol{q}_v) = \iint M_z(\boldsymbol{r}_0,\boldsymbol{v}_0)\, a(t_E,\boldsymbol{r}_0)\, \exp\{i\, [\boldsymbol{q}_v(t_E)\, \boldsymbol{v}_0(\boldsymbol{r}_0)]\}\, d\boldsymbol{r}_0 d\boldsymbol{v}_0$$

Flow imaging by phase encoding: $t = t_E$

$$M(\boldsymbol{k},\boldsymbol{q}_v) = \iint M_z(\boldsymbol{r}_0,\boldsymbol{v}_0)\, a(t_E,\boldsymbol{r}_0)\, \exp\{i\, [\boldsymbol{k}(t_E)\, \boldsymbol{r}_0 + \boldsymbol{q}_v(t_E)\, \boldsymbol{v}_0(\boldsymbol{r}_0)]\}\, d\boldsymbol{r}_0 d\boldsymbol{v}_0$$

Principles of 2D Imaging

- In *Fourier NMR* images are measured by acquiring the complex transverse magnetization $M = M_x + iM_y$ as a function of $\boldsymbol{k} = (k_x, k_y, k_z)^{\dagger}$ and subsequent Fourier transformation over $\boldsymbol{k}$
- The values of $\boldsymbol{k}$ are scanned on a discrete grid in one, two, or three dimensions
- Historically, two principle approaches are discriminated
- The grid can be defined on spherical/*cylindrical coordinates* and on *Cartesian coordinates*
- These schemes are denoted as *back-projection* (BP) *imaging* and as *Fourier* (FT) *imaging*
- The space-encoded data in one dimension are usually acquired directly in the presence of a time-invariant gradient field
- Throughout BP imaging this scheme is used with repeated acquisitions under different gradient directions
- In FT imaging, the data for further space dimensions are acquired indirectly by pulsing gradient fields in orthogonal directions in a *preparation period* prior to data acquisition
- Because a discrete *multi-dimensional Fourier transformation* is performed in Cartesian coordinates, the FT over imaging data acquired by the BP method involves the transformation from cylindrical to Cartesian coordinates

Sampling of *k* Space

cylindrical coordinates: back-projection imaging
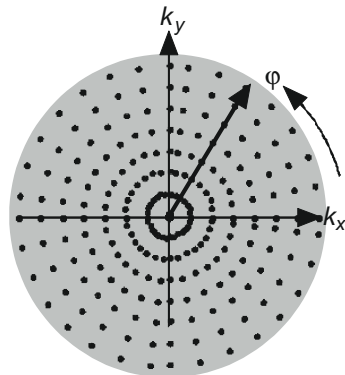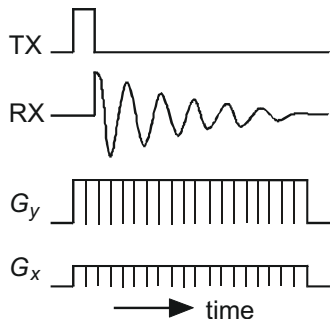
Cartesian coordinates: Fourier imaging
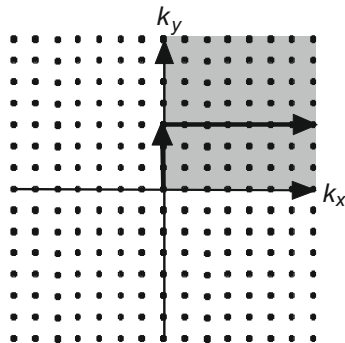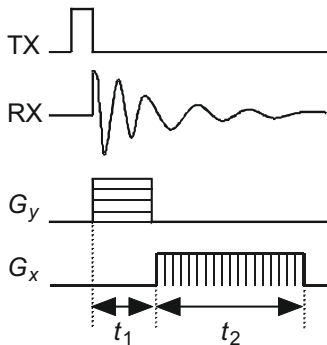
Space Encoding and Resolution

- The terminology of phase encoding and frequency encoding of the space information is historic
- The acquisition of the NMR signal in the presence of a time invariant gradient field is referred to as *frequency encoding* of the space information
- In frequency encoding k_x increases with the acquisition time t_2
- Because by changing t_2 also the signal attenuation by T_2 is affected, the *spatial resolution* $1/\Delta x$ is limited by the line width $\Delta\omega_{1/2} = 2/T_2$
- Modulation of the initial phase of the acquired magnetization in an *evolution time t_1* prior to the *acquisition time t_2* is referred to as *phase encoding*
- In phase encoding k_y is varied preferably by changing the gradient amplitude instead of the gradient duration. This avoids variable signal attenuation by transverse relaxation and signal modulations by the chemical shift and other spin interactions
- In phase encoding the spatial resolution $1/\Delta y$ is limited by the maximum gradient strength $n_{1max}\,\Delta G_y$
- Conventional 2D and 3D FT imaging methods combine phase and frequency encoding
- Pure phase encoding is used for *spectroscopic imaging* and for *imaging of solids*. It is referred to also as *single-point imaging* (SPI)

Frequency and Phase Encoding

TX

RX

G_y

G_x

t_1 t_2

$k_y = \gamma \, G_y \, t_1$

$k_x = \gamma \, G_x \, t_2$
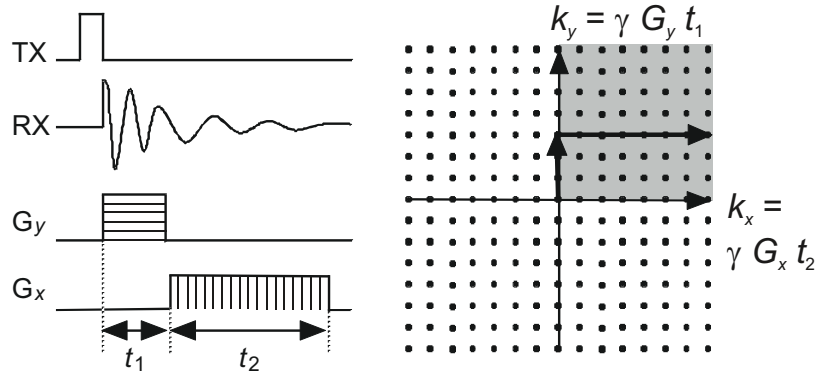
frequency encoding: vary t_2 in n_2 steps

$s(n_2) = \exp\{-[1/T_2 - i \, \gamma \, (B_0 + G_x \, x_0)] \, n_2 \, \Delta t_2\}$

spatial resolution limited by $\Delta\omega_{1/2}$

$\gamma \, G_x \, \Delta x_0 > 2/T_2 = \Delta\omega_{1/2}$

$1/\Delta x_0 = T_2 \, \gamma \, G_x \, / \, 2 = \gamma \, G_x \, / \, \Delta\omega_{1/2}$

phase encoding: vary G_y in n_1 steps

$s(n_1) = \exp\{-[1/T_2 - i \, \gamma \, (B_0 + n_1 \, \Delta G_y \, y_0)] \, t_1\}$

spatial resolution increases with $n_{1,max}$

$\gamma \, n_{1,max} \, \Delta G_y \, \Delta y_0 \, t_1 < 2\pi$

$1/\Delta y_0 = n_{1,max} \, \gamma \, \Delta G_y \, t_1/2\pi$

Walking Through *k* Space

- The information contained in an NMR image is localized near the origin of *k* *space*
- To acquire the NMR signal with spatial resolution, it needs to be acquired for a region of *k* space centered at *k* = 0
- The signal in this region is defined on a discrete grid of points
- The sequence in which these points are addressed is determined in the imaging experiment
- The signal of a group of points is often measured in one scan, which usually includes the origin of one of the components of *k*
- Typically many scans are needed to cover a complete region of *k* space
- Some *fast imaging methods* cover all relevant points of *k* space in one scan
- By *line-scan imaging methods*, the data from one line usually passing through the origin of *k* space are measured in one scan. An example is the back-projection method
- In *Fourier imaging*, the data are acquired from parallel lines in subsequent scans
- In *echo planar imaging* (*EPI*), the data of an entire image are acquired in a single shot where different traces through *k* space can be followed, for example meander and spiral traces

Scanning of 2D-*k* Space
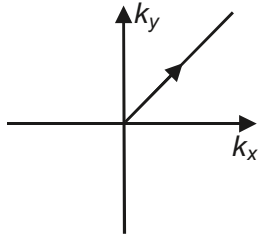
back-projection
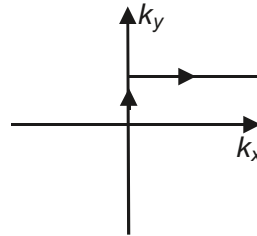
Fourier imaging
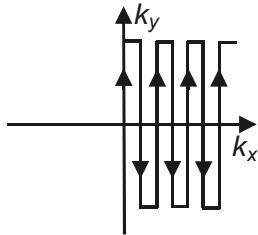
echo planar imaging (EPI)
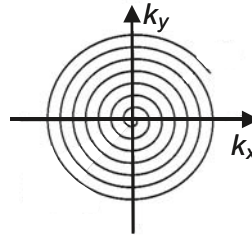
spiral EPI

Making 3D Objects Appear Like 2D Objects

- Usually, images of 2D slices through 3D objects are to be measured
- To make 3D objects appear two dimensional in NMR, a projection must be measured or the magnetization of a 2D *slice* through the object
- To select a slice, a *frequency selective pulse* is applied with the object exposed to an inhomogeneous magnetic field, which usually is a linear field with a space invariant gradient
- The linear field identifies different positions along the gradient direction by their NMR frequencies
- Constant frequencies are found in planes orthogonal to the gradient direction
- The frequency-selective pulse acts on the magnetization components within a limited frequency region only
- The width of the frequency region defines the thickness of the selected slice
- To a first approximation, the *Fourier transform* of the time-domain pulse shape defines the frequency-selection properties of the pulse
- A pulse with a sinc shape in the time domain exhibits a rectangular profile in the frequency domain
- To obtain pulses with finite durations, the lobes in the time domain are truncated on the expense of perfect *slice definition* in the frequency domain

B_1

principle

Ω

$B_{off} = G_x x$

$\Delta\Omega = \gamma \, G_x \, \Delta x$

0    $\Omega = \gamma \, G_x \, x$

Slice
Selection

Δx

z

y x

t

sinc pulse   FT

Ω
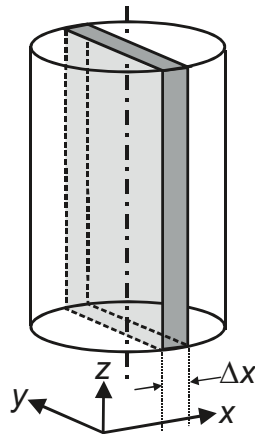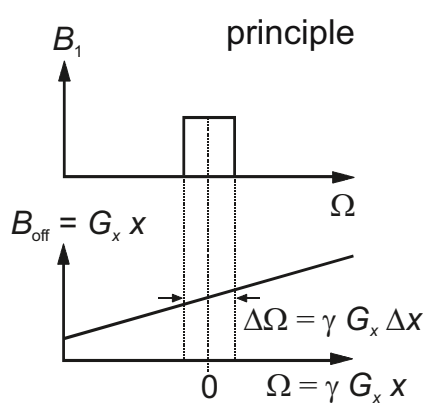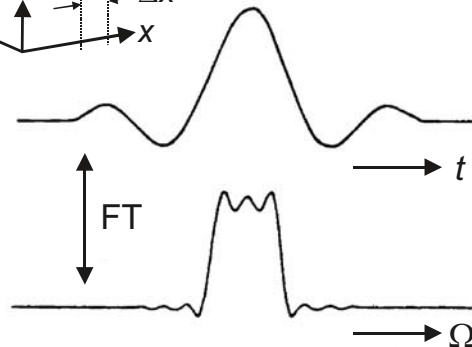
Restricting the Signal-Bearing Volume

- To investigate small regions within large objects by high-resolution NMR imaging or to measure NMR spectra from well defined regions within the object (*volume-selective spectroscopy*), the magnetization within the selected volume must be identified for measurement
- To avoid rapid decay of transverse magnetization, long-lived longitudinal magnetization is prepared
- Positions within the sample are labeled using magnetic gradient fields in the same way as in the selection of transverse magnetization of a 2D slice
- The longitudinal magnetization outside the selected volume is eliminated
- The sensitive volume is defined in the crossing of the three orthogonal *slices*
- Each pulse for selection of longitudinal magnetization consist of a package of three pulses, a selective 45° pulse, a nonselective 90° pulse, and another selective 45° pulse
- The first 45° pulse tips the magnetization within the selected plane by 45°
- The nonselective 90° pulse rotates the complete magnetization of the sample by 90°
- The last selective 45° continues to rotate the magnetization of the slice through another 45° so that it has been rotated through a total of 180° and ends up as longitudinal magnetization
- The unwanted magnetization has been rotated by 90° only and rapidly dephases as transverse magnetization

Volume Selection

90°

45° 45°

TX

RX

G_x

G_y

G_z

time

principle

pulse sequence

z

y

x
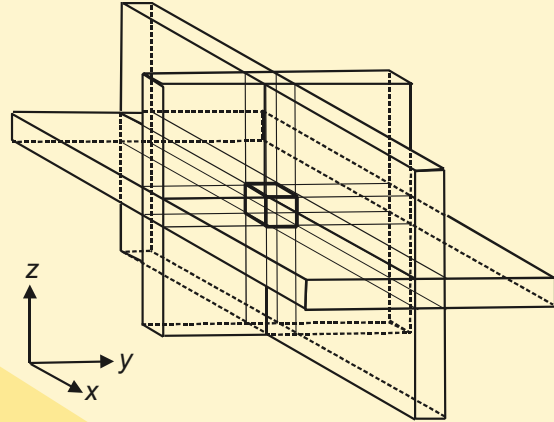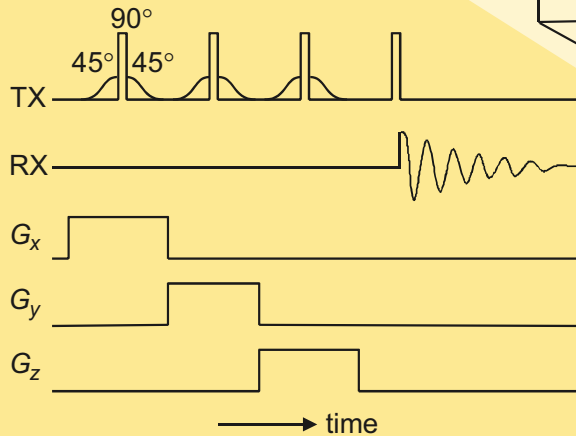
A Practical 2D Imaging Scheme

- A 2D imaging scheme starts by preparing the magnetization in a selected 2D *slice* with a suitably shaped pulse applied in the presence of a gradient field
- The *slice-selective pulse* is long, the magnetization dephases during the pulse in the gradient field
- This dephasing is refocused in a *gradient echo* generated by a second, negative gradient field pulse with an area half of that of the first gradient pulse
- The 2D space information is encoded into the transverse magnetization of the selected slice by *phase encoding* in an *evolution period* and by *frequency encoding* in the *detection period*
- The *gradient switching times* are finite, and some signal is lost during these times. This signal needs to be recovered
- Also, negative *k* components need to be encoded during the detection time
- Both conditions are met by forming a *gradient echo* during the detection time
- This echo is generated by extending the frequency encoding gradient with an initial negative lobe with an area half of that of the positive lobe
- Signal dephasing from chemical shift distributions and inhomogeneities of the polarizing field can be refocused in a *Hahn echo* by applying a 180° pulse separating evolution and detection periods
- Then, the sign of the field pulses applied in the frequency encoding direction during the evolution time needs to be inverted
- This method of 2D imaging is called *spin-echo imaging* or *spin-warp imaging*

Spin-Echo Imaging

(spin-warp imaging)

slice:

a) slice selection:
signal loss

TX — 90° ——→ time

RX

G_z

G_y

G_x

b) slice selection
with refocusing

TX — 90° ——→ time

RX

G_z

G_y

G_x

c) phase and frequency
encoding: half of *k* space

TX — 90° ——→ time

RX

slice: G_z

phase: G_y

read: G_x

d) phase and frequency
encoding: full *k* space

TX — 90° ——→ time

RX

G_z

G_y

G_x

e) refocusing of B_0
inhomogeneities

TX — 90° — 90° →time

t_E

RX

G_z

G_y

G_x
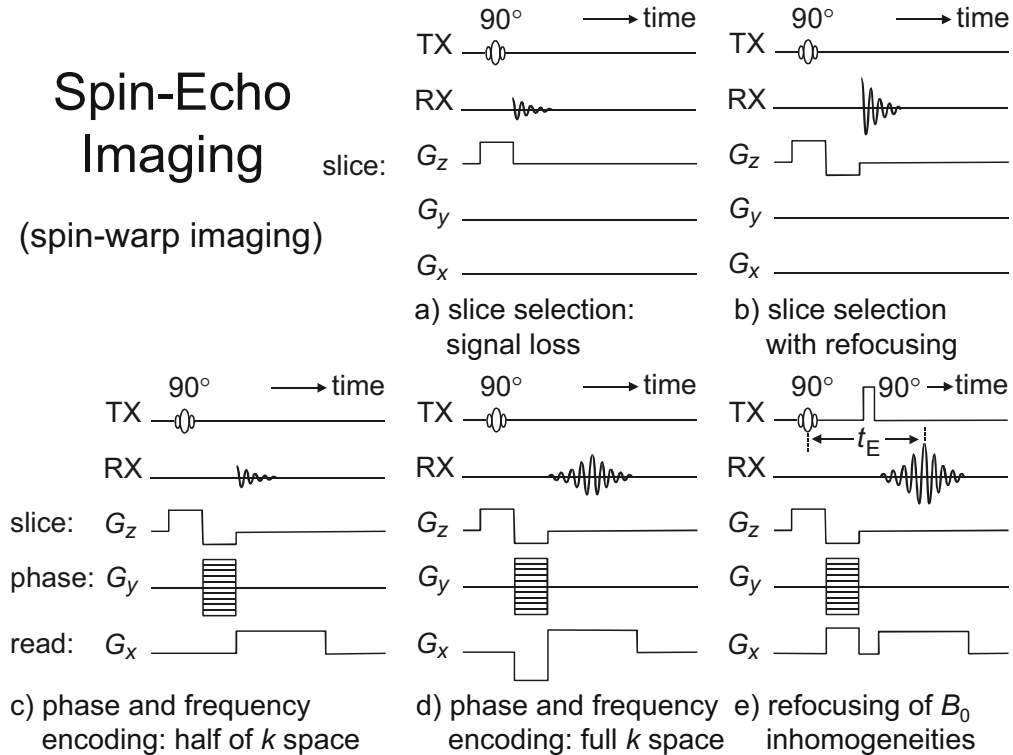
An Example of 2D Spin-Echo Imaging

- 2D *spin-echo imaging* used to be applied in medicine, but imaging times are long, because the longitudinal magnetization between each scan needs to recovered in preparation times of approximate duration 5 T_1
- Rubber is an inhomgeneous product especially when filled with carbon black. Consequently signal loss from magnetization dephasing in local field distortions originating from changes of the magnetic susceptibility within the sample may need to be refocused by the formation of a *spin echo*
- Spin-echo imaging is routinely applied in many tire development centers to probe the *vulcanization* state of the different rubber layers in sample sections cut from the *tire*
- The *image contrast* is largely defined by differences in transverse relaxation during the *echo time* following the initial selective pulse
- Sample regions with soft rubber and mobile additives have long T_2, hard rubber has shorter T_2, and solid polymers like textile fibers have very short T_2
- The typical *spatial resolution* in such images is 1/(0.1 mm) in both dimensions

Spin-Echo Imaging of Tire Samples

100

int. [%]

0

good tire

bad tire

defect region

tread   base

nylon cover   carcass
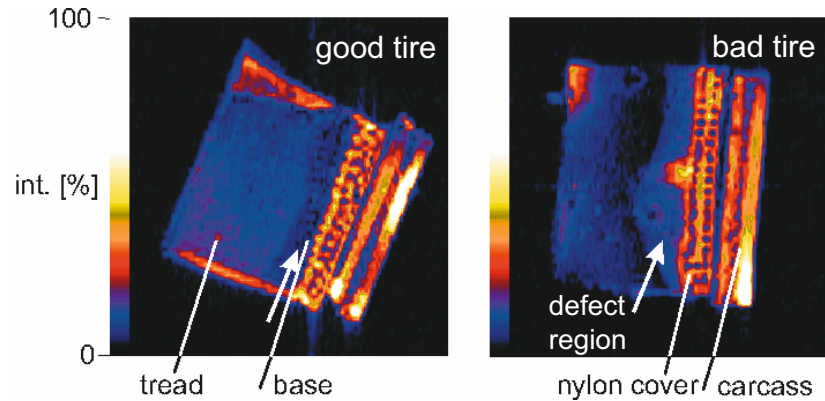
Pirelli pneumatico 1904

steel belt   nylon cover

carcass

liner   steel cord
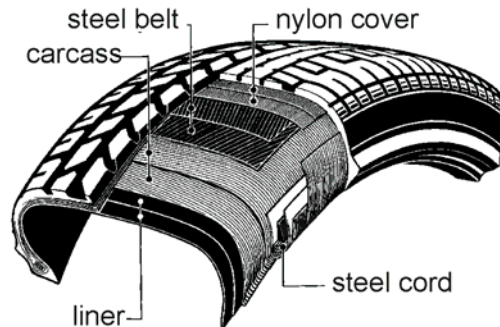
3D Imaging

- *3D images* can be obtained in different ways
- Successive 2D slices measured by slice-selective 2D imaging can be combined to constitute a 2D image
- Here, the spatial resolution perpendicular to the slice plane is low. During acquisition, the signal comes from one selected slice only, while the noise comes from the entire sample
- In *3D Fourier imaging*, the signal is acquired from the same volume which also produces the noise
- The slice-selective pulse is replaced by a non-selective pulse
- A further *phase-encoding gradient* field pulse is introduced and stepped through positive and negative values independent of the other gradient field pulses
- The image is obtained by *3D Fourier transformation* of the acquired data set

3D Spin-Echo Fourier Imaging
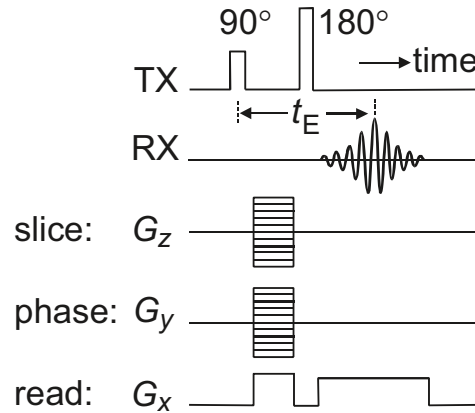
Reducing the Measurement Time

- The measurement time for a *spin-echo image* is determined by the number of lines in the image data matrix and the duration of the *recycle delay* for recovery of the longitudinal magnetization
- Due to the fact that in a spin echo the entire longitudinal magnetization is perturbed, the recycle delay is of the order of 5 T_1
- Shorter recycle delays can be employed if the longitudinal magnetization is only partially attenuated from its thermodynamic equilibrium value
- This is achieved by discarding the 180° refocusing pulse in the imaging sequence. Furthermore, a *small flip-angle pulse* is used instead of the initial 90° pulse to rotate the longitudinal magnetization only partially into the transverse plane
- Following Richard Ernst, the optimum flip angle α_E and the optimum recycle delay t_0 are determined by the longitudinal relaxation time T_1 according to $\cos\alpha_E = \exp\{-t_0/T_1\}$, where is the α_E *Ernst angle*
- The resultant imaging method is called *gradient echo imaging* or *fast low-angle shot* (*FLASH*) imaging
- It is a standard method in *medical imaging*
- It is also suitable for imaging slow dynamic processes in soft matter, such as chemical waves in oscillating reactions

Gradient-Echo Imaging
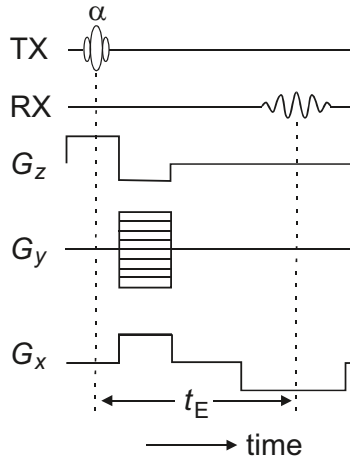
FLASH: fast low-angle shot

A. Haase, J. Frahm, D. Matthei, W. Hänicke, K. D. Merboldt, **J. Magn. Reson. 67** (1986) 258
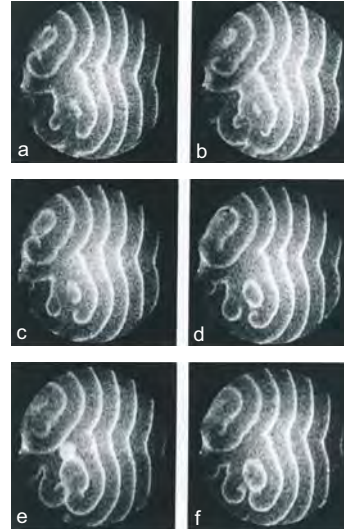
Mn catalyzed Belousov-Zhabotinsky reaction: images at 40 s intervals

A. Tzalmona, R. L. Armstrong, M. Menzinger, A. Cross, C. Lemaire, **Chem. Phys. Lett. 174** (1990) 199

Contrast and Artifacts

- In spin-echo imaging, the image *contrast* is determined by three factors
- 1) The *spin density*, i. e., the number of nuclei at position **r** contributes $M_{z0}(\mathbf{r})$
- 2) *Transverse relaxation* during the echo time t_E contributes $\exp\{-t_E/T_2(\mathbf{r})\}$
- 3) *Partial saturation* due to short recycle delays t_0 contributes $1-\exp\{-t_0/T_1(\mathbf{r})\}$
- In total, the image amplitude is given by $M_{z0}(\mathbf{r})\exp\{-t_E/T_2(\mathbf{r})\}(1-\exp\{-t_0/T_1(\mathbf{r})\})$
- In addition, the contrast is enhanced by *magnetic field distortions* in sample regions, where the *magnetic susceptibility* rapidly changes
- Examples are carbon black filler clusters embedded in a rubber matrix and the interface between distilled water and water doped with copper sulfate
- In *gradient-echo imaging*, the magnetization dephasing due to *magnetic field inhomogeneity is* not refocused, so that susceptibility distortions are enhanced in the frequency encoding direction
- The distortions do not appear in the *phase encoding* dimension because the encoding time t_1 is kept constant
- In *back-projection imaging* with frequency encoding in both dimensions, the artifacts appear symmetrically in both dimensions
- In pure *phase encoding imaging*, they are not observed at all
- In spin-echo imaging, the dephasing from magnetic field inhomogeneity is refocused in the echo maximum during frequency encoding
- *Susceptibility effects* can be considered artifacts in images, but can also be used to generate image contrast, e. g. in carbon-black filled *elastomers*

Susceptibility Contrast

susceptibility distortions

sample

14.15 mm
8.8 mm

distilled
water

28.3
mm

glass

0.6 mm

$Cu\ SO_4 \cdot 5\ H_2O$

spin-echo image

frequency encoding

phase encoding

back-projection
image

phase encoded
image

phase encoding

360° back projection

phase encoding
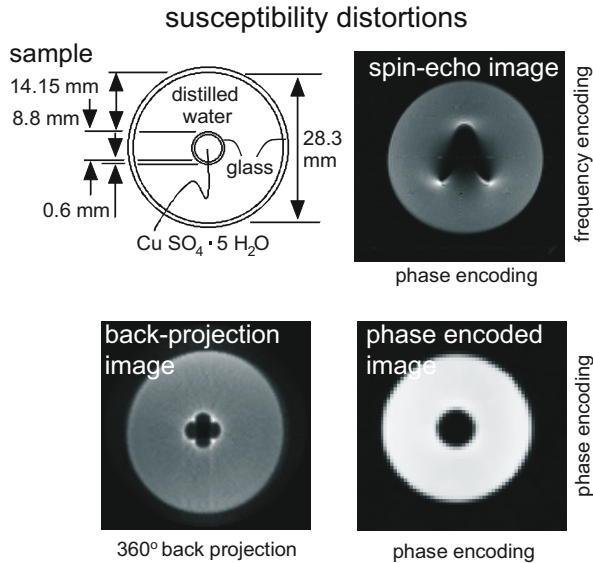
O. Beuf, A. Briguet, M. Lissac, R. Davis,
J. Magn. Reson. B 112 (1996) 111

stacked EPDM sheets

gradient-echo image

spin-echo image

10 mm
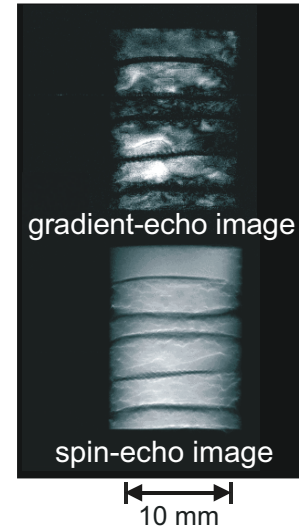
P. Blümler, V. Litvinov, H. G. Dikland,
M. van Duin, **Kautschuk Gummi
Kunststoffe 51** (1998) 865

Parameter Images

- Images of the spin density $M_{z0}(r)$ which are weighted by a function of other NMR parameters, for example by $\exp\{-t_E/T_2(r)\}$, are called *parameter-weighted images*
- By acquisition of several images with different echo times, the parameter $T_2(r)$ can be extracted from the set of images for every position *r*
- The resultant map of $T_2(r)$ is called a *parameter image*
- In rubber, T_2 is often found to be proportional to temperature within small temperature ranges
- Then, a T_2 parameter image $T_2(r)$ can be calibrated into a *temperature map*
- Such a temperature map has been determined by NMR for a carbon-black filled rubber cylinder undergoing small oscillatory shear deformation at a frequency of 10 Hz
- Due to the dynamic loss modulus, some deformation energy is dissipated as thermal energy
- The heating from inside the sample competes with the heat loss through the sample surfaces
- The resultant *temperature distribution* leads to a peak in the center of the sample
- Dynamic mechanical load thus leads to dynamic sample heterogeneity

Temperature Imaging from Relaxation Maps

T_2 calibration

T_2 [ms]

temperature [K]

- 10 phr
- 30 phr
- 50 phr
- 70 phr

temperature [K]

diameter [mm]

- 70 phr
- 50 phr
- 30 phr
- 10 phr
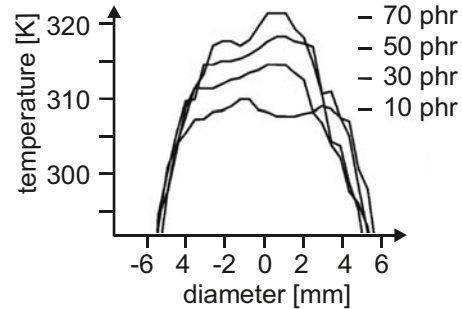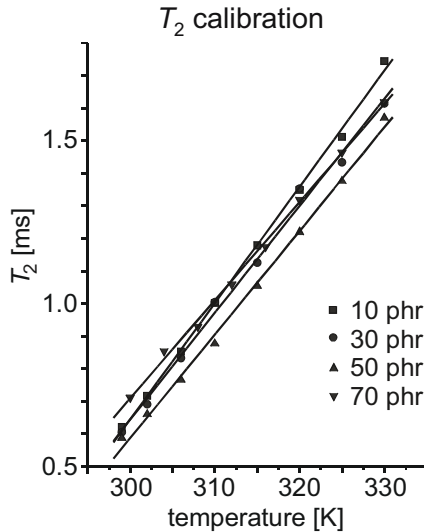
oscillatory
shear
at 10 Hz

carbon black
filled SBR
cylinder
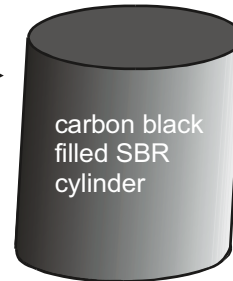
D. Hauck, P. Blümler, B. Blümich, *NMR Imaging of technical SBR vulcanizates under dynamic mechanical load*, **Macromol. Chem. Phys. 198** (1997) 2729 - 2741

Incorporating a Spectroscopic Dimension

- To measure an *NMR spectrum* at each point in space, the *spectroscopic information* is acquired either indirectly or directly
- Indirect acquisition is achieved by stepping through an evolution time point by point in different scans while the gradient field is off
- Direct acquisition corresponds to data sampling in the homogeneous field
- The typical *digital resolution* of an NMR image is 256 points in each dimension
- A 1D NMR spectrum consists of 1024 = 1k to 64 k data points
- For short measuring times, it is preferred to encode the spatial information in an evolution period t_1 indirectly in the signal phase and the frequency information directly in the detection period t_2
- From such *spectroscopic images*, other images can be derived, where the *contrast* is defined by the amplitude of a given line in the NMR spectrum
- This way, the distribution of different chemical compounds can be imaged, for example, in plants, muscles, and the human brain

Spectroscopic Spin-Echo Imaging

with water suppression

c   b a

fennel fruit

without water suppression

d   x 16

9 8 7 6 5 4 3 2 1 0
ppm

$90°$ $180°$

TX ——— → time

t_E t_2

RX

slice: G_z

phase: G_y

phase: G_x

a

water suppressed

b

methoxy

c

aromatic & olefinic

d

water image

H. Rumpel, J. M. Pope, **Magn. Reson. Imag. 10** (1992) 187
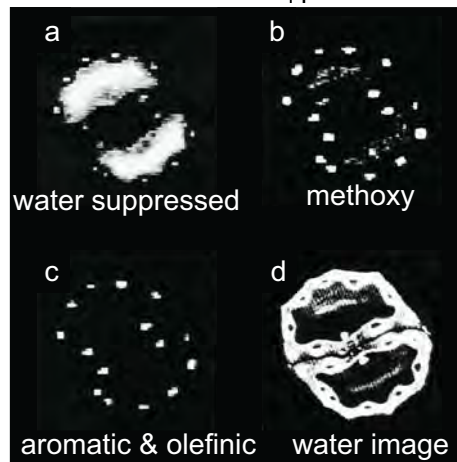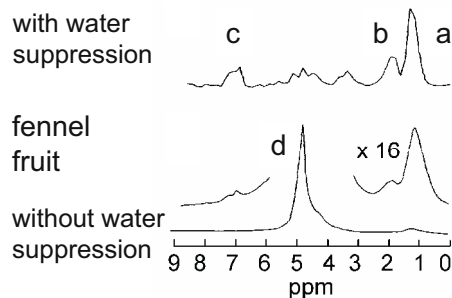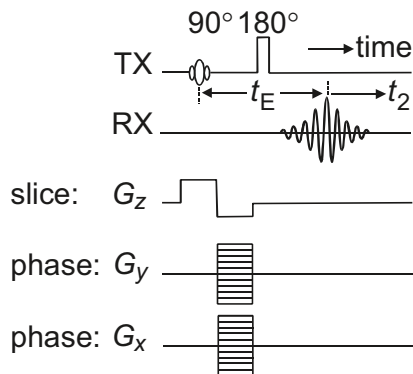
Acquiring Images in a Single Scan

- Fast imaging methods exploit different principles
- In the *steady state free precession* method the transverse magnetization stays in dynamic equilibrium with the excitation and with relaxation
- Other methods use multiple scans in rapid succession without recovery time by avoiding Hahn echoes in favor of gradient echoes. One such method is the *FLASH* method
- But the entire image can also be acquired in one shot by generating multiple echoes, where each echo encodes a different trace through k space.
- Methods of this type are referred to as *echo planar imaging* (*EPI*)
- In medical imaging, they are usually pure gradient-echo methods to avoid excessive rf exposure
- In the original EPI method, k space is scanned in either a zig-zag trace or in parallel traces on a Cartesian grid by rapidly pulsing gradient fields
- A method less demanding on hardware and less noisy to the environment is the *spiral imaging* scheme, where the trace through k space forms a spiral

Echo-Planar Imaging (EPI)

TX

RX

G_z

G_y

G_x

time

Cartesian EPI

TX

RX gate

G_z

G_y

G_x

time
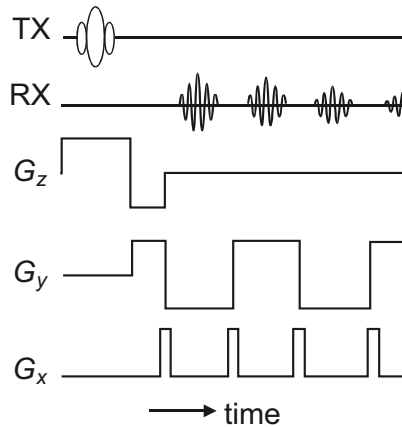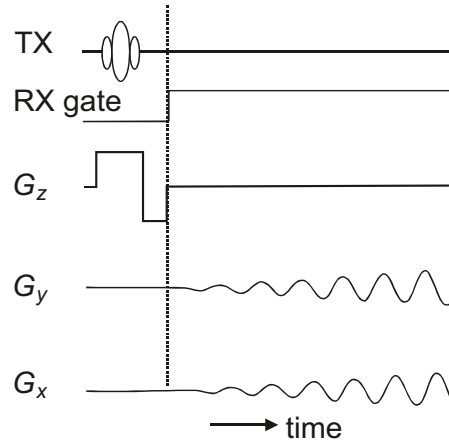
spiral EPI

$k_x(t) = \gamma \, k_0 \, t \sin \omega_k t$

$k_y(t) = \gamma \, k_0 \, t \cos\omega_k t$

$\gamma \, G_{xy}(t) = d/dt \, k_{xy}(t)$

Space Encoding with B_1 Gradient Fields

- Most NMR experiments in the laboratory frame have a counterpart in the rotating frame
- For *imaging in the rotating frame* magnetic gradient field can be the rf field, for example in the *y* direction
- Using *anti-Helmholtz coils* (*Maxwell coils*) or simple unilateral current loops to generate this field, the gradient points in the same direction as the rf fields, i. e. the coil generates the component G_{yy} of the gradient tensor
- Excitation with such a B_1 gradient field generates space dependent flip angles θ, for example along the *x* direction
- With a homogeneous 90° pulse along the *x* direction generated by a *saddle coil,* this flip-angle dependent excitation is converted into a phase-angle distribution of the transverse magnetization
- Signals with pure amplitude modulation are obtained by combination of two data sets, one acquired with a $+90°_x$ pulse and the other with a $-90°_x$ pulse
- The saddle coil with the homogeneous B_1 field is also used for signal detection
- Space encoding in the *z* direction is done via a gradient G_{zz} in the polarization field
- The advantage of B_1 *imaging* is short gradient switching times
- The disadvantage is a complicated scenario for the rf coils in 3D imaging

Rotating Frame Imaging
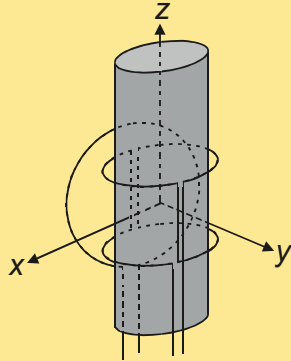
G_{yy} TX, RX
coil arrangement with the B_1
gradient field in the y direction

G_{yy}

G_{zz}

TX $90^\circ_{\pm x}$

t_1 t_2

M_0 θ 90°_x M_0

M_0 θ 90°_{-x} M_0
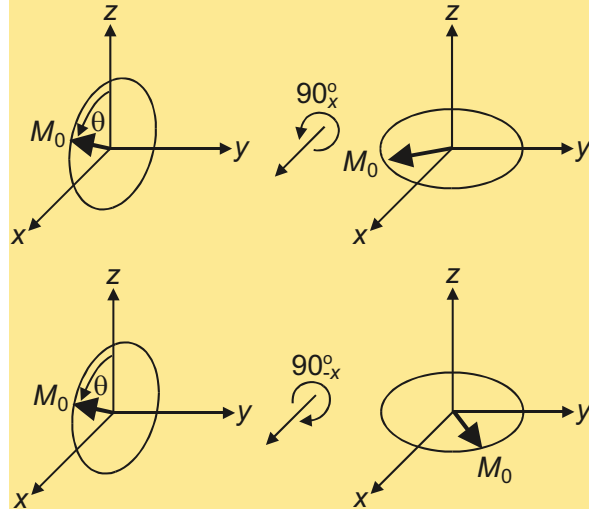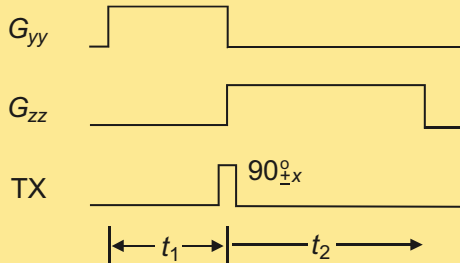
pulse sequence for 2D imaging with amplitude modulation: acquire two data sets

principle pulse sequence for 2D
Fourier imaging: phase modulation

Ultra-High Time-Invariant Gradient Fields

- Solids usually exhibit wide lines due to *dipolar* or *quadrupolar broadening*
- Approaches to *high-resolution NMR imaging of solids* rely on either strong field gradients, on line narrowing, or on combinations of both
- The strongest field gradients are encountered in *stray fields* of, for example, super-conducting magnets
- For many magnets, planes of constant gradient strength are found outside the magnet hole
- For imaging, the sample is physically shifted through that plane, and the amplitude of the NMR echo is acquired for each position
- For a given sample orientation, the collection of NMR echoes for each position shift is a *projection* of the T_2-weighted spin density
- Different projections are acquired for different sample orientations, so that an image of the sample can be reconstructed from these projections
- The technique works well for rigid solids, but sample shifting is somewhat awkward
- Instead of mechanically shifting the sample through the sensitive plane, the position of the plane can be shifted through the sample by means of an additional field in *z* direction which is adjustable in its strength

Stray-Field Imaging (STRAFI)

principle set-up

magnet cryostat

main field coil

profile with sweep coils energized

initial profile

field-sweep coil

STRAFI plane moves with field

B_0

z

12.8 mm

12.8 mm

STRAFI image of a composite from layers of PPS (bright) and PPS with carbon fibers (dark).
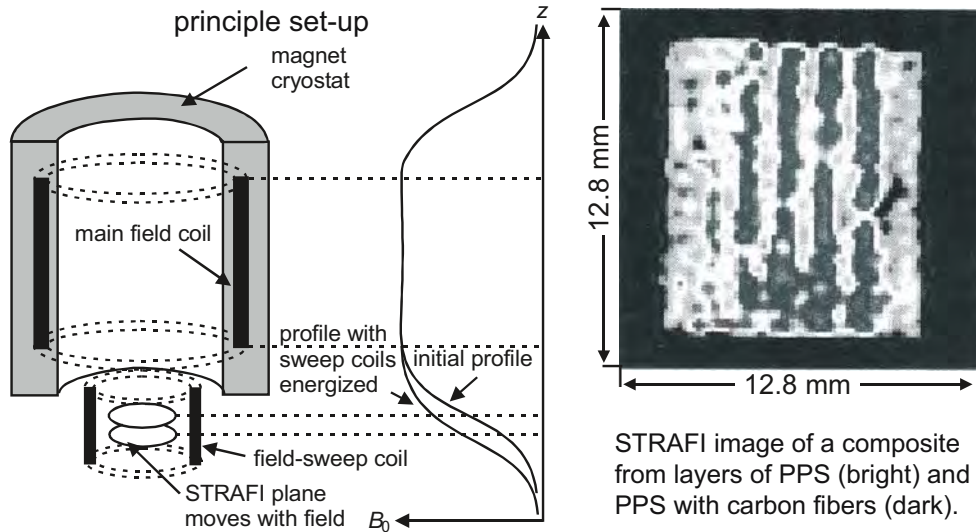
A. A. Samoilenko et al., **Bruker Report 2** (1987) 30;
R. Kimmich et al., **J. Magn. Reson. 91** (1991) 136;
M. J. D. Mallet, M. R. Halse, J. H. Strange, **J. Magn. Reson. 132** (1998) 172

J. H. Iwajima, S. W. Sinton, **Solid-State Nucl. Magn. Reson. 6** (1996) 333

B. Blümich, *NMR Imaging of Materials*, Clarendon Press, Oxford, 2000 (by permission of Oxford University Press)

High, Time-Dependent Gradient Fields

- Time dependent gradient fields can be generated by driving the gradient field coils in resonant mode by a sine wave
- The resonant mode maximizes the current in the coils for maximum field strength
- By driving the *x* gradient with a negative lobe of area k_{xmax} and a positive lobe of area $2k_{xmax}$, a gradient echo is formed in the maximum of the *x* gradient, and frequency encoding can be used to scan k_x
- The phase encoding gradients are simple sine waves with variable amplitude and their periods adjusted to twice the echo time
- The rf pulse is applied in the amplitude node common to all three *oscillating gradients*
- The sampling grid in **k** space is distorted from a regular square pattern due to the varying gradient strength in *imaging with oscillating gradients*
- Numerical routines should be used for data extrapolation to a Cartesian grid before Fourier transforming the data to obtain an image
- The technique works well for soft solids

Imaging with Oscillating Gradients

pulse scheme

TX

G_x 2 A A A

G_y

G_z

RX detection

time

k-space coverage

k_y

k_x

0
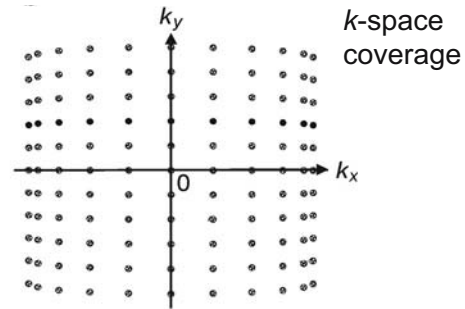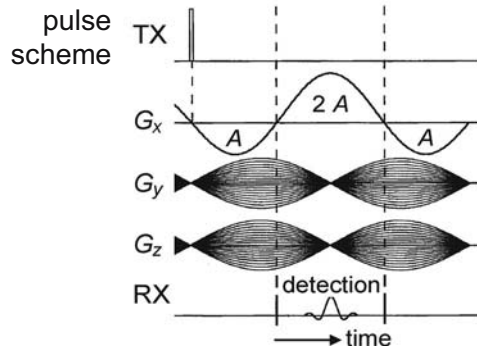
surface-rendered images of a Lego brick

S. L. Codd, M. J. D. Mallet, R. Halse, J. H. Strange, W. Vennart, T. van Doorn, **J. Magn. Reson. B 113** (1996) 214

Imaging with Pure Phase Encoding

- The most successful technique for imaging solid samples is *single-point imaging* (*SPI*)
- k space is sampled by pure phase encoding
- A short rf pulse with a small flip angle is applied in the presence of a gradient field
- A single point of the FID is sampled after a short dead time t_1
- The gradient is ramped to a different value and the experiment is repeated
- Depending on the flip angle and the repetition time, T_1 contrast is introduced
- Different filters can be introduced to prepare the initial longitudinal magnetization, for example, an inversion recovery filter for T_1 contrast and a spin echo filter for T_2 contrast
- Despite the pure phase-encoding procedure, the acquisition of images can be rather fast, such as 50 s for a single scan of an image with 128×64 data points

Single-Point Imaging (SPI)
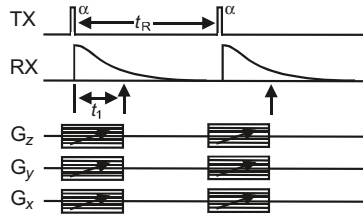
basic pulse sequence
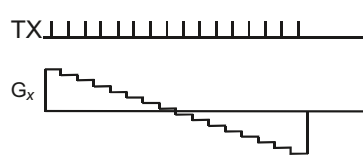
SPRITE: single-point ramped imaging with T_1 enhancement
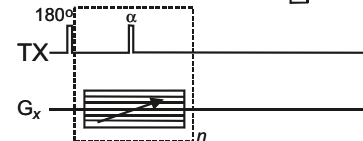
T_1 filter
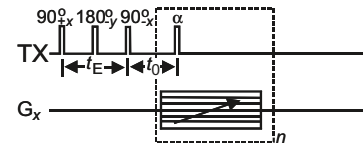
T_2 filter

P. Prado, B. J. Balcom, M. Jama, **J. Magn. Reson. 137** (1999) 59

external layer

fabric

20 mm

10 mm
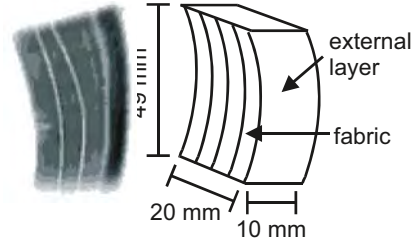
tire section: 200 s acquisition time
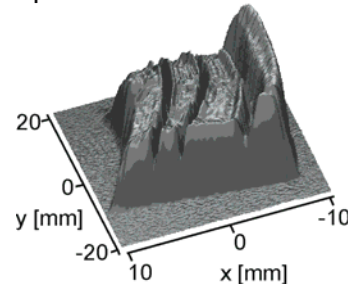
P. Prado et al, **Macromol. Mat. Eng. 274** (2000) 13 - 19

Imaging Solids by Manipulation of Spin Interactions

- If the NMR line is narrow in a homogeneous field, high-resolution imaging can be achieved with low gradient strengths
- Broad lines from solids can be narrowed to obtain good spatial resolution with low gradient strengths
- Optimum *line narrowing* is obtained when all spin interactions are refocused
- The dominating spin interactions in solids are the *dipole-dipole interaction* and the *chemical shift* including the chemical shift anisotropy
- The dipole-dipole interaction is refocused by the *magic echo*
- The chemical shift is refocused by the *Hahn echo*
- Both interactions are refocused by a combination of both echoes, the so-called *mixed echo*
- Good results are already obtained with the magic echo only
- For the magic echo, the phase encoding gradients can be on during the whole length of the magic-echo pulse sequence
- *Slice selection in solids* is a difficult task
- Acceptable results are obtained with the *spin-lock sequence* applied in the presence of a gradient field
- The stronger the lock field, the thicker the selected slice

Magic-Echo Phase Encoding

slice selection   space encoding   spectro-scopic detection

pulse sequence with spin-lock slice selection

TX

x $-x$ x y $-y$

SL_y SL_x SL_{-x}

0   τ 2τ 3τ 4τ 5τ 6τ

RX

G_x

G_y

G_z

time

HMB
PTFE
HMB

2.4 mm
2.9 mm
3.2 mm
4.8 mm

application to a phantom from HMB and PTFE
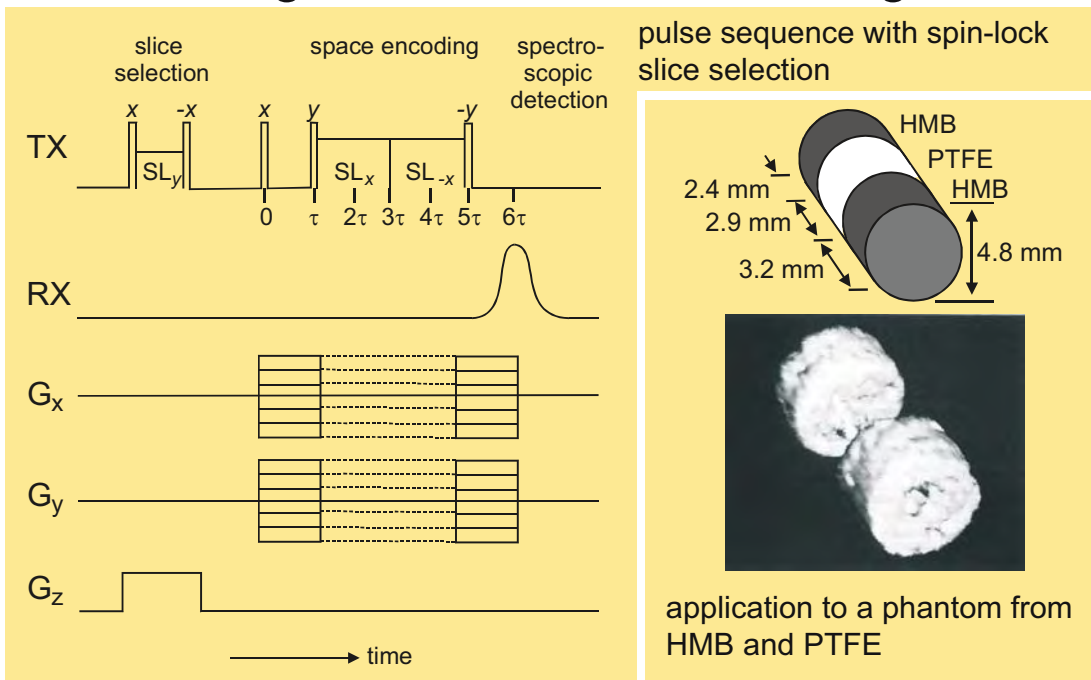
S. Hafner, D. E. Demco, R. Kimmich, **Solid State Nucl. Magn. Reson 6** (1996) 275
B. Blümich, *NMR Imaging of Materials*, Clarendon Press, Oxford, 2000 (by permission of Oxford University Press)

Tricks With Coupled Spins

- Systems of *coupled spins* and *quadrupolar spins* give rise to *multi-quantum coherences*
- The dephasing angle of coherences by precession in gradients fields is proportional to the *coherence order*
- A double-quantum coherence dephases twice as fast as a single-quantum coherence
- Phase encoding of multi-quantum coherences effectively multiplies the strength of the gradient field by the coherence order
- Such an approach only works if the multi-quantum relaxation time is long enough, as in the case of the double-quantum coherence of deuterons
- In other cases, the multi-quantum coherence can still be exploited to separate signals from uncoupled and coupled spins or from isotropic and anisotropic material regions
- *Double-quantum imaging* and *double-quantum filtered imaging* have successfully been applied to image local stress and strain in rubber bands by discriminating the signals from differently deformed macromolecular coils in the rubber network

Imaging of Double-Quantum Coherences

application to a strained rubber band with a cut

pulse sequence:
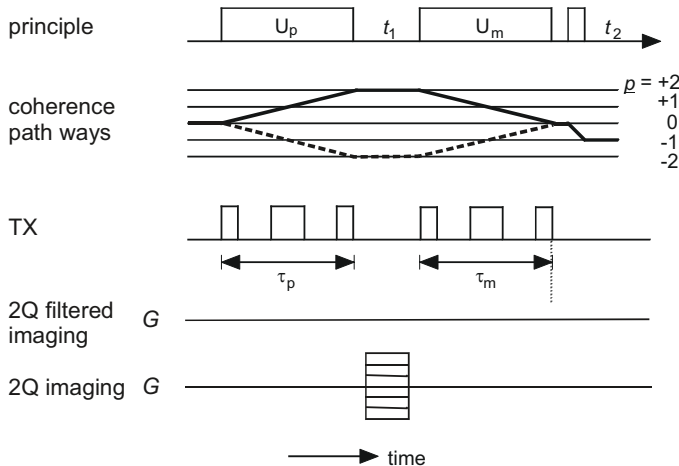
¹H 2Q-filtered image

2H 2Q image
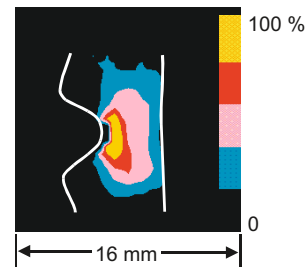
M. Schneider, D. E. Demco, B. Blümich, **J. Magn. Reson. 140** (1999) 432;
M. Klinkenberg, P. Blümler, B. Blümich, **Macromolecules 30** (1997) 1038

Imaging of Double-Quantum Coherences

application to a strained rubber band with a cut

Early Medical Images

- The first medical images were measured in 1978 by Raymond Damadian and co-workers by the *FONAR* method
- They acquired images point-by-point in real space by shifting the patient through the sensitive region of an inhomogeneous field
- The sensitive region was defined by a saddle point of the B_0 field profile
- The acquisition time was several hours, and the image quality was low
- Yet, 10 years later NMR imaging was already an indispensable diagnostic tool in hospitals all around the world
- However, it was not the clumsy FONAR method reaching the finishing line, but the *spin warp imaging* technology developed at General Electric by W. Edelstein and collaborators
- Spin warp imaging is spin-echo imaging with a fixed evolution time in which the gradients are incremented to scan *k* space
- Already in the original spin-warp publication promising *parameter images* of the *spin density* and of T_1 from slices through different parts of the human body were published

FONAR versus Spin Warp Imaging

FONAR: Field Focused Nuclear Magnetic Resonance
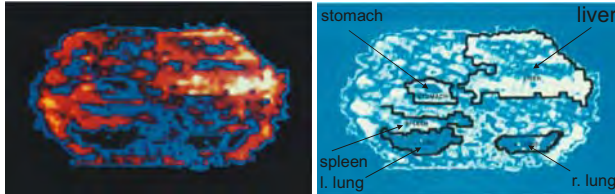
R. Damadian, L. Minkoff, M. Goldsmith, NMR in Cancer: XXI. FONAR Scan of the Live Human Abdomen, **Physiol. Chem. & Physics 10** (1978)
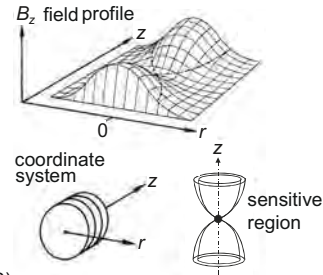
Spin Warp Imaging: head section, 25 mm below the eyes
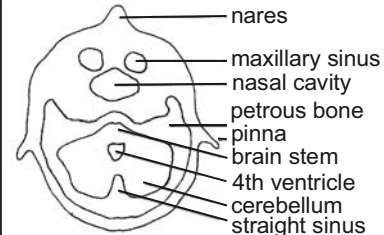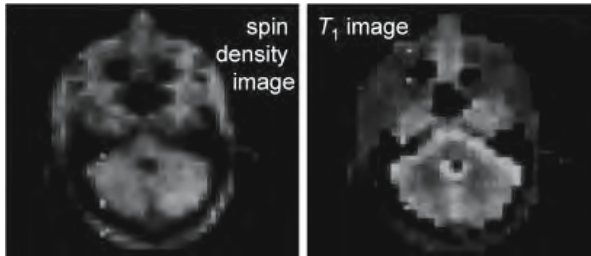
W. A. Edelstein, J. M. S. Hutchison, G. Johnson, T. Redpath, *Spin Warp Imaging and Applications to Human Whole-Body Imaging*, **Physics in Medicine and Biology 25** (1980) 751 – 756 (by permission of IOP Publishing, Bristol)

Imaging Flowing Liquids

- Probably the most important application areas of imaging outside biomedicine are in *chemical engineering* and *materials science*
- Many questions of interest in chemical engineering concern the characterization of *flow phenomena* often in optically opaque media such as fluid flow, granular flow, and molecular self- and interdiffusion
- As long as these media are non-magnetic and radio-frequency transparent, the particle transport can be measured by NMR
- Usually, the phenomenon in question has to be reproduced inside the magnet unless unilateral NMR techniques are employed and the object is investigated from one side
- An important, optically non-transparent fluid is *blood*. Its rheological properties are of interest in medical technology for building devices like artificial arteries and veins, hemodialyzers, and blood pumps. Only the blood substitute water/glycerol is sufficiently transparent for optical velocity analysis
- Using NMR with pulsed gradient fields, *velocity vector fields* can be imaged
- It is useful to select a slice of the moving fluid, which stays inside the resonator for the duration of space and velocity encoding as well as detection
- A complete velocity image has six dimensions: 3 for space and 3 for velocity
- Also, the velocity distribution can be determined in each pixel

Flow Imaging of Blood
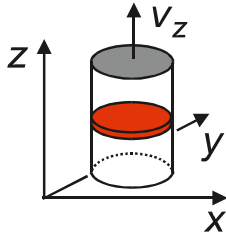
S. Han, O. Marseille, C. Gehlen,
B. Blümich, *Rheology of blood
by NMR,* **J. Magn. Reson. 152**
(2001) 87 – 94
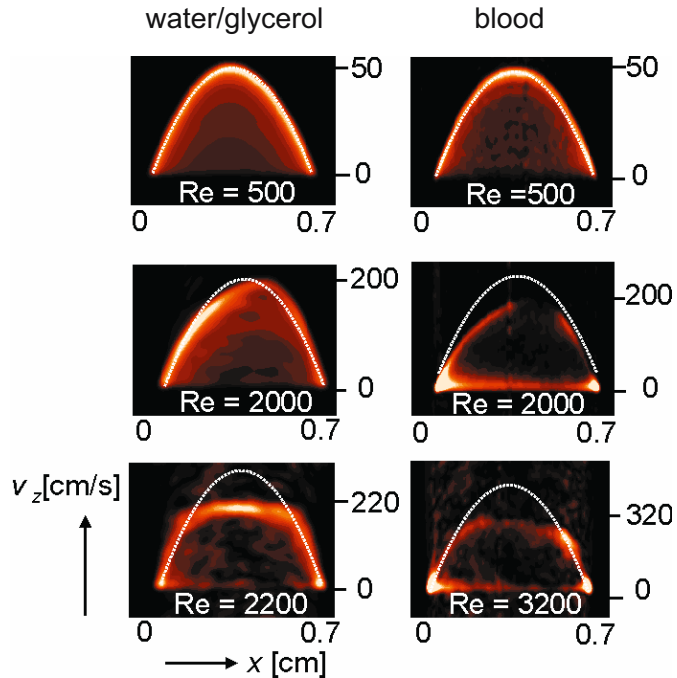
Pulse-Sequence Design

- Pulse sequences for *velocity imaging* have to incorporate *space encoding* by scanning **k** space and *flow encoding* by scanning $\boldsymbol{q}_v$ space
- The encoding of **k** and $\boldsymbol{q}_v$ spaces must be done independently within one pulse sequence, that is, during data acquisition only one **k** or one $\boldsymbol{q}_v$ component can be varied. The other components must be constant
- Typically, one **k** component is frequency encoded for direct acquisition and the other components of **k** and $\boldsymbol{q}_v$ are phase encoded in the acquired signal
- A compromise has to be made for the velocity component in the same direction as the frequency encoded space component. Here, complete decoupling is not possible
- For example, to image $v_z(x,y)$, an *xy* slice is selected, and k_x, k_y, q_{vz} are varied
- The components q_{vx}, q_{vy}, and k_z should be zero during data acquisition
- If frequency encoding is used for k_x, then q_{vx} also varies during the detection time
- The optimum gradient timing scheme for such sequences is usually determined using a computer
- After Fourier transformation over k_x, k_y, and q_{vz}, the possibly relaxation-weighted spin density $M_z(x,y,v_z)$ is obtained
- The components $v_z(x)$ and $v_z(y)$ can readily be extracted from it

Pulse Sequence for Flow Imaging

slice selection and phase encoding of v_z

phase encoding of y

frequency encoding of x

evolution of moments of orders 0 and 1 for position and velocity encoding in x, y an z directions

B. Blümich, *NMR Imaging of Materials*, Clarendon Press, Oxford, 2000

90°   180°

TX

RX

slice / flow
G_z

phase
G_y

read
G_x

k_x

$q_{vx}/12$

k_y

q_{vy}

k_z

$q_{vz}/7$
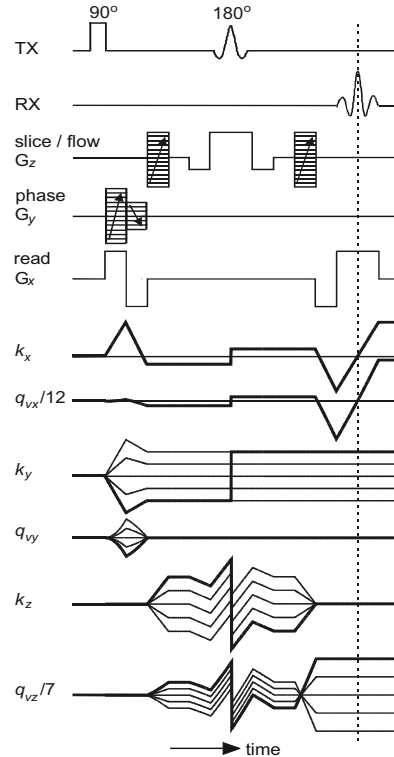
time

Imaging Velocity Fields

- *Flow imaging* by NMR usually requires long acquisition times ranging from several minutes to several hours
- Flow processes suitable to NMR imaging must, therefore, be either stationary or repetitive
- An example of a repetitive process is the *vortex motion* in a drop of water falling through the NMR magnet
- Due to the short residence time of the drop in the receiver coil, *single-point acquisition* is necessary for all points in k and q_v space
- Drops from different dripping experiments show different velocity profiles
- A *water drop* covered with a surfactant does not show internal motion
- A 2D velocity vector field is composed of two data sets, each providing one of the two in-plane velocity components
- If k or q_v space is traced in only one or two dimensions, a projection is acquired in real space or in velocity space (see below: *projection – cross-section theorem*), i. e. the spin density is integrated over the missing space and velocity components

NMR Imaging of the Falling Drop

zx projection of the velocity vector field
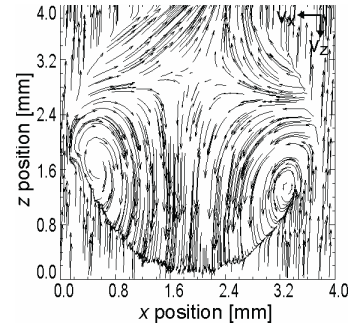
maps of velocity components

water drop I   water drop II   surfactant drop
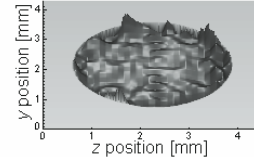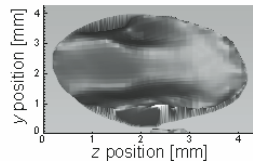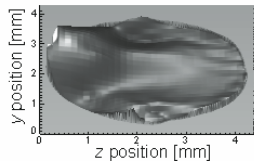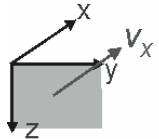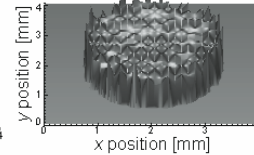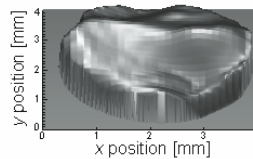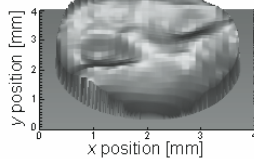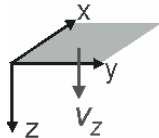
Probability Densities of Velocity

- *Probability densities* are called *distributions* in short
- A *distribution of velocity* is the Fourier transform of the NMR signal as a function of q_v
- Usually, only one component of q_v is varied and the distribution is plotted against *displacement* in a given time instead of against velocity
- This notation is popular for diffusive motion. In the NMR community, the corresponding *distribution of displacements* is called the *propagator*
- The distribution of velocities is most simply measured with pulsed gradient fields by a pair of anti-phase gradient field pulses, and the amplitude of the associated echo is recorded as a function of the gradient amplitude
- In principle, the experiment can be conducted with time invariant gradient fields as well by varying the echo time t_E in an echo experiment
- For *laminar flow through a circular pipe* the *velocity profile* is parabolic
- The velocity distribution is obtained by equating the probability density $P(v)$ dv of finding a velocity component between v and $v + $ dv with the area of the ring at radius r and of width dr in which these velocity components are found
- The distribution is constant for all velocities between 0 near the tube wall and v_{max} in the center, and zero elsewhere; it has the shape of a *hat function*
- *Velocity distributions* are very sensitive against slight imperfections in the experimental set-up; they may provide better fingerprints of the flow process than *velocity images*

Laminar Flow in a Circular Pipe

theory: $v(r) = \dfrac{v_{max}}{R^2}(R^2 - r^2)$ $P(v)\,dv = \dfrac{2\,\pi\,r\,dr}{\pi\,R^2}$

$$P(v) = \frac{2\,\pi\,r}{\pi\,R^2\,\dfrac{dv}{dr}} = \frac{1}{v_{max}}$$

$<v>$ = 4.6 cm/s

$<v>$ = 9.2 cm/s

$\dfrac{1}{v_{max}}$

data acquired in a time-invariant and space-invariant gradient field

-30   -20   -10   0   10   20   30

v_{max}

v [cm/s]

experimental data
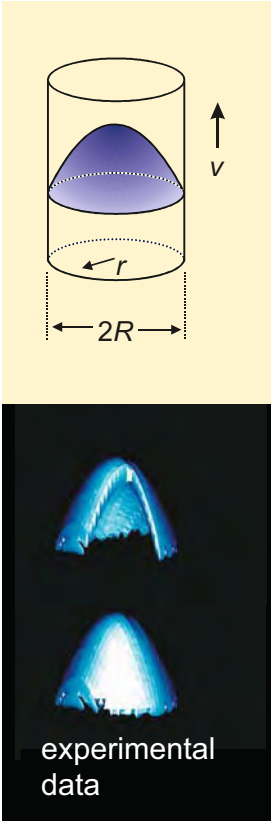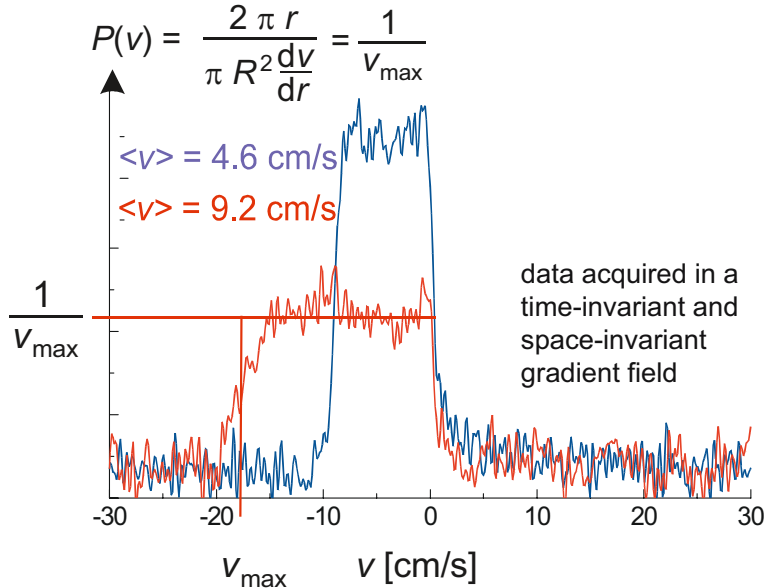
Velocity-Vector Distributions

- *1D velocity distributions* are *projections* of 3D velocity distributions obtained by integration over the missing velocity components
- *2D velocity distributions* provide much more detailed information than 1D distributions
- They are obtained by measuring the NMR signal corresponding to the number of spins as a function of two components of the wave vector q_v and subsequent 2D Fourier transformation
- Flow through circular pipes filled with glass beads or cotton fibers can readily be distinguished by the associated 2D distributions of radial and axial velocities
- For the cotton fibers, strong radial dispersion is observed at high axial flow
- For the glass beads, considerable axial backflow is observed at zero radial flow
- The observed velocities are *finite difference approximations* of velocities corresponding to the displacements R experienced in the encoding time Δ_v
- For field gradient pulses with durations δ no longer short compared to the characteristic times of motion, the *slow motion approximation* fails and the finite difference interpretation can no longer be applied

2D Velocity Distributions

glass beads

polymer-fiber plug
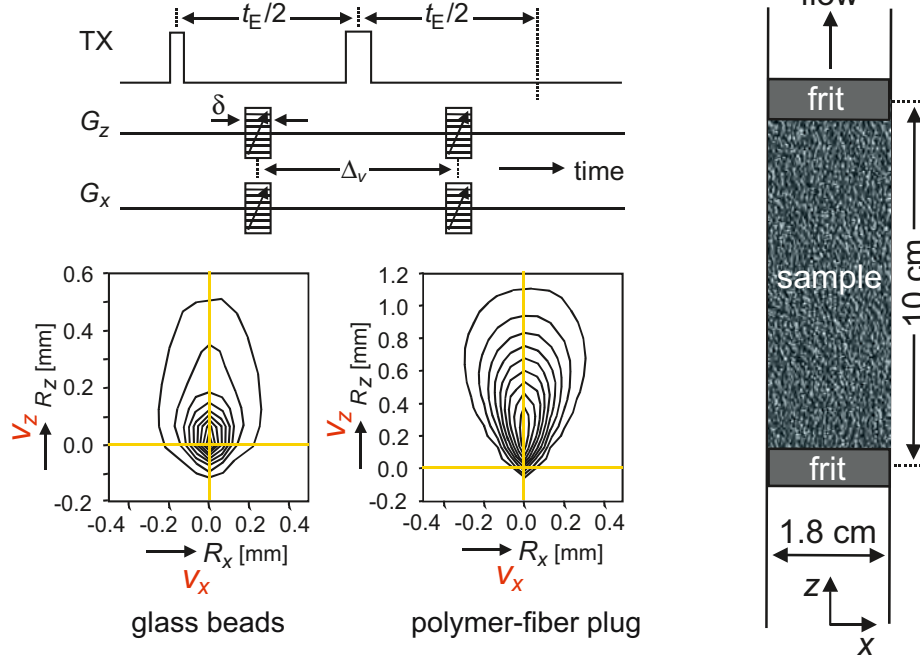
B. Blümich, *NMR Imaging of Materials*, Clarendon Press, Oxford, 2000

Diffusion in Anisotropic Media

- *Translational diffusion* leads to *incoherent displacements* as opposed to *coherent displacement* of molecules by flow
- To probe incoherent motion, displacements *X, Y, Z* are measured in given time intervals Δ_v by the use of *pulsed gradient fields* (*PFG NMR*: pulsed field gradient NMR)
- For free diffusion, the *distribution of displacements* (*propagator*) has a Gaussian form, and the diffusion length scales with the square root of the diffusion time
- For *restricted diffusion* in narrow pores, for example in rocks and hetero-geneoeus catalysts, the confining pore walls limit the diffusion path length
- For short diffusion times, a *Gaussian distribution* is observed. For long diffusion times, the confinements lead to deviations from a Gaussian distribution
- Macroscopically anisotropic porous media, such as oriented biological tissue and ice formed from salt water can readily be identified by comparing the 1D distributions of displacements in different space directions
- Another method is the analysis of *2D distributions of displacements* for deviations from circular symmetry

Oriented Salt-Water Ice

1D distributions

2D distribution
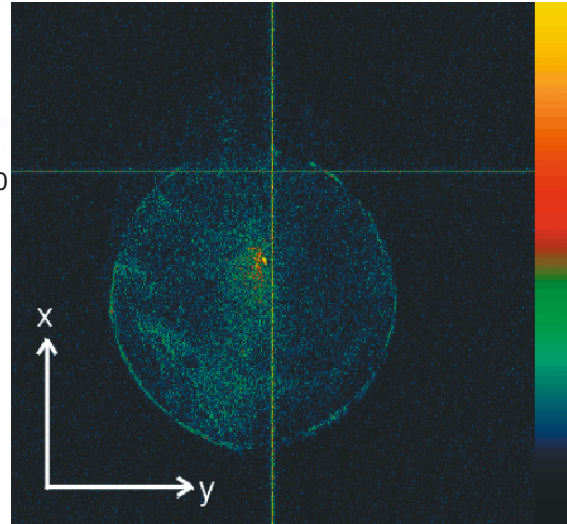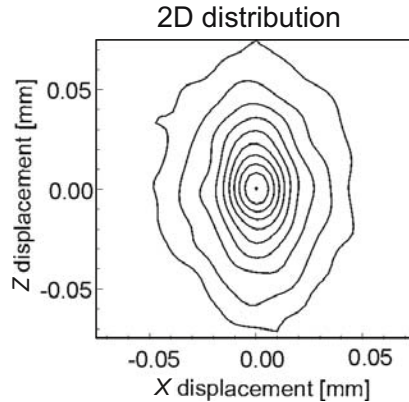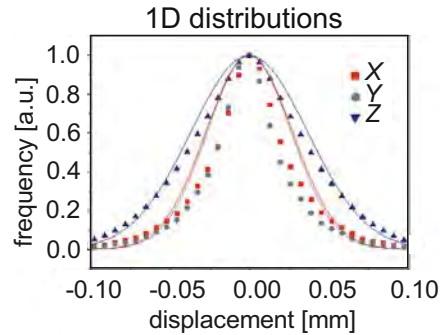
M. Menzel, S.-I. Han, S. Stapf, B. Blümich, *NMR Characterization of the Pore Structure and Anisotropic Self-Diffusion in Salt Water Ice,* **J. Magn. Reson. 143**, 376 – 381 (2000)

Position Exchange NMR

- Measurements of *flow* or *displacements* in given times are achieved by pulsed anti-phase gradient pairs, the second, positive pulse marking final position and the first, negative one initial position
- For measurements of displacements, both gradients pulses are locked to equal magnitude in each amplitude step, i. e. $k_2 = -k_1$ at all times
- Stepping both gradient pulses independently leads to a 2D experiment
- The Fourier transform of the acquired data is the joint probability density of finding a particle at a particular initial position and a time Δ later at a particular final position
- On the principal diagonal, the average of the initial and final particle positions is identified; on the secondary diagonal, the difference between final and initial positions, i. e. displacement or velocity, is identified
- The experiment is called *position exchange spectroscopy* (*POXSY*) in close analogy to frequency *exchange spectroscopy* (*EXSY*) in NMR spectroscopy
- A 4D exchange experiment results with four gradient pulses
- Conditions on the gradient variations, such as the formation of *gradient echoes* for detection, reduce the dimensionality of the experiment
- The conditions $k_2 = -k_1$ and $k_4 = -k_3$ imposed on the 4D POXSY sequence lead to *velocity exchange spectroscopy* (*VEXSY*)
- Here, *average velocity* is identified along the principal diagonal and velocity difference or *acceleration* along the secondary diagonal
- The additional condition $k_4 = -k_3 = -k_2 = k_1$ leads to a 1D experiment by which the *distribution of accelerations* can be measured

Pulsed Gradient Field NMR

$G_z z_0$ — k_1 k_2 k_3 k_4 — time

4D PFG exchange NMR

t_{m1} t_{m2} t_{m3}

q_{v1} q_{v2}

$G_z z_0$ — $-k_1 = k_2$ $-k_3 = k_4$ — time

Δ_1 t_m Δ_2

$k = 0$ $k = 0$

2 echo conditions:
$k_2 = -k_1$; $k_4 = -k_3$

ε_z

$-q_{v1} = q_{v2}$

$G_z z_0$ — $k_1 = -k_2 = -k_3 = k_4$ — time

Δ_v Δ_a Δ_v

$k = 0$ $k = 0$
$q_v = 0$

further condition:
$q_{v2} = -q_{v1}$
probability density
of acceleration
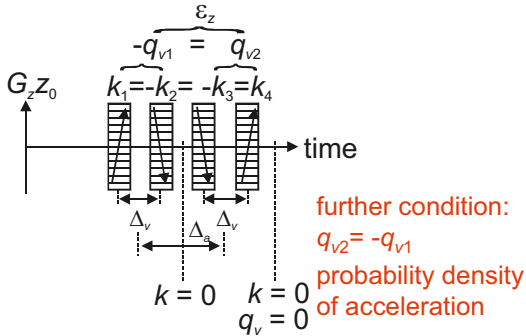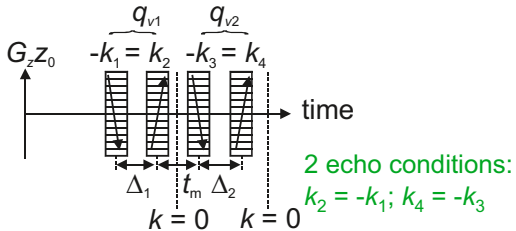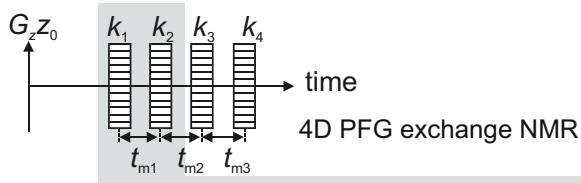
2D PFG exchange
NMR: POXSY

k_2 $\propto q_v$ $\bar{k}$ k_1

VEXSY

q_{v2} $\propto \varepsilon$ $\bar{q}_v$ q_{v1}
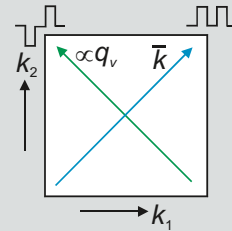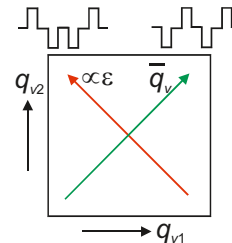
Demonstration of Position Exchange NMR

- An instructive example of a *position exchange experiment* is that performed on the falling *water drop*
- Initial and final positions are marked in the Fourier domain by the wave numbers k_1 and k_2
- The maximum of a Hahn or a stimulated echo with a gradient pulse in each free evolution period is recorded for all values of k_1 and k_2
- The 2D Fourier transform of the experimental data set is the position exchange spectrum
- Along the principal diagonal, the projection of the drop onto the gradient direction appears
- Along the secondary diagonal, the drop displacement during the encoding time Δ corresponding to the *velocity* of the falling drop appears
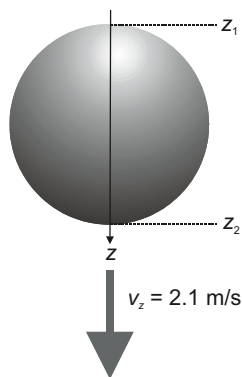
Position Velocity Correlation of a Falling Drop of Water

$v_z = 2.1$ m/s

90°   180°

TX

RX

k_1 k_2

G

Δ

t_1 t_2 time

$v = \mathrm{d}z / \mathrm{d}t$

$\approx (z_2 - z_1) / \Delta$

position Z_1 [mm]

average position

3 mm   4 mm   5 mm   6 mm   7 mm

2.1 m/s

velocity
$(Z_2 - Z_1)/\Delta$

position Z_2 [mm]
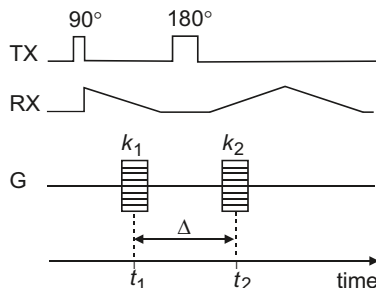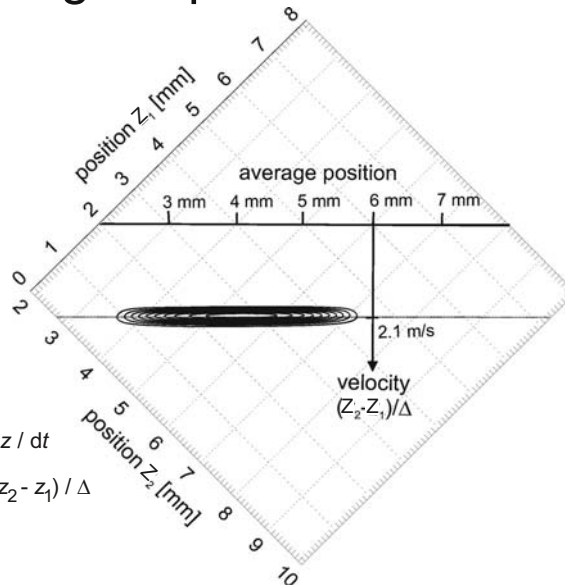
S. Han, B. Blümich, *Two-dimensional representation of position, velocity, and acceleration by PFG-NMR,* **Appl. Magn. Res. 18** (2000) 101 – 114

Velocity Exchange NMR

- Similar to the *position exchange NMR*, initial and final velocities can be encoded in terms of q_{v1} and q_{v2} along the axes of a 2D data matrix, leading to *velocity exchange NMR*
- Velocity exchange NMR has been used to study *cross-filtration* in hollow-fiber filtration modules which are used in hemodialysis as artificial kidneys
- Water was passed inside and outside the hollow fibers in counter flow
- Water molecules crossing the membrane must change their direction and lead to off-diagonal peaks in a velocity exchange spectrum
- On the diagonal, the distribution of *average velocity* is observed
- For negative velocities it is the *hat function* corresponding to *laminar flow* within the circular membranes. For positive velocities, the distribution corresponds to the interstitial flow and depends on the packing of the fibers
- The projection along the principal diagonal and onto the secondary diagonal of the velocity exchange spectrum eliminates average velocity from the data set, and the remaining variable is velocity difference or *acceleration*
- For two different membrane materials, the velocity exchange spectra are different and so are the projections onto the secondary diagonals, i. e. the *acceleration distributions*
- The SPAN material shows signal at high accelerations corresponding to efficient interactions of the passing molecules with the membrane walls

Cross Filtration by VEXSY
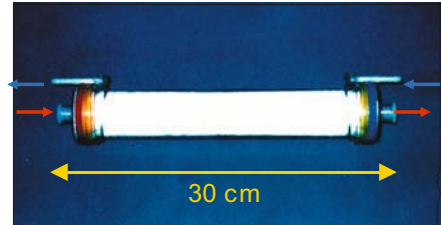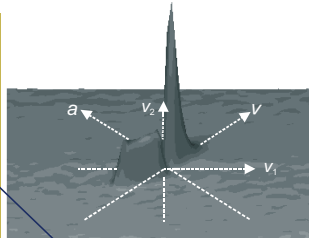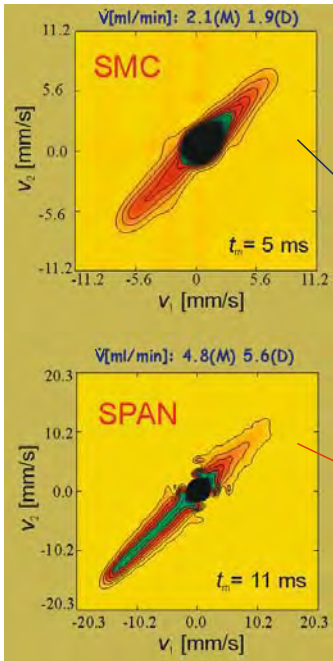
SMC: synthetically modified cellulose
SPAN: special poly acrylo nitrile
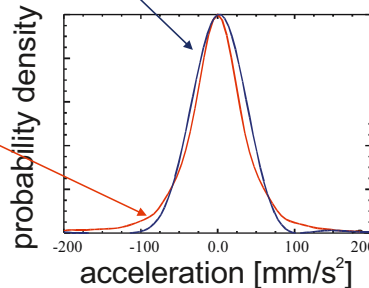
projections onto the secondary diagonals

S, Han, S. Stapf, B. Blümich, *Two-Dimensional PFG NMR for Encoding Correlations of Position, Velocity, and Acceleration in Fluid Transport*, **J. Magn. Reson. 146** (2000) 169 – 180;

B. Blümich, S.Han, C. Heine, R. Eymael, M. Bertmer, S. Stapf, *Analysis of Slow Motion by Multidimensional NMR*, J. Fraissard, O. Lapina, eds., **Magnetic Resonance in Colloid and Interface Science**, Kluwer, Academic Publishers, Amsterdam, 2002, pp. 3 - 14

Projections in Multi-Dimensional Fourier NMR

- In *multi-dimensional Fourier NMR* the data are acquired in *Fourier space* (t, $\boldsymbol{k}$, $\boldsymbol{q}_v$) and, subsequently, Fourier transformed into the space (ω, $\boldsymbol{r}$, $\boldsymbol{v}$) appropriate for data interpretation
- A *slice* in one space corresponds to a *projection* in Fourier space
- For example, a 1D slice in (k_1,k_2) space along the secondary diagonal corresponds to a projection in Fourier space along the principal diagonal so that the data are projected onto the secondary diagonal
- The term "projection" means "integration" of the multivariable function so that the number of variables is reduced and the variable in the direction of the projection is the variable of the integration
- This relationship can readily be derived from the expression for the *multi-dimensional Fourier transformation*
- It is known as the *projection – cross-section theorem*

Projection - Cross-Section Theorem
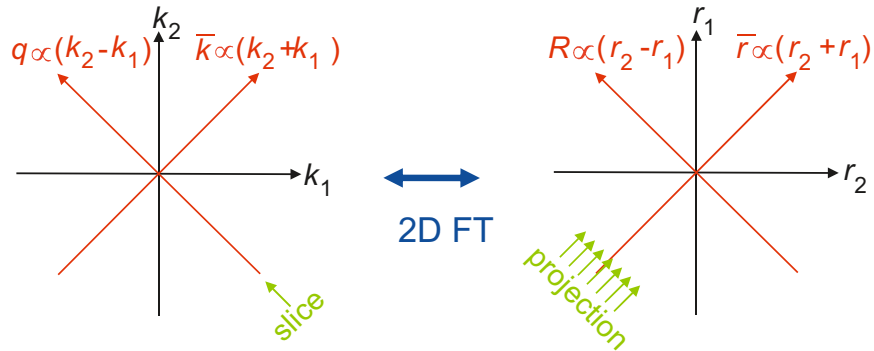
3D Position Exchange NMR

- The *VEXSY* experiment uses two anti-phase PFG pairs for encoding initial and final velocities
- However, only three and not four gradient pulses (k_1, k_2, k_3) are necessary to encode two position differences at different times, i. e. k_3-k_2 and k_2-k_1
- The scheme for *multiple position encoding* in Fourier space has been dubbed *SERPENT* for SEquential RePhasing by pulsed field gradiENTs
- The gradient amplitudes are adjusted to form an echo at the time of signal detection
- Given the echo condition k_1+k_2+k_3=0, the SERPENT scheme with three gradient pulses has two independent variables to adjust the amplitudes of the three gradient pulses
- In the 3D position exchange spectrum, these variables define the plane perpendicular to the vector $\boldsymbol{k}_1$+$\boldsymbol{k}_2$+$\boldsymbol{k}_3$ in (k_1,k_2,k_3) space, where the $\boldsymbol{k}_i$ are the unit vectors along the axes of the (k_1,k_2,k_3) exchange space
- Following the *projection – cross-section theorem*, the Fourier transform of this 2D plane in (k_1,k_2,k_3) space is the projection of the *3D exchange spectrum* along the direction of average position, leaving two position differences as the remaining variables in the 2D spectrum
- This shows that the SERPENT experiment with three gradient pulses is equivalent to a VEXSY experiment
- *Multi-dimensional Fourier NMR* usually employs *differential time coordinates*, while in non-linear systems theory *integral time coordinates* are preferred

SERPENT and VEXSY

3D scheme:
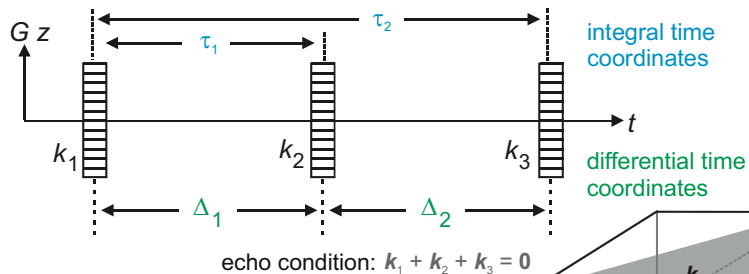
echo condition: $k_1 + k_2 + k_3 = 0$

integral time coordinates

differential time coordinates

B. Blümich, S.Han, C. Heine, R. Eymael, M. Bertmer, S. Stapf, *Analysis of Slow Motion by Multidimensional NMR*, J. Fraissard, O. Lapina, eds., **Magnetic Resonance in Colloid and Interface Science**, Kluwer, Academic Publishers, Amsterdam, 2002, pp. 3 - 14

$(k_1 + k_2 + k_3)/3^{1/2}$

$1/2(3^{-1/2}-1)k_1+1/2(3^{-1/2}+1)k_2-3^{-1/2}k_3$

$1/2(3^{-1/2}+1)k_1+1/2(3^{-1/2}-1)k_2-3^{-1/2}k_3$
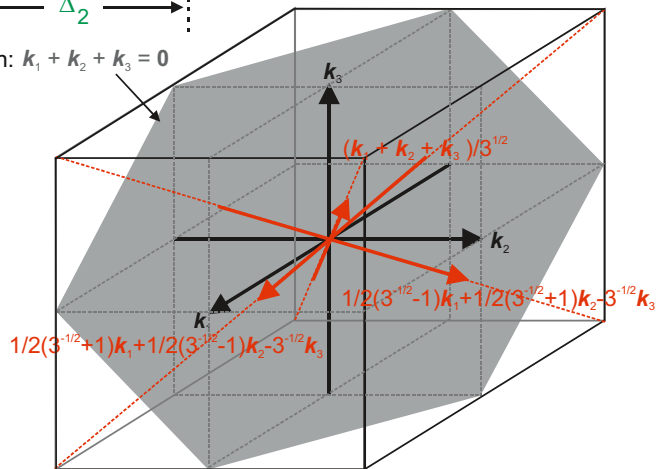
5. Low-Field and Unilateral NMR

NMR for process and quality control
Unilateral NMR: NMR-MOUSE
Soft matter: rubber
Relaxation anisotropy
Multi-quantum NMR
Spatial resolution
Transport phenomena
Spectroscopy

NMR Spectroscopy for Process Control

- *Low-field NMR* can be realized by small and less expensive instruments
- Often *permanent magnets* are employed, which hardly need maintenance
- A typical field strength for such magnets is between 0.5 to 1 T
- The field of permanent magnets is weakly inhomogeneous, but can be shimmed to a homogeneity sufficient for *spectroscopic resolution*
- Low-field NMR in homogeneous fields is established for *process control* in oil refineries
- The product stream is analyzed spectroscopically and a feedback signal is generated from a parameter of the ^{1}H NMR spectrum to optimize the product stream (www.foxboro.com)
- Without shims spectroscopic resolution is hard to achieve, but many simple and some more sophisticated NMR experiments can be conducted with *spin-echo detection*
- Simple experiments are measurements of echo amplitudes at different echo times and transverse relaxation decays as *CPMG echo trains* and envelopes of sets of *Hahn echoes*
- Sophisticated experiments use *multi-quantum filters*, *translational diffusion filters*, *saturation or inversion recovery filters*, *spin-lock filters*, etc., to prepare the detection of magnetization by a *Hahn echo* or a *CPMG echo train*. Also, *imaging* can be employed

NMR Monitoring of Fluid Product Streams

www.foxboro.com
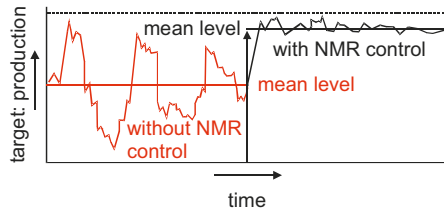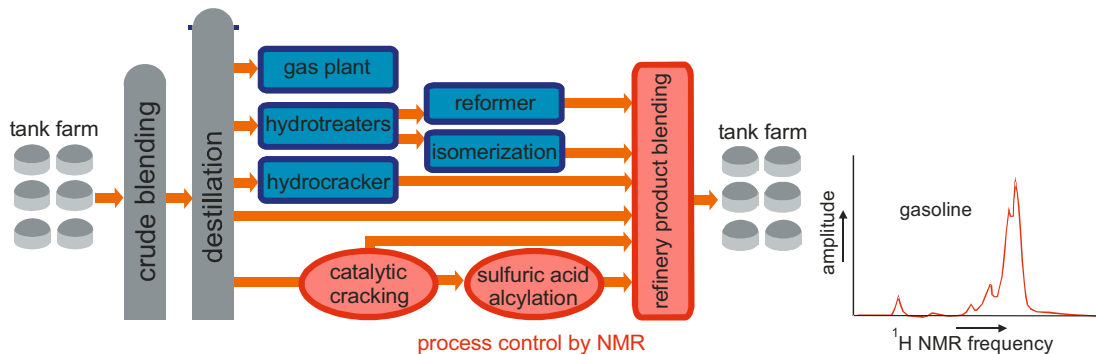
NMR Relaxometry for Process and Quality Control

- The field of *permanent magnets* is inhomogeneous and changes with temperature
- Nevertheless, spectrometers with permanent magnets are widely employed and typically measure echoes or FIDs in *weakly inhomogeneous fields* to characterize a diverse range of products like food, cosmetics, and polymers
- Initial amplitudes $a(t_0)$, relaxation-weighted relative intensities $I(t_2 - t_1)/a(t_0)$, and relaxation times T_2 can be extracted from the *FIDs* and *echo envelopes* for sample characterization
- Amplitudes and intensities can be determined without fitting functions to the recorded data
- Relaxation times are extracted with the help of *fit functions* such as the *stretched exponential function* $a(t) = a(0) \exp\{(t/T_2)^b/b\}$
- This approach has been employed in the construction of sensors that monitor *moisture* in food on-line during the production process
- It is also employed in desk-top NMR spectrometers to determine quantities such as moisture content, solid content, fat content, viscosity, droplet size distribution, extent of cure, etc.
- When conducted properly, the accuracy of such measurements can be as good as 0.1%

Process and Quality Control by Relaxometry

$$a(0) \exp\{(t/T_2)^b/b$$

$$a(0) \qquad I(t_2 - t_1)$$

amplitude a

time t

product stream

sensor

rf coil

magnet heater

sample chamber

magnet yoke

magnet pole piece

piston

B_1

B_0
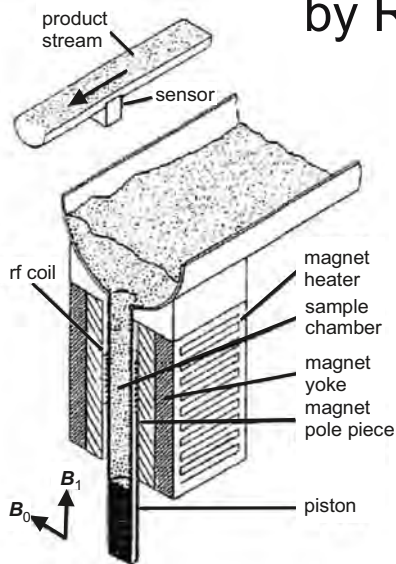
A. Nordon, C. A. McGill, D. Littlejohn, *Process NMR spectrometry*, **Analyst 126** (2001) 260 – 272.

desk-top NMR in weakly inhomogeneous fields: quality control of samples from food, polymers, cosmetics, etc.
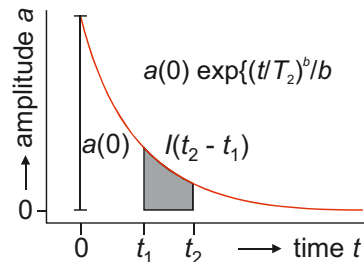
NMR Tomography for Quality Control

- Although convenient, homogeneous polarization fields are not a necessary requirement for *NMR imaging*
- Low image resolution can be achieved by simple means and is sufficient for some types of quality control, for example, the inspection of foodstuff such as dairy products packaged in boxes at fixed positions
- In an imaging experiment, one voxel can be placed inside each item in the box, and the signal of each voxel can be explored to measure the *product quality*
- The signals are compared against a moving average, and inferior products are identified by deviations exceeding a predetermined norm
- Such a setup has been proposed for analysis of dairy products by Intermagnetics General Corporation, Latham, New York, where the boxed goods are transported through the magnet on a *conveyor belt*
- A similar setup with a conveyor belt has been suggested by them to inspect raw rubber to detect moisture contaminations

Quality Control by NMR Imaging

MR inspection: packaged goods, spoilage of food
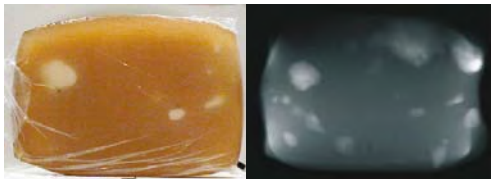
moisture in butadiene rubber:
10 kg sample from a production
bale; photo and NMR image

www.igc.com

Well-Logging NMR

- One of the oldest commercial interests in NMR is in logging oil wells
- In the fifties it was thought that the earth's magnetic field could be utilized for NMR in the bore hole wall
- Later *permanent magnets* were used to enhance the nuclear polarization
- In such a NMR set-up, where the sample sits outside the magnet, the magnetic polarization and rf fields penetrating the *bore-hole* wall are inhomogeneous, because the fields are applied from one side
- NMR of this kind is also referred to as *inside-out NMR* or *unilateral NMR*
- In *well-logging NMR*, the signal of the fluids in the bore-hole wall is acquired
- Typically, CPMG-type multi-echo trains are generated to measure the transverse relaxation
- The relaxation of fluids confined in pores is governed by *wall relaxation*
- In the *fast diffusion limit*, all molecules in a pore have the same contact with the wall
- Then the relaxation times T_1 and T_2 are proportional to the pore diameter
- The envelope of a *CPMG echo train* from fluid in pores with a distribution of sizes exhibits a multi-exponential decay
- An inverse *Laplace transformation* of this decay yields the T_2 distribution which maps the *pore size distribution*
- In the end, the T_2 distribution provides retrieval information about the type of fluid and the pore connectivity

Inside-Out NMR

NMR sensor

"homogeneous" region of B_0

half-coaxial antenna

10 cm

S   N

S   N

R. L. Kleinberg in: D. M. Grant, R. K. Harris, eds., *Encyclopedia of NMR*, Wiley, New York, 1996, p. 4960

biexponential fit
T_{2short} = (0.18 ± 0.01) ms
T_{2long} = (1.75 ± 0.04) ms

rel. echo amplitude [%]

time [ms]

inverse Laplace-Transformation

frequency

T_{2eff} [ms]
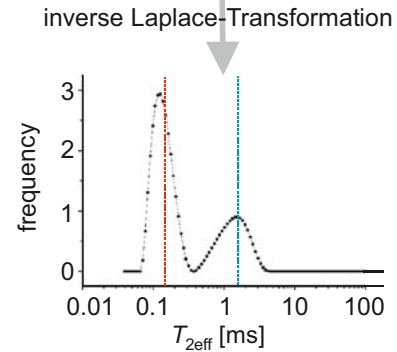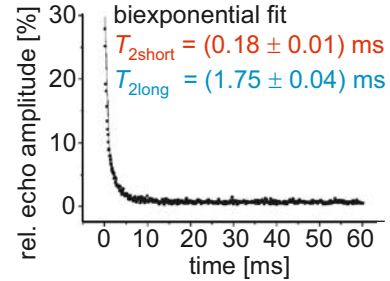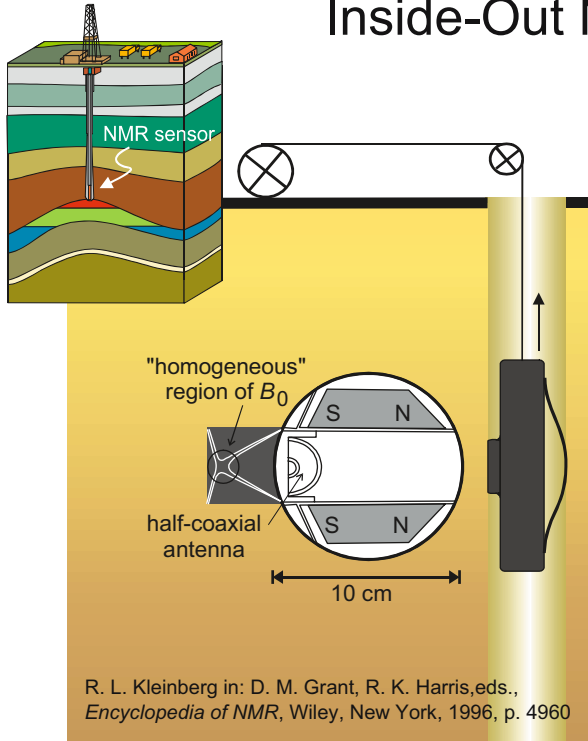
Mobile NMR for Nondestructive Testing

- *Well-logging NMR* is the oldest form of *mobile NMR*, where the NMR equipment is brought to the object for investigation
- The idea has been adapted in the seventies for *moisture determination* in buildings, food stuffs, soil, and other materials
- The instrumentation employed permanent as well as electromagnets designed in such a way as to inspect the object from one side
- With the focus on moisture detection the polarization field B_0 was sought to be as homogeneous as possible to avoid signal attenuation from *diffusion*
- Penetration depths of a few centimeters required large and heavy magnets weighing a few hundred kilograms
- To test rubber and polymer products, a few millimeters of depth resolution are often sufficient and translational diffusion is absent, so that the highly inhomogenous fields generated by small magnets can be employed
- The *NMR-MOUSE*® (mobile universal surface explorer) has been developed for *materials testing* by *unilateral NMR* following the concept of well-logging NMR
- With *permanent magnets*, field strengths near 0.5 T are readily produced in depth up to a few millimeters with average field gradients of 10 to 20 T/m
- The envelope of the FID is sampled stroboscopically via *echo trains*
- The resultant *effective relaxation times* $T_{2\text{eff}}$ are modified by the inhomogeneities in B_0 and B_1, where $T_{2\text{eff}} > T_{2\text{Hahn}}$ is often observed

Unilateral NMR: NMR-MOUSE

mobile unilateral NMR

magnetic field and gradient profiles

B_z

G_z

e^{-t/T_2}

time t

time-domain signals in spectroscopy and relaxation in a homogeneous $\boldsymbol{B}_0$ field and echo train in an inhomogeneous $\boldsymbol{B}_0$ field

NMR-MOUSE: MObile Universal Surface Explorer

← 85 mm →

magnet
rf coil

N   S

sensitive volume

magnetic field: 0.5 T

radio-frequency field: 20 MHz
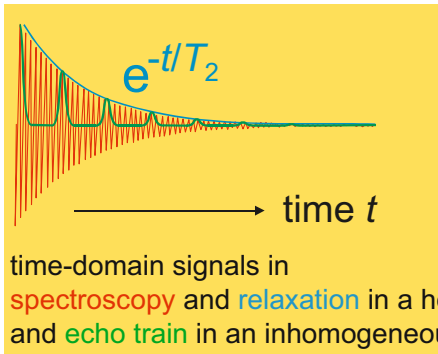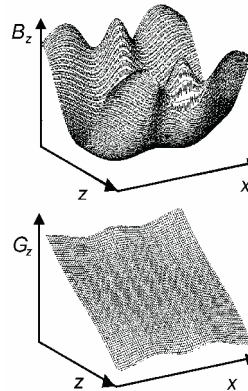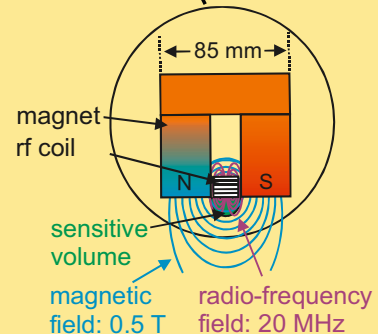
Transverse Relaxation and Glass Temperature in Rubber

- In soft organic matter the NMR *relaxation times* are determined by the *residual dipole-dipole interaction* among [1]H
- In *elastomers* the residual dipole-dipole interaction depends on the time scale and the anisotropy of the segmental motion
- 60 to 80 K above the *glass temperature* T_g the motion is fast and the anisotropy is determined by the *cross-link density*
- Closer to T_g the chain stiffness also determines the relaxation times
- Measurements of $T_{2\text{eff}}$ can be employed to characterize the cross-link density, the glass temperature, and other physical parameters of materials
- For *quality control* of *rubber products*, the experimental values of $T_{2\text{eff}}$ need to be extrapolated to a reference temperature and correlated with material properties by means of calibration curves
- Calibration curves are obtained on small samples in physical testing laboratories, for example by swelling, rheometry, and dynamic-mechanical relaxation
- By mapping these data onto NMR relaxation times, parameters such as the glass temperature, the *elastic modulus*, and the cross-link density can be determined nondestructively in selected spots at production intermediates and the final product

Cross-Linked Rubber: T_2 Versus T_g
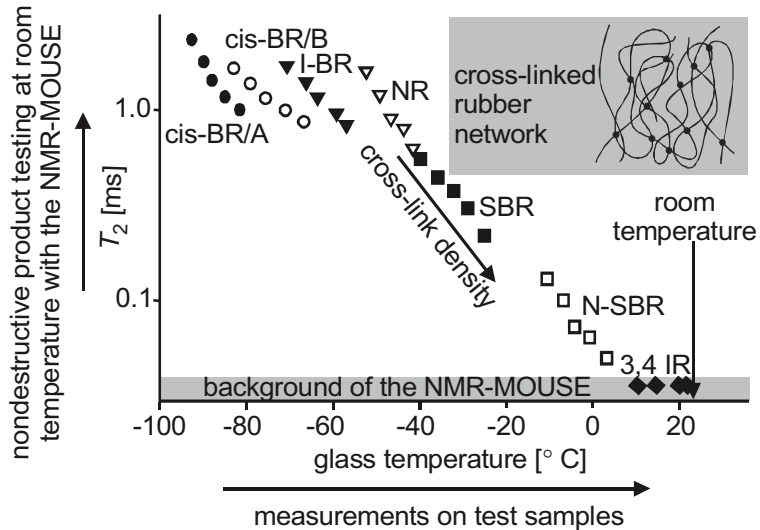
V. Herrmann, K. Unseld, H.-B. Fuchs, B. Blümich, *Molecular Dynamics of Elastomers Investigated by DMTA and the NMR-MOUSE®*, **Colloid and Polymer Science 280** (2002) 738 - 746

Analysis of Technical Rubber

- *Technical rubber* is a cross-linked polymer network with various additives including fillers, cross-linker, accelerators, processing aids, etc.
- Depending on the formulation and the conditions of use, aging, cross-linking, and chain-scission reactions proceed in the finished product
- The prevailing state of rubber products can be assessed nondestructively by *unilateral NMR* in different depths of the sample
- Overcure cannot be identified through measurements of the degree of swelling or the *rheometer torque* by the *cross-link density* itself as these values are identical at curing times t_{90} and t_{R90}, where the rheometer torque is at 90 % of its maximum
- Depending on the formulation and the vulcanization conditions, T_{2eff} may discriminate these states, as the chain stiffness changes with *overcure* caused by different reactions dominating the sample evolution
- Errors in the formulation as well as changes in the processing steps may be identified by NMR
- The correlation of T_{2eff} with chain stiffness is nicely exemplified by the dependence of T_{2eff} on the curing time of a moisture curing poly(urethane) adhesive used for mounting windshields in cars
- As the *windshield* is an element providing stability to the car, proper curing of the adhesive is a matter of safety

Curing of Rubber
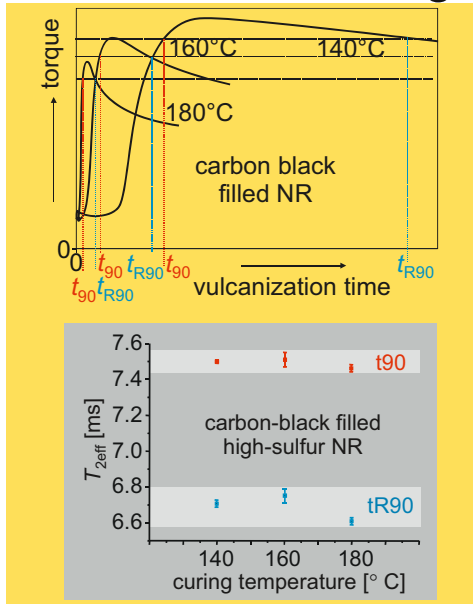
B. Blümich, S. Anferova, K. Kremer, S. Sharma, V. Herrmann, A. Segre, *Unilateral NMR for Quality Control: The NMR-MOUSE®*, **Spectroscopy 18** (2003) 18 - 32
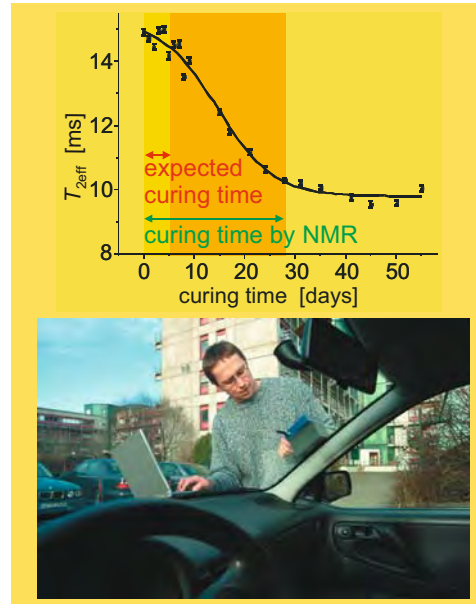
K. Kremer, H. Kühn, B. Blümich, J. Seitzer, F. P. Schmitz, *NMR-MOUSE ermöglicht Online Quali-tätskontrolle im KFZ-Bau*, **Adhäsion 11** (2002) 32 – 36

Reproducibility of Measuring T_2

- *Technical rubber* is a statistical product produced by mixing, diffusion, and the reaction of various compounds
- Depending on the miscibility and the processing conditions, some compounds may agglomerate
- Even on a macroscopic scale technical rubber appears inhomogeneous in NMR images which reveal the statistical nature of the material
- Measurements with the *NMR-MOUSE* collect signal from a volume element the size of a small coin
- While the uncertainty of reproducing $T_{2\text{eff}}$ from repetitive measurements at one point is often less than 1 %, values of $T_{2\text{eff}}$ differing by as much as 10 % are found for measurements at different points due to the variance of the network properties
- For *quality control of rubber* products several measurements need to be conducted at equivalent spots of the product. The mean fit parameters characterize the average material properties and the variance the heterogeneity of the product
- A similar approach may be required to characterize other matter such as semi-crystalline polymers and food

Technical Rubber

rel. amplitude

experimental data and fit function
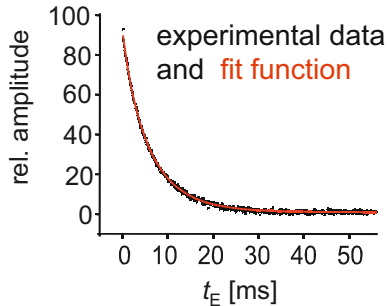
NMR image of a technical rubber sample

10 mm
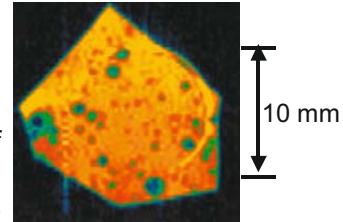
$a(t_E) = A \exp\{-(1/b)(t_E/T_2)^b\}$

distributions of fit parameter T_2

relative number of counts

measurements at the same position

measurements at different positions

variance

mean value

relaxation time T_2
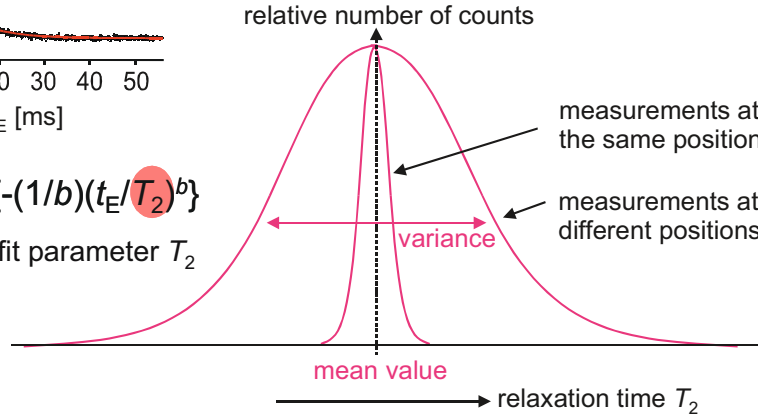
B. Blümich, S. Anferova, K. Kremer, S. Sharma, V. Herrmann, A. L. Segre, *Unilateral Nuclear Magnetic Resonance for Quality Control: The NMR-MOUSE*, **Spectroscopy 18** (2003) 18 - 32

Semi-Crystalline Polymers

- Polymers consist of assemblies of macromolecular chains
- *Semi-crystalline polymers* are solids with disordered amorphous and ordered crystalline domains
- In the *crystalline domains*, the chain packing is dense, the degrees of freedom for molecular motion are restricted, and T_2 is short
- In the *amorphous domains*, the chains are disordered, their degrees of molecular motion are less restricted, and T_2 is longer
- In polymers like poly(ethylene), poly(propylene), and Nylon, spherulitic crystal structures form upon cooling of the polymer melt
- Within the spherulites the polymer chains are arranged in stacks consisting of chain-folded lamellae alternating with amorphous layers
- Upon drawing, the macromolecular chains become realigned
- Upon annealing, a fibrillar structure forms with the alternating layers of chain-folded lamellae and amorphous domains arranged in the drawing direction
- Depending on the temperature variation and the shear fields applied during processing, different overall *crystallinity*, different size distribution of the crystallites, and different order in the amorphous domains are achieved
- The *transverse relaxation* function of such polymers can be fitted with a *bi-exponential decay*, where the rapidly and the slowly relaxing components are assigned to the crystalline and the amorphous domains, respectively

Morphology of Semi-Crystalline Polymers

spherulite

crystalline polymer

amorphous polymer

strain

annealing

crystalline polymer

amorphous polymer
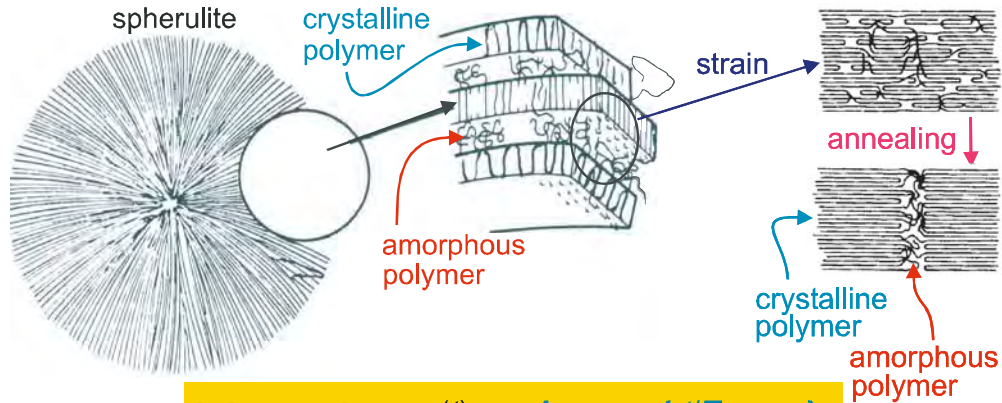
fit function for CPMG decays

$$s(t) = A_{short} \exp\{-t/T_{2eff,short}\} + A_{long} \exp\{-t/T_{2eff,long}\}$$

Analysis of Poly(ethylene) Pipes

- Plastic pipes are increasingly being installed by communities in the ground for water and gas transport
- During installation and repair it is common practice to stop the transport of gas or water by squeezing the pipes, and welding lines are introduced when adding or replacing pipe sections
- The mechanical treatment as well as heat treatment at temperatures well below the melting temperature (T_m = 120° C) of the crystallites change the *polymer morphology*
- Such changes in the polymer morphology can be monitored by the *NMR-MOUSE* for state assessment and safety inspection
- The parameters of a *bi-exponential fit* of the experimental CPMG decays can be interpreted in terms of the *crystallinity*, the average crystallite size, and the order in the amorphous domains
- Like rubber, *PE pipes* are inhomogeneous products, where the morphology changes with the measurement position
- Upon deformation the crystallinity and the average crystallite size decrease, while the order of the amorphous domains increases
- Upon annealing at low temperature, crystallinity and the average crystallite size decrease further while the order in the amorphous domains decreases as well

PE 100 Water Pipes

deformed PE pipe and measurement positions

relative amplitude $A_{short}/(A_{short}+A_{long})$

"crystallinity"

1)new
2)after deformation (3 days)
3)after annealing (24h, 80° C)

position at circumference

$1/T_{2eff,short}$ [1/ms]

"size of crystallites"

1)new
2)after deformation (3 days)
3)after annealing (24h, 80° C)

position at circumference

$1/T_{2eff,long}$ [1/ms]

"order in amorphous domains"

1)new
2)after deformation (3 days)
3)after annealing (24h, 80° C)

position at circumference

Moisture and Pore-Size Distributions

- In homogeneous B_0 fields the T_2 *distribution* maps the *pore-size distribution* of fluid-filled media in the fast diffusion limit
- In the strongly inhomogeneous B_0 field of the *NMR-MOUSE*, diffusive attenuation of the transverse magnetization compresses the *relaxation time distribution* at large relaxation times
- Nevertheless, information about the fluid distribution can be obtained in a non-destructive fashion by unilateral NMR
- The time-domain signal may be fitted e. g. by a *bi-exponential function*
- A map of $T_{2\text{eff}}$ as a function of depth reveals *average pore sizes*
- This way, pore size reductions from treatments of stones in conservation efforts can be mapped and the success of the treatment determined
- In liquid-saturated porous media, the amplitude of the signal measured by unilateral NMR is proportional to *porosity*, where the measurement volume is given by the sensitive volume
- T_2 distributions undistorted by diffusive attenuation need to be measured in homogeneous or slightly inhomogenous B_0 fields
- Such fields can be generated from blocks of permanent magnets arranged in the Halbach geometry, where B_0 points transverse to the axial direction for convenient use of solenoidal B_1 coils
- *Halbach magnets* can be designed at low weight to obtain portable systems

Mobile NMR of Wet Porous Materials

wet ancient fresco near Colle Oppio in Rome

wall near fresco

dryer, newer wall orthogonal to fresco

fresco

small pores

large pores

relative frequency of occurence

relaxation time T_{2eff} [ms]

S. Sharma, F. Casanova, W. Wache, A. Segre, B. Blümich, *Analysis of Historical Por-ous Building Materials by the NMR-MOUSE*, **Magn. Reson. Imag.** **21** (2003) 245 – 255

pore reduction in sandstone

relaxation time T_{2eff} [ms]

$T_{2eff,long}$
$T_{2eff,short} \times 10$

surface: small pores

inside: large pores

depth [mm]

T_{2eff} distributions in geological drill cores

frequency

NMR-MOUSE

Halbach magnet

T_{2eff} [ms]

8 kg Halbach magnet and po-larizations

Relaxation Anisotropy in Oriented Materials

- The dominant relaxation mechanism in ^{1}H NMR is the *dipole-dipole interaction*
- In macroscopically ordered solids the dipole-dipole coupling tensors are distributed anisotropically, so that the relaxation rates depend on the orientation of the polarization field B_0 with respect to the direction n of molecular orientation
- *Tendons* are *biological tissues* with a high degree of *macroscopic order* of the collagen triple helices
- Strained rubber is an example of synthetic soft matter with a low degree of molecular order which depends on the elongation ration $\Lambda = L/L_0$
- In ordered matter, the transverse relaxation rate $1/T_{2eff}$ is the sum of an orientation-dependent part which depends on the square of the second Legendre polynomial $P_2(\beta) = 3(\cos^2 \beta - 1)/2$ and an isotropic part
- The isotropic and the *anisotropic relaxation* rates increase with increasing elongation
- The anisotropy leads to minima of the relaxation rate at the magic angle
- In the human Achilles tendon the observed angle dependence of relaxation rates $1/T_{2eff}$ suggests a bimodal *orientational distribution* of the interaction tensors in agreement with a twisted structure of the collagen fibrils

Macroscopic Molecular Order
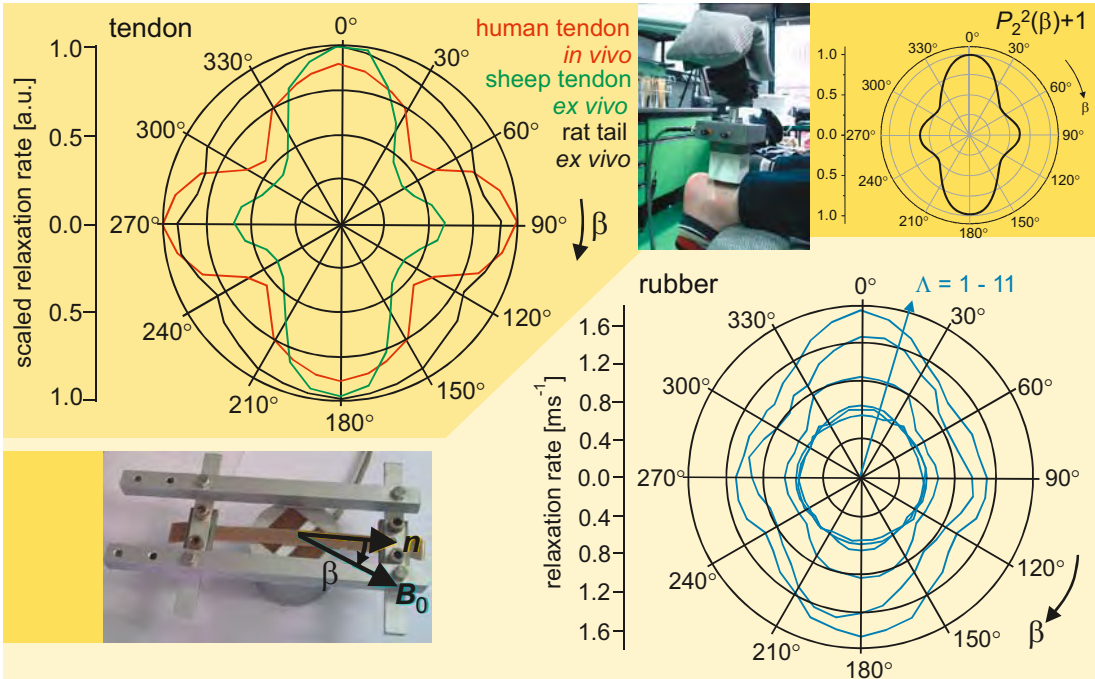
K. Hailu, R. Fechete, D. E. Demco, B. Blümich, *Segmental Anisotropy in Strained Elastomers Detected with a Portable NMR Scanner*, **Solid State Nucl. Magn. Reson. 22** (2002) 327 – 343

Spin Modes in Inhomogeneous Fields

- *Multi-quantum coherences* are *spin modes* in coupled spin systems
- *Transverse magnetization*, *dipolar encoded longitudinal magnetization*, and *dipolar order* are other *spin modes*
- Spin modes other than single-quantum coherences can only be detected indirectly by preparing different initial states before data acquisition
- The preparation of such states follows the general scheme of *multi-quantum NMR* consisting of a preparation, an evolution, and a mixing period
- A *z* filter often precedes the detection period to eliminate unwanted signal contributions
- In the inhomogeneous fields of unilateral NMR refocusing pulses need to be centered in each period, where *density-matrix elements* evolve
- *Double-quantum build-up curves* are obtained by varying the preparation time τ which is equal to the mixing time
- The build-up curves measured in *inhomogeneous fields* are in agreement with those measured in homogeneous fields
- Relative but no absolute values of dipolar couplings can be extracted at short τ from the slopes of the curves measured in inhomogeneous fields
- The same information can be obtained from *double-quantum decay curves* which start at the maximum of the build-up curves
- The relative dipolar couplings obtained in this way at low and inhomogeneous fields agree with those obtained at high and homogeneous fields

Unilateral Multi-Quantum NMR of Rubber

$$\text{short } \tau: \quad \frac{S_{2Q}(\tau)}{S_0} = \langle\sin^4\theta\rangle_\theta \langle\langle\sin^2\{(3/2)^{1/2}\omega_d\tau\}\rangle\rangle$$

$$\approx \langle\sin^4\theta\rangle_\theta \; 3/2 \; \langle\omega_d^2\rangle \, \tau^2$$
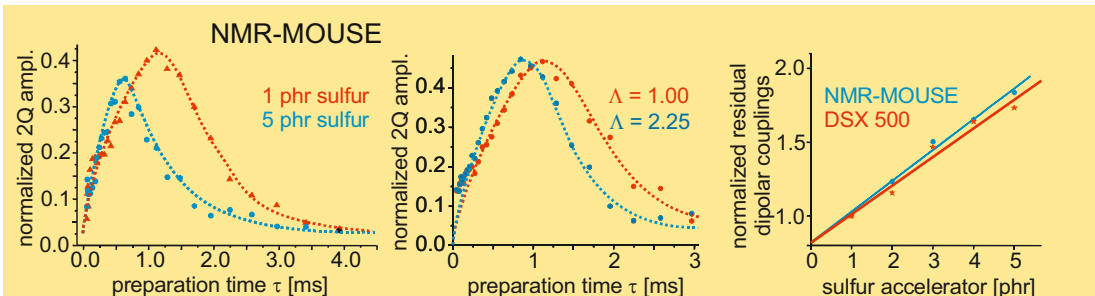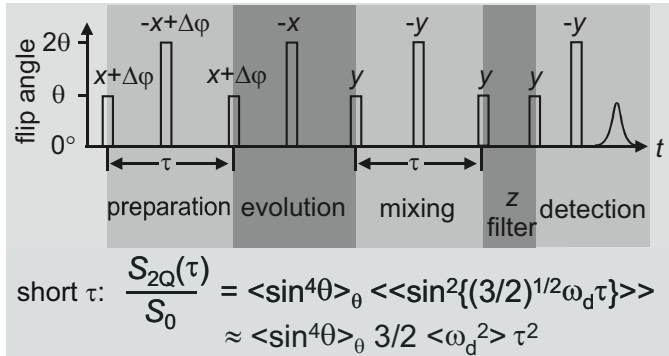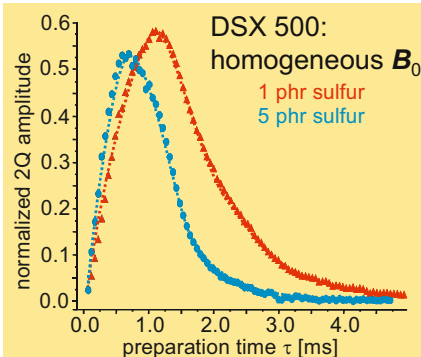
A. Wiesmath, C. Filip, D.E. Demco, B. Blümich, *Double-Quantum-Filtered NMR Signals in Inhomogeneous Magnetic Fields*, **J. Magn. Reson. 149** (2001) 258-263; *NMR of Multipolar Spin States Excited in Strongly Inhomogeneous Magnetic Fields,* **J. Magn. Reson. 154** (2002) 60 - 72

Depth Selectivity

- In *inhomogeneous magnetic fields*, the signal comes from a limited region of the sample, which is called the *sensitive volume*
- By lowering the radio frequency, deeper lying sample regions are probed in *unilateral NMR* at the expense of a loss in sensitivity
- *Depth profiles* can be obtained either by adjusting the radio frequency or by tuning it to a fixed value for a distant sensitive volume and changing the distance between sensor and sample
- Depending on the field profiles the sensitive volume is curved or flat
- Curved shapes are preferred for thick slices, flat volumes for thin slices
- Depth profiles of car-tire treads have been obtained to identify inferior tires in a collection of new tires. The depth profiles are in agreement with the morphological shapes revealed in NMR images
- With optimized field profiles, the sensitive volume can be shaped into a sensitive plane that is 30 μm thick
- By adjusting the distance between the *NMR-MOUSE*® and the object, depth profiles of water in polymer sheets and skin at different parts of the human body were obtained
- Such profiles are appreciated in the optimization of painting plastic parts and in the development of skin care products

Depth Profiles by the NMR-MOUSE

T_2 weighted spin density images of tire tread sections and depth profiles by the NMR-MOUSE

good tire

bad tire

T_2 [ms]

T_2 [ms]

depth [mm]

depth [mm]

(by permission of Oxford University Press)

days after soaking

amplitude [a.u.]

drying of a polymer sheet

depth [mm]

sensitive volume

depth [mm]

z [mm]

slice definition

amplitude [a.u.]

regular

optimized

depth [mm]

epidermis

dermis papillare

dermis reticulare

subcutis

amplitude [a.u.]

hand

lower arm

skin profiles

depth [μm]
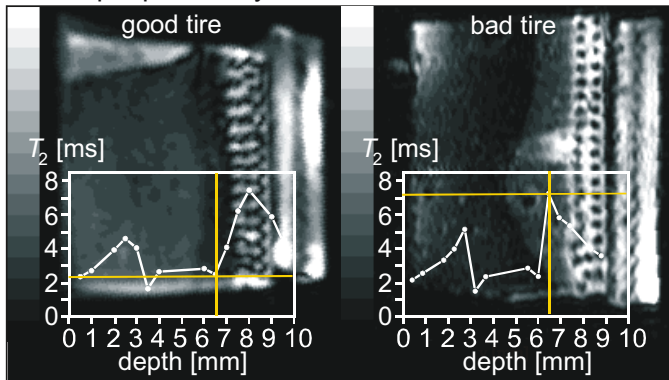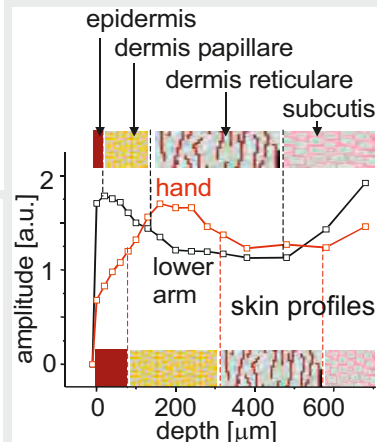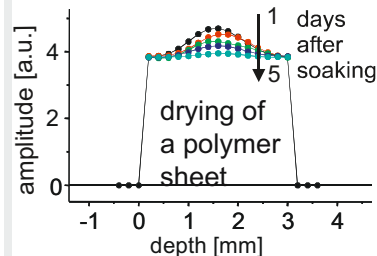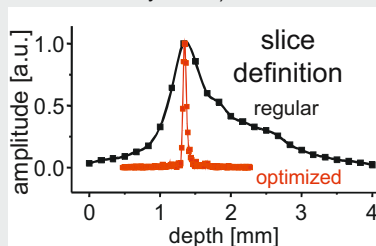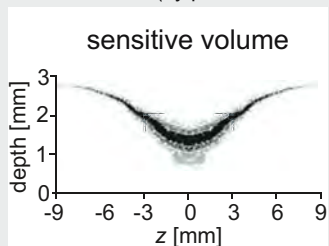
Unilateral Imaging

- *Unilateral tomographs* can be built by furnishing the *NMR-MOUSE* with gradient coils for lateral 2D space encoding to measure 2D slice images parallel to the scanner surface
- Due to the inhomogeneous B_0 field, echo-based *single-point imaging* methods are used which sample k space point by point
- The signal-to-noise ratio is improved by detecting multiple echoes and integrating their amplitudes
- Depending on the length of the multi-echo decay, imaging times of a few minutes to 1 hour are obtained
- Images obtained by unilateral NMR reveal details of the object similarly to a magnifying glass but accessing sub-surface structures
- Applications are envisioned in nondestructive *defect analysis* and *quality control*
- If unilateral imagers are to be built very small, their fields of view and the penetration depths are small as well

Defect Analysis by Unilateral NMR

a small unilateral tomograh

Foto: Peter Winandy

open tomograph measuring a rubber hose

textile reinforced rubber hose with a defect

unilateral-NMR image of the defect
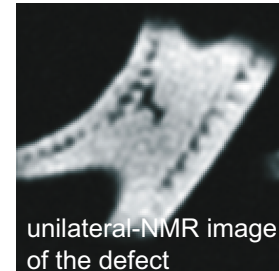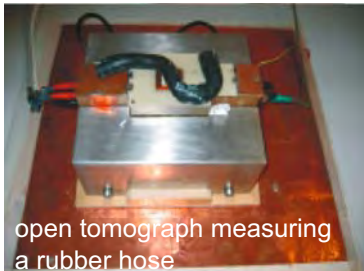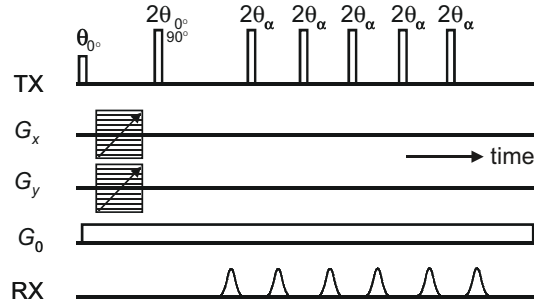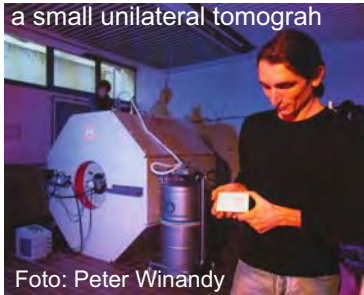
F. Casanova, J. Perlo, B. Blümich, K. Kremer, *Multi-Echo Imaging in Highly Inhomogeneous Magnetic Fields,* **J. Magn. Res. 166 (2004)** 76 – 81; J. Perlo, F. Casanova, B. Blümich, *3D imaging with a single-sided sensor: an open tomograph,* **J. Magn. Res. 166 (2004)** 228 – 235

Unilateral Flow Imaging

- Despite large field inhomogeneities, *unilateral NMR* can be employed to measure flow by using combined gradient and Hahn echoes for position encoding with background gradient compensation
- Two such position encodings with opposite signs encode *displacement* corresponding to average velocity when divided by the lime lag Δ_v between the encodings
- The *velocity encoding* is detected by an *echo train* with short echo time, and the echoes are integrated for signal-to-noise improvement
- By systematically varying the pulsed gradient amplitudes, q_v space is scanned for the slice defined by the frequency of the excitation
- Fourier transformation of the q_v-space signal provides the *velocity distribution* in the slice through the object, a pipe in this case
- The sum of all velocity distributions from contingent slices is the velocity distribution in the pipe
- By placing the velocity profiles adjacent to each other in a 2D matrix and plotting the frequency of occurrence of each velocity component in a different gray shade, a 1D *velocity image* is obtained
- For laminar flow through a circular pipe, the sum velocity distribution is a *hat function*, and the velocity image shows the *flow parabola*

Velocity Distributions and Flow Images
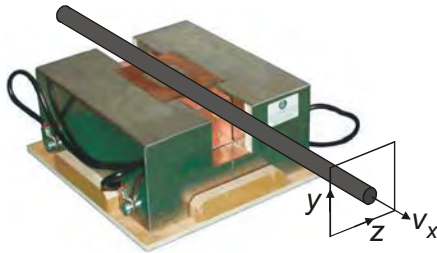
pulse sequence for background gradient elimination
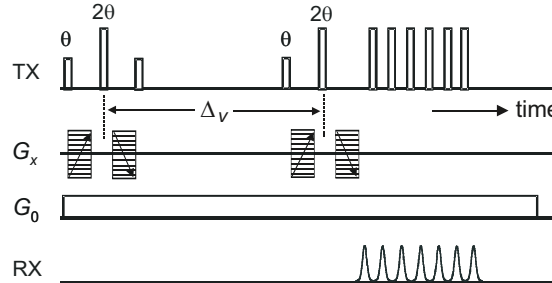
slice-selective measurements
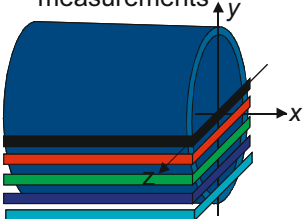
slice-selective velocity distributions
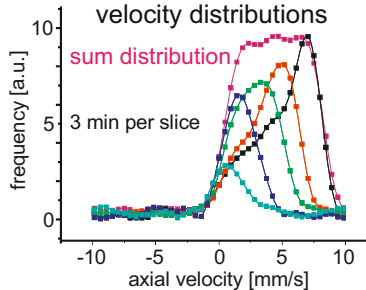
reconstructed velocity image
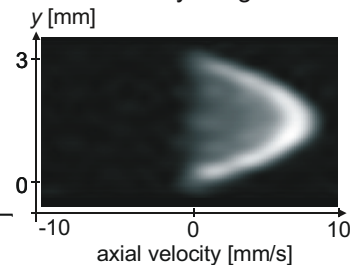
Spectroscopy in Inhomogeneous Fields

- *Chemical shifts* can be sampled in *inhomogeneous fields* by acquiring a *mixed nutation echo* train
- A mixed nutation echo is generated by matching the phase evolutions of the transverse magnetization in inhomogeneous B_0 and B_1 fields in an appreciable sample volume
- In linear field profiles, a *Hahn echo* is generated in a B_0 gradient field by matching the wave numbers k_{01} in an evolution period t_1 to the wave number k_{02} in a detection period t_2. The echo maximum arises at $k_{01} + k_{02} = 0$
- Similarly, a *nutation echo* is generated in a B_1 gradient field by matching the wave numbers k_{11} in an evolution period t_1 to the wave number k_{12} in a detection period t_2. The echo maximum arises at $k_{11} + k_{12} = 0$
- For a mixed nutation echo $k_{11} + k_{02} = 0 = k_{01} + k_{12}$
- As rf pulses are insensitive to chemical shifts, k_{11} is free of chemical shift evolution, but the evolution in B_0 according to k_{02} is not
- Consequently, the chemical shift evolution is preserved at the maximum of the mixed nutation echo, and the field inhomogeneities do not lead to line broadening
- Among other methods, mixed nutation echoes are of potential use for measuring NMR spectra *ex situ*, i. e. in the fringe field outside the magnet by unilateral NMR

Mixed Nutation Echoes in Matched Fields

$B_0 \propto \omega_0$

matched B_0 and B_1 gradient fields

y

$B_1 \propto \omega_1$
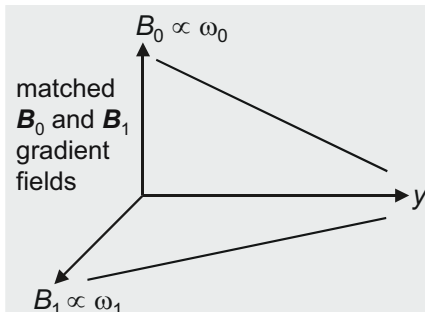
pulse sequence to generate a train of mixed nutation echoes. The β_x pulses use inhomogeneous B_1

acquire   acquire

90°_y 90°_y β_x 90°_{-y} 90°_{-y} β_{-x} 90°_y 90°_y β_x 90°_{-y}

k_1 k_0 k_1 k_0 repeat

time

CH$_2$-CH$_2$ H
C=C
H   COOH

chemical shift [ppm]
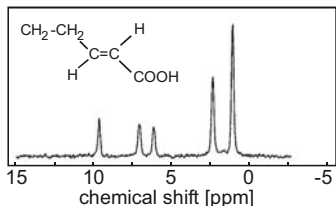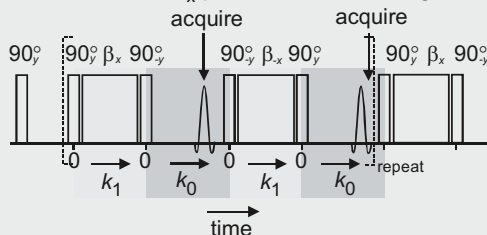
Fourier transform of the FID acquired in a homogeneous field

chemical shift [ppm]
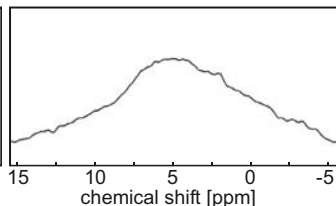
Fourier transform of the FID acquired in an inhomogeneous field

chemical shift [ppm]
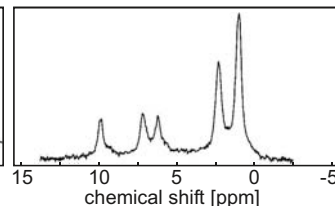
Fourier transform of the modulation of mixed nutation echoes acquired in an inhomogeneous field

Index